Solutions for Tractor-trailer Path following at Low Speed

by

Tong Wu

A dissertation submitted to the Graduate Faculty of
Auburn University
in partial fulfillment of the
requirements for the Degree of
Doctor of Philosophy

Auburn, Alabama
August 5, 2017

Keywords: Tractor-trailer System, Path Following Control, Model Predictive Control, Integral Separation, Unscented Kalman Filter

Approved by

John Y. Hung, Chair, Professor of Electrical and Computer Engineering
George T. Flowers, Professor of Mechanical Engineering
Bogdan M. Wilamowski, Professor of Electrical and Computer Engineering
Thaddeus A. Roppel, Associate Professor of Electrical and Computer Engineering

Abstract

Autonomous tractor-trailer systems have become more and more popular in real life. This dissertation focuses on control and estimation for the path following problem where space-based path is used as reference. The goal is to make the trailer path follow the reference path as closely as possible. A kinematic model is derived and is applicable when the tractor velocity is relatively low.

To reduce tracking error near the intersection between two different kinds of reference paths, a new approach is first developed based on a proper local coordinate transformation. Then, an alternative solution based on model predictive control is developed to solve the challenge mentioned above in an optimal way. Two linearization methods for the nonlinear model, based on current measurements and steady-state values of time-varying terms, are given. The result shows that both of these two approaches can greatly reduce the tracking error near the intersections of different reference paths. For the trailer far from the reference, a controller focusing on heading control is then proposed.

Two methods are then given to eliminate the steady-state error for curved reference path. One is to add a feed-forward part in the control law. The other is to use tractor steering rate as the control input instead of steering angle. The steady-state error may exist when there is a bias in the measurement and process. An additional integrator is added in the model and adaptive integral separation is applied to accumulate position error only when it is close to zero. The proposed approaches are verified by simulations.

To reduce the sensor cost, an estimator based on adaptive unscented Kalman filter is proposed when the positions of the trailer are measurable. Simulation results verify the proposed algorithm.

Acknowledgments

First of all, I would like to thank my advisor, Prof. John Hung. He gave me much assistance for my study in Electrical and Computer Engineering in Auburn University. Furthermore, he helped me a lot on my research, including the academic suggestions and paper publications. I really appreciate his extensive knowledge and good character. I also would like to thank the other committee members Prof. George Flowers, Prof. Bogdan Wilamowski, Prof. Thaddeus Roppel and Prof. David Beale as the university reader for my course work and their assessment of my research and dissertation.

I want to thank my father Guohong Wu, my mother Yanjie Liu, my grandma Peizhu Shi, and my wife Xufang Wang. My parents and my grandma brought me up with a large amount of dedication. My wife also gave me much support. Thank you all I love.

I also thank my friends in Auburn, Xiaolong Cao, Jianliang Hao, and Xianglin Wang. Thank you for your help and companion. I would cherish the friendship and pray for you.

Last but not the least, I would like to thank China Scholarship Council for the financial support.

Table of Contents

List of Figures

List of Tables

Chapter 1

Introduction

A tractor-trailer is a common vehicle that can do various tasks depending on the equipment on the trailer. With the development of computer technology, autonomous tractor-trailer systems can be applied in many fields. For example, the system can be used to spread seed and fertilizer in the agriculture. In the previous work from Auburn University, a metal sensor is placed on the trailer to detect unexploded ordnance underground. All these applications require accurate path following. As a robot, the tractor controls the speed and direction and drives the trailer to track a given path. This dissertation focuses on control system design for the trailer path following problem. which is more difficult than single robot control. One reason is that a tractor-trailer system is a high order system. The position of the trailer is changed by the heading angles of tractor and trailer, while the direction of a single robot is decided by itself. The other difficulty is that it's a non-collocated system. For most tractor-trailer systems, the steerable wheels are the front wheels of the tractor. Therefore, the control input is from the tractor while the control objective is the trailer position. Furthermore, a tractor-trailer system is nonlinear. When classical linear approach is applied, the system may be unstable in some cases.

1.1 Some classical control approaches

Proportional-integral-derivative (PID) control may be the most popular control algorithm for single-input-single-output (SISO) systems. The control law in continuous time domain is [1] :

$$u(t) = K_P[e(t) + \frac{1}{T_I}\int_0^\infty e(\tau)d\tau + T_D\frac{\mathrm{d}e(t)}{\mathrm{d}t}] \tag{1.1}$$

Figure 1.1: An example of a tractor-trailer system

where $e(t)$ is the error signal, $u(t)$ is the control command, and K_P, T_I, and T_D are the PID controller gains. In discrete time domain, the control law becomes:

$$u(k) = k_P[e(k) + k_I \sum_{0}^{k} e(k) + k_D(e(k) - e(k-1))] \tag{1.2}$$

Unfortunately, PID control is unable to give a satisfactory result for tractor-trailer systems, even when the system is near the reference. The main reason is that PID controller doesn't include any information about the tractor heading angle, which is critical to the direction of the trailer. Some researchers have used state feedback approach and good results have been achieved. The heading angles and trailer lateral position can be treated as system state variables by constructing a state-space model:

$$\begin{aligned} \dot{x} &= Ax + Bu \\ y &= Cx \end{aligned} \tag{1.3}$$

where variable x is the state vector. A control law can be designed using state feedback, making all the poles in the closed-loop system locate in the left-half plain:

$$u = -kx$$

There are several methods to determine the control gain k. Hodo uses pole placement method [2] where the control input is the tractor yaw rate. Payne uses an optimal linear quadratic regulator (LQR) algorithm in [3] where the control effort minimizes the cost function:

$$J = \sum_{k=0}^{\infty} (x_k^T Q x_k + u_k^T R u_k) \tag{1.4}$$

One advantage of LQR over pole placement is that the algorithm considers not only the output errors, but also the magnitude of control effort. The restriction of control effort for most control systems is useful because any control signal, such as wheel steering angle, torque in mechanical system, or current in the electrical system, can not be infinitely large.

Model predictive control (MPC) is another optimal control approach. The control law is also obtained from minimizing a cost function like (1.4), but with a finite prediction horizon. MPC has two main advantages over LQR. One is the reference output signal $r(k)$ can be flexibly set, and the other is the constraints can be integrated in the controller design. However, the cost is that the amount of computation is much more than LQR, especially for nonlinear MPC (NMPC) because calculating the optimal solution using numerical method is very time-consuming. Falcone *et al.* apply so-called linear time-varying model predictive control (LTV-MPC) for an autonomous robot where a discrete linear approximation model was used at every step [4]. In other words, the nonlinear model was linearized by $(A(k), B(k), C(k), D(k))$. Backman *et al.* applies NMPC for an agriculture machine. To overcome the computation burden, the prediction horizon is reduced to ten samples when trailer tracks a curve. Besides, the controller effort calculated at the last step is used when NMPC fails to provide the solution in real-time. Kayacan also uses NMPC to control the

position of tractor and trailer with the help of a code generation tool "ACADO" which solves the nonlinear programming problem relatively fast [5].

Some other control approaches based on linear or nonlinear model can be also applied for a tractor-trailer system. A linearized dynamic model is developed in [6]. The tracking error e is defined where a look-ahead point is selected as the reference point. A sliding model controller is designed to eliminate the lateral error. Sliding surface is:

$$s = \dot{e} + \lambda e$$

where λ is a positive number and the control effort is chosen to guarantee the following equation:

$$s\dot{s} < 0$$

A hybrid back stepping controller is applied in [7]. The lateral position of the trailer, heading angle of the trailer and the hitch angle are stabilized using pseudo feedback respectively. In [8], the original nonlinear kinematic model is replaced with a set of linear models by fuzzification.

$$\dot{x}(t) = A_i(t)x(t) + B_i(t)u(t)$$
$$y(t) = C_i(t)x(t)$$

Parallel distributed compensation (PDC) is proposed based on the Takagi-Sugeno (TS) fuzzy model:

$$u(t) = -\sum_{i=1}^{r} h_i(z(t))K_i x_i$$

where r is the number of IF-THEN rules, and $z_i(t)$ is the premise variable. Other controller design techniques can be seen in [9][10][11]

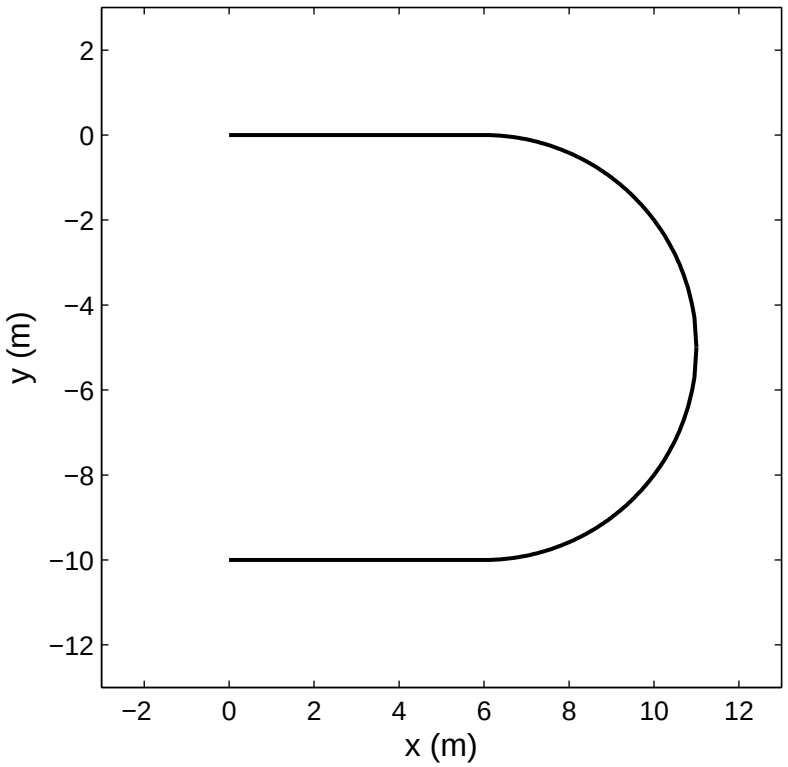

Figure 1.2: An example of a space-based path

1.2 Type of reference paths

Basically, there are two kinds of reference path: space-based path and time-based path. Space-based path is defined in the space, and usually doesn't depend on the time, while the desired path is defined specifically as a function of time. Fig. 1.2 shows an example of space-based reference path with U shape, and Fig. 1.3 shows an example of time-based reference path with the following differential equations:

$$\dot{x}(t) = t$$

$$\dot{y}(t) = 2\sin t$$

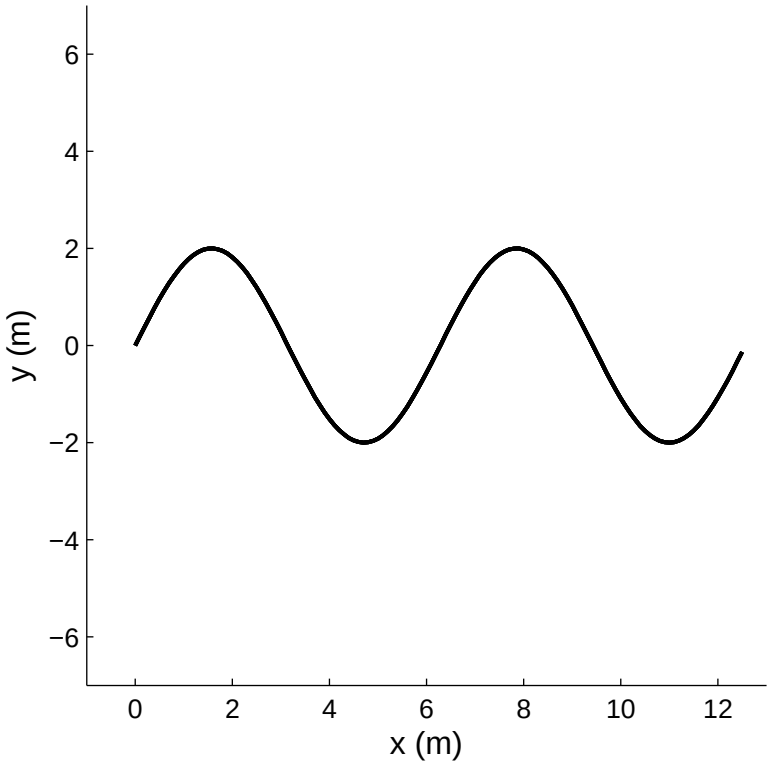

Figure 1.3: An example of a time-based path

The main difference is that in the case of time-based reference path, the desired position at each moment can be clearly expressed but it's not true in the case of space-based path. In this dissertation, the space-based path is selected to be the reference. Fig. 1.4 shows a straight path in global coordinates and local coordinates. Local coordinates x and y are defined based on the reference path and the vehicle position. Actually, the vehicle would be on the reference path as long as the lateral position error along the y axis is equal to zero. Therefore, the lateral position is much more important than the longitudinal position for path following.

1.3 The research focus

Even though a large amount of research has been done to stabilize the system, there are still some challenges remaining to be solved. First, the tracking error near the intersections

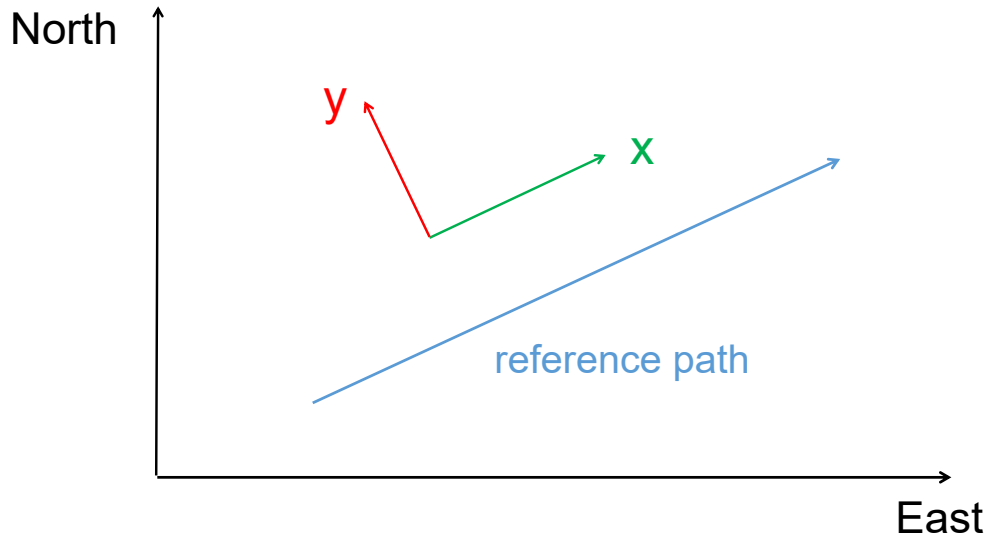

Figure 1.4: Reference path in global coordinate and local coordinates

of two different reference paths are usually very large. Second, the linear controller, which is easy to implement, may fail to make the trailer follow the reference when the position error is large. Last, the tracking error is difficult to remove for curved reference path. Besides, the steady-state error exists when there is a bias in the measurement.

All the variables, including the positions and heading angles of tractor and trailer, should be measurable to make the controller work well. To implement this, one solution is to use two sets of Global Navigation Satellite System/Inertial Navigation System (GNSS/INS) with real-time kinematic (RTK) corrections placed on tractor and trailer. The measurements are very accurate. The position error can be less than 1 centimeter [12]. However, the implement cost becomes very high. Instead, an encoder can be used to measure the hitch angle, the angle difference between the tractor bearing and trailer bearing. Thus, the tractor bearing can be calculated rather than measured, as well as the positions of the tractor. But the sensor is often fragile and the signal from the encoder is usually very noisy.

1.4 Overview of the contributions

In the following chapters, the solutions to the challenges mentioned above are proposed. In Chapter 2, the kinematic and dynamic model of a general tractor-trailer system is deduced and compared. In Chapter 3, two methods are introduced to reduce the trailer position error near the intersections of two different reference paths. One method is based on a coordinate transformation strategy which is properly selected. The other is based on model predictive control [13]. Then an alternate controller used when the vehicle is far away from the reference is designed to stabilize the system [14]. In Chapter 4, methods to remove the tracking error for curved reference path and with the present of sensor bias are given [15]. In Chapter 5, a state observer based on an adaptive unscented Kalman filter is proposed to overcome the changes of road condition and disturbances [16]. Conclusions and future work are given in Chapter 6.

Chapter 2

Modeling of a Tractor-trailer System

Many controllers are designed based on a mathematic model. Therefore, the model is critical to the closed-loop system for both transient and steady-state behaviors. In this chapter, two models for a tractor-trailer system are derived. First, a relatively simple kinematic model is obtained, and then a more complicated dynamic model is given.

2.1 System kinematic model

Fig. 2.1 shows the construction of a kinematic model and Table 2.1 shows the variable definitions. In a kinematic model, it's assumed that there is no lateral tire slip, which means the direction of vehicle velocity is the same as the heading of vehicle body.

From the kinematic relationships of tractor and trailer, the nonlinear kinematic model can be obtained as follows [17]:

$$\dot{\varphi}_r = \omega_r = \frac{v_r \tan\delta}{l_r} \tag{2.1}$$

$$\dot{\varphi}_t = \omega_t = \frac{v_r \sin\theta - l_h \omega_r \cos\theta}{l_t} \tag{2.2}$$

$$\dot{x}_t = v_t \cos(\varphi_t) \tag{2.3}$$

$$\dot{y}_t = v_t \sin(\varphi_t) \tag{2.4}$$

$$v_t = v_r \cos\theta + l_h \omega_r \sin\theta \tag{2.5}$$

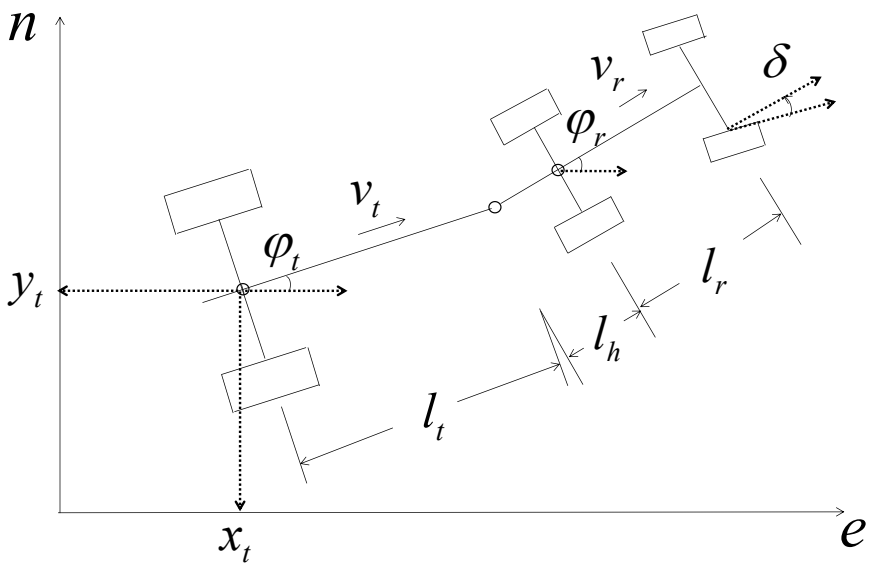

Figure 2.1: Kinematic model of a tractor-trailer system

Here x axis and y axis represent the local geographic Cartesian coordinates and variable θ is the hitch angle:

$$\theta = \varphi_r - \varphi_t$$

In (2.1), the tractor yaw rate is modeled to be linear with $\tan\delta$ [18]. In fact, equation (2.2) and (2.5) can be extended for systems with more trailers. Generally, yaw rate of trailer k is:

$$\dot{\varphi}_k = \omega_k = \frac{v_{k-1}\sin\theta_{k-1} - l_{h,k}\omega_{k-1}\cos\theta_k}{l_{t,k}} \tag{2.6}$$

where φ_k means the heading angle of the kth trailer, variable θ_{k-1} means the $(k-1)$ hitch angle, variables v_{k-1} and $l_{h,k}$ represent the velocity of the trailer $(k-1)$ and the distance between the hitch point $(k-1)$ and the center of rear wheel axle of the trailer $(k-1)$. The velocity of the trailer k is:

$$v_k = v_{k-1}\cos\theta_{k-1} + l_{h,k-1}\omega_{k-1}\sin\theta_{k-1} \tag{2.7}$$

Table 2.1: Parameters of tractor-trailer system

Variable	Description
l_r	Length from front tire of tractor to rear tire of tractor
l_h	Length from back tire of the tractor to hitch
l_t	length from hitch to the rear tire of trailer
v_r	velocity of tractor
v_t	velocity of trailer
δ	tractor steering angle
x_t	longitudinal position of trailer
y_t	lateral position of trailer

Treating the robot speed v_r as a constant and using the small angle assumption, a state-space model in $\dot{X} = AX + BU$ form can be obtained:

$$\begin{bmatrix} \dot{\varphi}_r \\ \dot{\varphi}_t \\ \dot{y}_t \end{bmatrix} = \begin{bmatrix} 0 & 0 & 0 \\ \frac{v_r}{l_t} & -\frac{v_r}{l_t} & 0 \\ 0 & v_r & 0 \end{bmatrix} \begin{bmatrix} \varphi_r \\ \varphi_t \\ y_t \end{bmatrix} + \begin{bmatrix} \frac{v_r}{l_r} \\ -\frac{l_h v_r}{l_r l_t} \\ 0 \end{bmatrix} \delta \tag{2.8}$$

The state vector contains tractor heading angle, trailer heading angle, and the trailer lateral position. The longitudinal position x_t disappears because we focus on the lateral position control, and the other three variables have no relation to variable x_t.

2.1.1 On-axle vs. Off-axle hitching models

There are two kinds of connection between a tractor and a trailer: on-axle hitching (shown in Fig. 2.2) and off-axle hitching (shown in Fig. 2.3). In an on-axle hitching system, the trailer is directly connected to the center of tractor rear wheel axle, while there exists a distance l_h between the joint point and the tractor rear axle. In the linearized kinematic model, an off-axle hitching system has an additional right-half plane zero at $z = \frac{v}{l_h}$, resulting in an opposite motion of trailer with respect to the tractor yaw rate at the beginning of a new command.

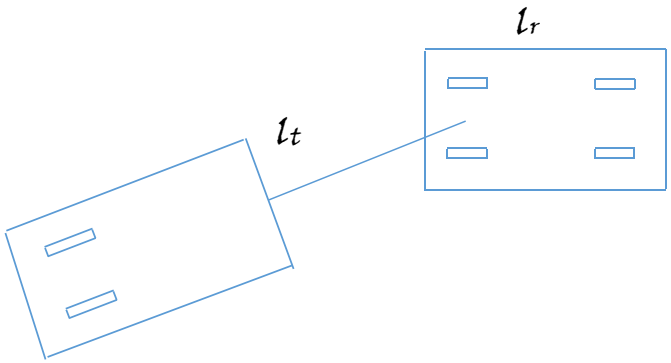

Figure 2.2: On-axle hitching system

2.1.2 Comparison of on-axle and off-axle transient response

Fig. 2.4 shows a step response of trailer heading. The input is tractor yaw rate with a magnitude of 0.5. The lateral position first becomes negative, then has a positive value which corresponds to the direction the tractor guides to after about 1.5 seconds. Therefore, the tracking error for a tractor-trailer system with off-axle hitching is usually larger than that for on-axle hitching system. Besides, The right-half plane zero also prohibits the use of high gain feedback control.

2.2 System dynamic model

A dynamic model considers lateral forces and side slip for both tractor and trailer. Variables used in a dynamic model are shown in Table 2.2. A difficulty to model the tractor-trailer system is the force at the hitch. The trailer is regarded as a third axle behind the tractor and the force at the hitch is modeled as an additional tire [19]. It's not accurate since the trailer dynamic is not considered. A force analysis using "Bicycle" approach deduced from Newton's law is studied in [20]. However, the position and velocity of tractor rather than the trailer are addressed. For the trailer dynamic analysis, the model and a linearized

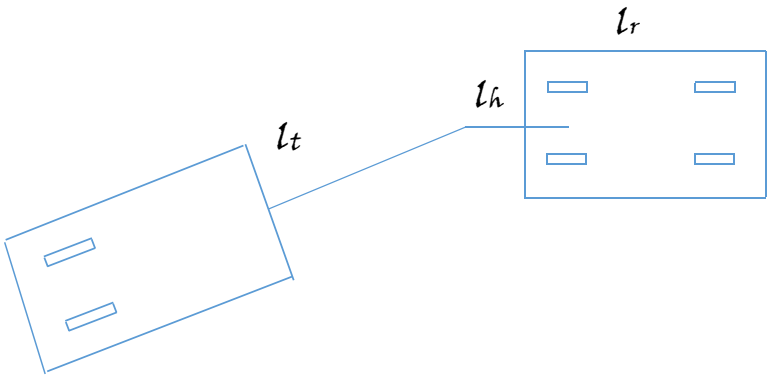

Figure 2.3: Off-axle hitching system

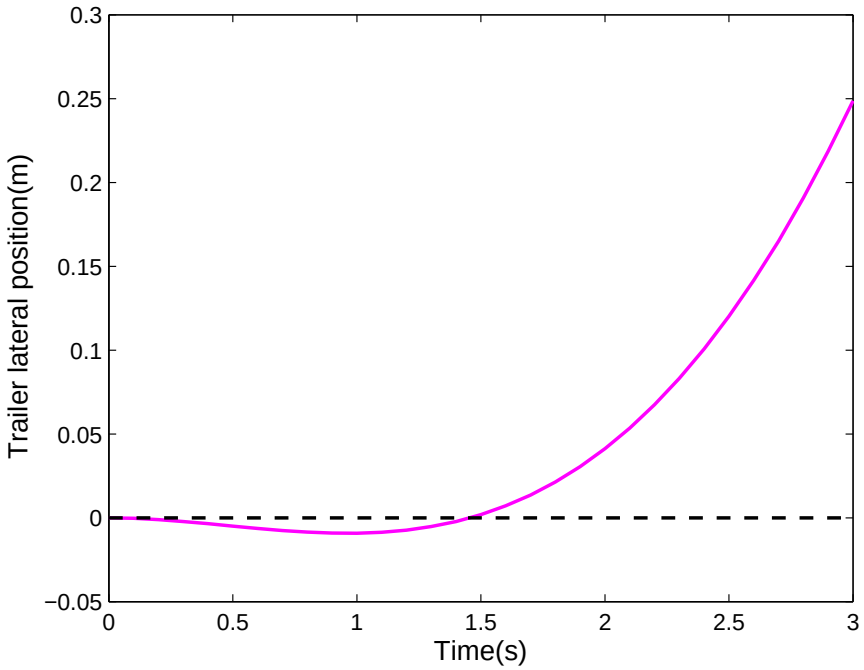

Figure 2.4: Step response of off-axle hitched trailer lateral position using tractor yaw rate as input, showing initial change in the negative direction

Table 2.2: Parameters of dynamic model for tractor-trailer system

Variable	Description
C_f^r	Cornering stiffness of tractor front tire
C_r^r	Cornering stiffness of tractor rear tire
C_r^t	Cornering stiffness of trailer rear tire
m_r	Mass of tractor
m_t	Mass of trailer
α_r^f	side slip angle of tractor front tire
α_r^r	side slip angle of tractor rear tire
α_t	side slip angle of trailer rear tire
v_c^r	Lateral velocity of tractor
v_c^t	Lateral velocity of trailer
a	Length from tractor front tire to CG
b	Length from tractor CG to rear tire
c	Length from rear tire to hitch
d	Length from hitch to CG of trailer
e	Length from CG of trailer to rear tire
I_z^r	Tractor yaw moment of inertia
I_z^t	Trailer yaw moment of inertia
σ_f	Relaxation length of tractor front tire
σ_r	Relaxation length of tractor rear tire
σ_t	Relaxation length of trailer rear tire

dynamic model are derived below in which the lateral velocity and position of trailer are used as state variables.

Using Newton's Law, the following two equations can be applied for both tractor and trailer:

$$F_y = m\dot{v}_y \tag{2.9}$$

$$M_z = I_z\dot{\omega} \tag{2.10}$$

where F_y is the lateral force, M_z is the moment about the center of gravity (CG), and v_y is the lateral velocity. Fig. 2.5 shows the forces on the vehicles. The two equations above can

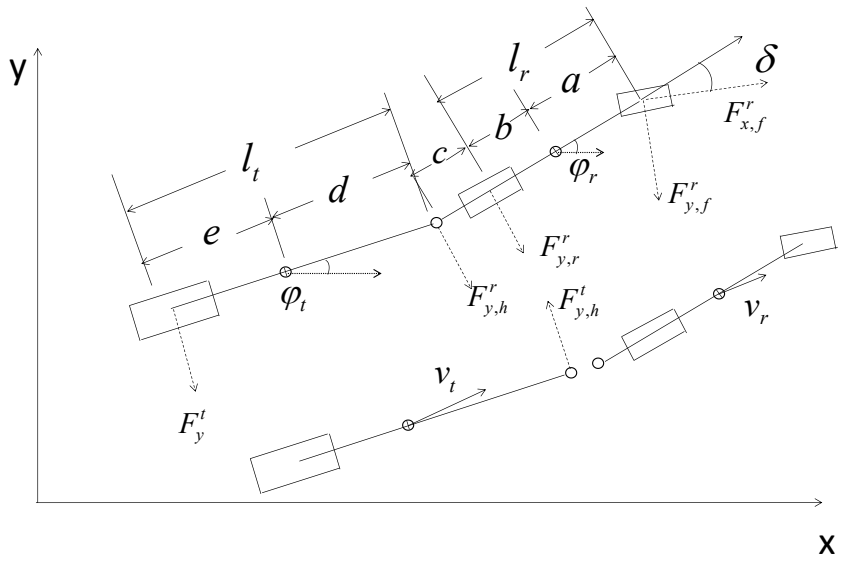

Figure 2.5: Dynamic model of the tractor-trailer system

be extended as follows:

$$m_r \dot{v}_c^r = F_{x,f}^r \sin\delta + F_{y,f}^r \cos\delta + F_{y,r}^r + F_{y,h}^r \tag{2.11}$$

$$I_z^r \dot{\omega}_r = a(F_{x,f}^r \sin\delta + F_{y,f}^r \cos\delta) - bF_{y,r}^r - cF_{y,h}^r \tag{2.12}$$

$$m_i(\dot{v}_c^t + v_x^t \omega_t) = F_{y,h}^t + F_y^t \tag{2.13}$$

$$I_z^t \dot{\omega}_t = dF_{y,h}^t - eF_y^t \tag{2.14}$$

Using a linear tire model, which is valid for small side slip angles, the lateral forces on front tire of tractor, rear tire of tractor, and rear tire of trailer can be obtained by:

$$F_{y,f}^r = -C_f^r \alpha_r^f = -C_f^r(\frac{v_c^r + a\omega_r}{v_x^r} - \delta) \tag{2.15}$$

$$F_{y,r}^r = -C_r^r \alpha_r^r = -C_r^r \frac{v_c^r - b\omega_r}{v_x^r} \tag{2.16}$$

$$F_r^t = -C_r^t \alpha_r^t = -C_r^t \frac{v_c^t - e\omega_t}{v_x^t} \tag{2.17}$$

Moreover, the relationship between $F^r_{y,h}$ and $F^t_{y,h}$ is:

$$F^r_{y,h} = -F^t_{y,h}\cos\theta + F^r_{x,h}\sin\theta \tag{2.18}$$

Thus, the lateral force at the hitch for trailer and tractor $F^t_{y,h}$ and $F^r_{y,h}$ can be calculated from (2.13) and (2.18). The lateral velocity of trailer's center of gravity is:

$$v^t_c = v^r_x\sin\theta + (v^r_c - c\omega_r)\cos\theta - d\omega_t \tag{2.19}$$

Then the system dynamic can be represented by equations (2.11), (2.12) and (2.14) with the linear tire model (2.15)-(2.17) and the equation on velocity (2.19). With small angle assumption, a linearized sixth-order state-space model can be derived:

$$M\dot{x} = Nx + P\delta \tag{2.20}$$

where

$$M = \begin{bmatrix} m_r + m_t & m_t(b+c) & dm_t & 0 & 0 & 0 \\ -m_t(b+c) & I^r_z & 0 & 0 & 0 & 0 \\ -m_t d & 0 & I^t_z & 0 & 0 & 0 \\ 0 & 0 & 0 & 1 & 0 & 0 \\ 0 & 0 & 0 & 0 & 1 & 0 \\ 0 & 0 & 0 & 0 & 0 & 1 \end{bmatrix}$$

$$P = \begin{bmatrix} C^r_f & aC^r_f & 0 & 0 & 0 & 0 \end{bmatrix}^T$$

$$x = \begin{bmatrix} v^t_c & \omega_r & \omega_t & y_t & \varphi_r & \varphi_t \end{bmatrix}^T$$

Define n_{ij} as the element in ith row and the jth column of N matrix, then: $N=$

$$\begin{bmatrix} n_{11} & n_{12} & n_{13} & 0 & n_{15} & n_{16} \\ n_{21} & n_{22} & n_{23} & 0 & n_{25} & n_{26} \\ n_{31} & 0 & n_{33} & 0 & 0 & 0 \\ 1 & 0 & 0 & 0 & 0 & v_x^r \\ 0 & 1 & 0 & 0 & 0 & 0 \\ 0 & 0 & 1 & 0 & 0 & 0 \end{bmatrix}$$

The details of n_{ij} are given in the appendix.

2.3 Comparison between kinematic model and dynamic model

A third-order kinematic model and a sixth-order dynamic model are derived. It turns out that three variables in the dynamic model are the same as the variables in the kinematic model: tractor heading angle, trailer heading angle and trailer lateral position. The other three variables are higher-order terms of the variables mentioned above respectively, which are the yaw rate of tractor, yaw rate of trailer and the trailer lateral velocity.

If the parameters in both models are accurate, the dynamic model has less modeling error than the kinematic model because it takes the high-order behaviors into account. Next, the open-loop eigenvalues of linearized models, which determine the main dynamic of the system, are checked and compared to see when the high-order variables are necessary. The data shown in Table 2.3 are from a Kubota RTV [21]. In the kinematic model, variable l_h is same as c in the dynamic model, and l_r, l_t are equal to:

$$l_r = a + b$$

$$l_t = d + e$$

Table 2.3: Parameter values for a tractor-trailer system

Variable	Value
C_f^r	45000 N/rad
C_r^r	45000 N/rad
C_r^t	4000 N/rad
m_r	900 kg
m_t	50 kg
a	0.75 m
b	1.21 m
c	0.53 m
d	3 m
e	1 m
v_r	1m/s
I_z^r	810 kg$\cdot m^2$
I_z^t	150 kg$\cdot m^2$

When the parameters in the table are determined, the only variable that can changes the open-loop poles is the tractor velocity. Table 2.4 shows the non-zero poles closest and second closest to the imaginary axis with the change of tractor velocity from 0.5 m/s to 10 m/s:

Table 2.4: Nonzero pole locations of kinematic model and dynamic model

tractor velocity	closest nonzero pole imaginary axis in kinematic model	closest nonzero pole to to imaginary axis in dynamic model	second-closest nonzero pole to imaginary axis in dynamic model
0.5m/s	-0.125	-0.125	-162.476
1m/s	-0.25	-0.251	-81.626
2m/s	-0.5	-0.505	-41.629
3m/s	-0.75	-0.766	-28.779
4m/s	-1	-1.041	-23.017
5m/s	-1.25	-1.333	-20
6m/s	-1.5	-1.654	-16.124
10m/s	-2.5	-4	-6.667

It can be seen that when the tractor velocity is small (less than 5m/s), the closest nonzero poles in the two models are quite similar. Furthermore, the other poles are much

far away. Therefore, the kinematic model can represent the system as well as the dynamic model. When the tractor velocity gets higher, the difference between the dominant poles in two models becomes larger, and the other poles are closer to the dominant pole. Especially when the velocity is 10 m/s or higher, the closest non-zero pole to the imaginary axis in dynamic model is no longer dominant. In this case, the kinematic model is insufficient.

2.4 Summary

In the kinematic model, the geometrical information of tractor and trailer are measured and used, namely the length of tractor, the length between the rear wheel axle of tractor to hitch point, and the length of trailer. These variables are easy to measure and the measurements of the length can be very accurate. In the dynamic model, the geometrical variables are needed as well as the moment of inertia and cornering stiffness which are difficult to measure. Sometimes engineers can only estimate these variables. As a result, even though the dynamic model is more complicate, the parameters in the model may be not accurate.

When the tractor velocity is small, the higher-order dynamic vanishes very fast, and the simpler kinematic model is sufficient to describe the system. The following work of controller and estimator design is based on the kinematic model. When the tractor moves faster, the higher-order terms should not be ignored and the dynamic model is suggested to be used instead. In the next chapter, the controllers for trailer near the intersections of different reference paths and far from the reference path are introduced.

Chapter 3

Controller Design for Trailer Near the Intersections and Far From the Reference

Reference paths are often compositions of straight lines and arc segments. Both linear state feedback and nonlinear approaches can make the trailer track a straight line very well [22] [7]. For time-based curved reference, tracking error can be clearly defined, and control law is able to drive the trailer match the desired yaw rate [10]. Basically, a controller can be designed to do the path following for one type of reference path, either straight lines or arc segments. However, there are few researches on the system performance in the region where two different segments join. The tracking error following one type of reference path can be small, but the error near the intersections is usually large because the controller is often designed for a fixed curvature, which is not suitable for the path near the joining point. In this chapter, methods to reduce the tracking error near the joint point of two reference paths are proposed, which are ignored by most of other researchers.

Another challenge for path following is that the system might be unstable when initial error is large under a linear control law. In other words, the stability is not guaranteed using linear methods when the vehicle is far from the reference because the system is nonlinear. This problem also exists in the control of a single robot. Nonlinear control with input saturation may solve the problem [23] [24]. It's realized that the system transient performance using linear state feedback is very satisfactory. Nonlinear controller can solve the stability problem, but the transient behavior, represented by overshoot and settle time, may get worse. Some nonlinear controllers are difficult to design, e.g. feedback linearization. In this chapter, a simple, alternate control strategy is given to drive the tractor-trailer system to the reference when the vehicle is initially far from the desired path. The original controller is

only used when the vehicle is close to the reference to have less overshoot and shorter settle time.

3.1 Modification of the kinematic model

In Chapter 2, a linearized kinematic model of a tractor-trailer system is given by (2.8). The system input is the tractor steering angle. When a new control command is provided, it's assumed that the new control effort can be implemented instantly. However, it's not realistic because the steering rate of the tractor can't be infinite. So the steering dynamic should be considered. The tractor steering dynamic can be modeled as a first-order process[25]:

$$\dot{\delta}_r = -d^v \delta_r + K^v u \tag{3.1}$$

where δ_r is the actual steering angle, d^v is the damping constant, K^v is the input gain, and u is control input. Using δ_r as an additional state variable, the augmented linear model of a tractor-trailer system can be describe as:

$$\begin{bmatrix} \dot{\varphi}_r \\ \dot{\varphi}_t \\ \dot{y}_t \\ \dot{\delta}_r \end{bmatrix} = \begin{bmatrix} 0 & 0 & 0 & \frac{v_r}{l_r} \\ \frac{v_r}{l_t} & -\frac{v_r}{l_t} & 0 & -\frac{l_h v_r}{l_r l_t} \\ 0 & v_r & 0 & 0 \\ 0 & 0 & 0 & -d^v \end{bmatrix} \begin{bmatrix} \varphi_r \\ \varphi_t \\ y_t \\ \delta_r \end{bmatrix} + \begin{bmatrix} 0 \\ 0 \\ 0 \\ K^v \end{bmatrix} u \tag{3.2}$$

The state-space model becomes a fourth-order model. In the following part of this chapter, the new model is used.

3.2 Controllers to reduce the error near the intersections

The reference path is usually defined in the global coordinate. In the controller, however, a local coordinate should be used to define the error state. Fig. 3.1 shows a common way to define the tracking error for heading angles and lateral position. For curved reference path,

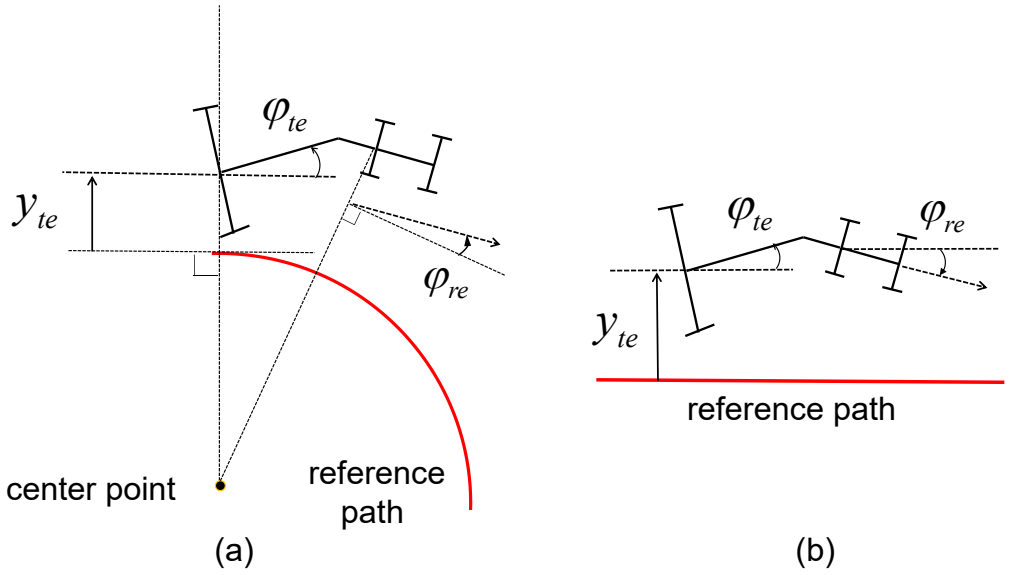

Figure 3.1: State error definitions: (a) curved reference path, (b) straight reference path

the desired heading angles are decided by the positions of tractor and trailer, and the center point of the curve. It can be found that the desired heading angles for tractor and trailer are different. The trailer lateral position error is defined as the nearest distance between the center of trailer rear axle and the reference path. For the straight reference path, the desired heading angles for tractor and trailer are same. Next, two methods to reduce the tracking error near the intersections are given.

3.2.1 Controller using new coordinate transformation strategy

Using the above local coordinate produces large tracking error when the path types change. Fig. 3.2 shows system performance to track a U-shape path using the local coordinate above and linear state feedback. Point 1 and point 2 are two intersection points from line to curve and from curve to line, respectively. The trailer path drawn in blue deviates from desired path at both two points.

It can be also found in Fig. 3.2 that the trailer begins to turn right too early, resulting in the path inside the desired circle path. The reason is shown in Fig. 3.3. At this moment, the

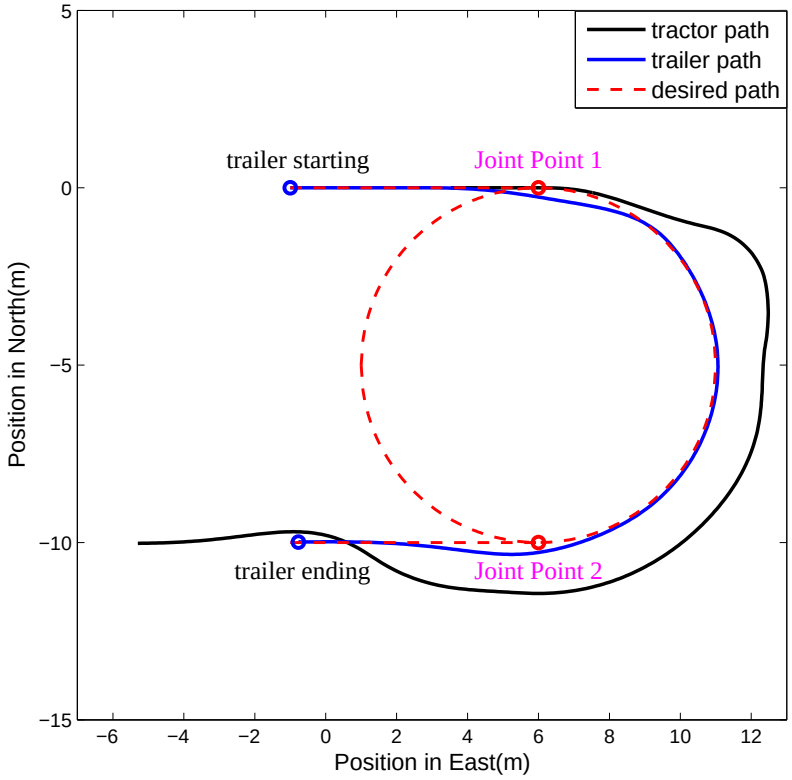

Figure 3.2: System performance tracking U-shape path using present linear state-of-the-art approach

tractor is just at the intersection point P_1 and the trailer is at point A. From the next time instant, since the the desired path of tractor changes from line to curve, the desired bearing of tractor would be different from that of trailer, and the tractor would drive the system to turn in clockwise. As a result, the trailer starts to turn before it reaches the intersection point. So the key point is that the tractor and trailer have different reference paths and different type of local coordinates. This phenomenon only happens when the system is near the joining point.

A local coordinate definition considering both the positions of tractor and trailer seems to be a solution to reduce the tracking error. If the coordinate of the trailer is designed to be always the same with the trailer, unfortunately, the error would be still large because the trailer path in Fig. 3.3 would be outside the desired circle path, and the system performance

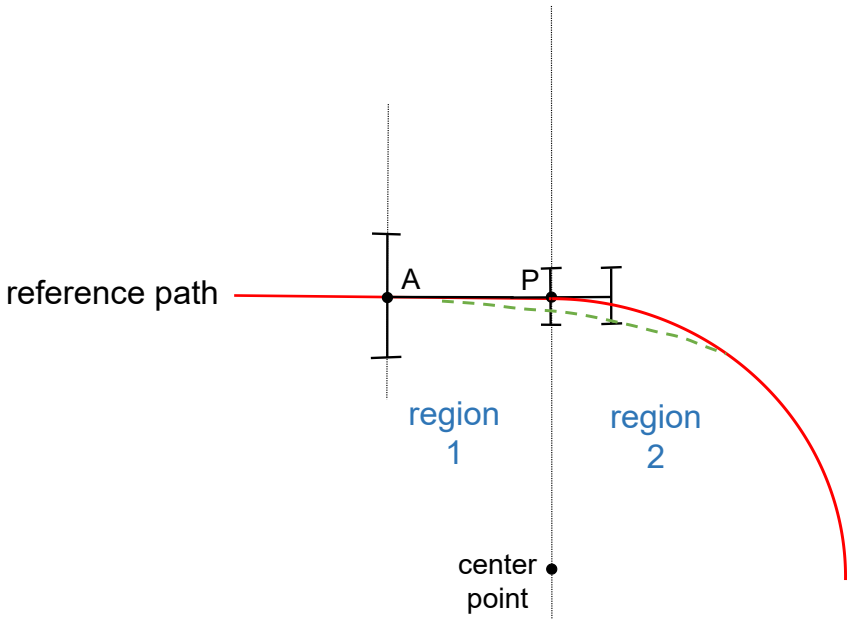

Figure 3.3: The tractor and trailer are located in different regions

under this strategy is shown in Fig. 3.4. The tractor begins to turn too late actually. The large tracking error can't be smaller even with nonlinear control algorithms as long as the local coordinate above is used. Furthermore, tuning the control gains can't obtain better results either.

From the analysis, it can be realized that using the existing coordinate transformation strategy makes the trailer yaw rate mismatch the yaw rate of reference path because the system changes the heading angle either too early or too late. The tracking error near the intersection may become smaller if an appropriate moment that tractor begins to apply coordinate for new reference path can be chosen correctly [14]. In the case of Fig. 3.3, point A and point P are trailer positions without tracking error using two strategies mentioned above. Neither of two points are suitable to indicate when the tractor begins to use new type of local coordinate for region 2. A better selection can be located between these two points. In other words, the new strategy considers the tractor and trailer together instead of defining local coordinate based on positions of tractor and trailer individually. Variable D indicates the distance between the trailer position and the joint point. A threshold of D

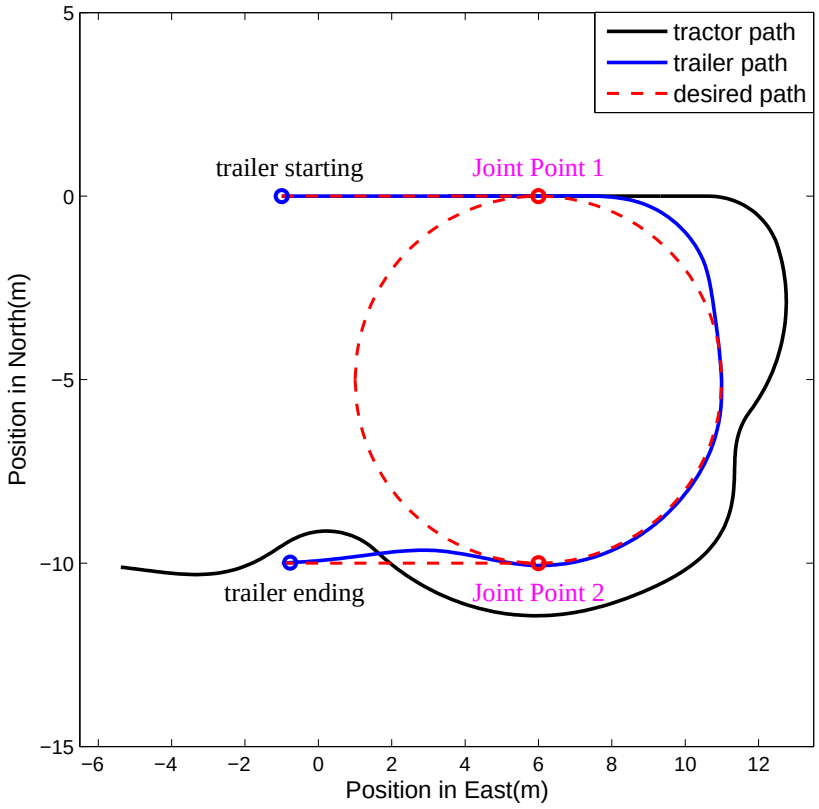

Figure 3.4: The system performance tracking U-shape path when tractor and trailer use same type of local coordinate

can be defined which is in the range of:

$$D_{th} \in [0, l_h + l_t]$$

As shown in Fig. 3.5(a), if the distance of between trailer position to joint point P is larger than D_{th}, the coordinate definition for straight line in region 1 is still use for the tractor, even though the tractor is already located in region 2. In other words, the tractor should track the extension line of the previous reference path. When the distance is equal or smaller than D_{th} (shown in Fig. 3.5(b)), the new type of local coordinate, which is for the curved path in region 2, is applied for the tractor.

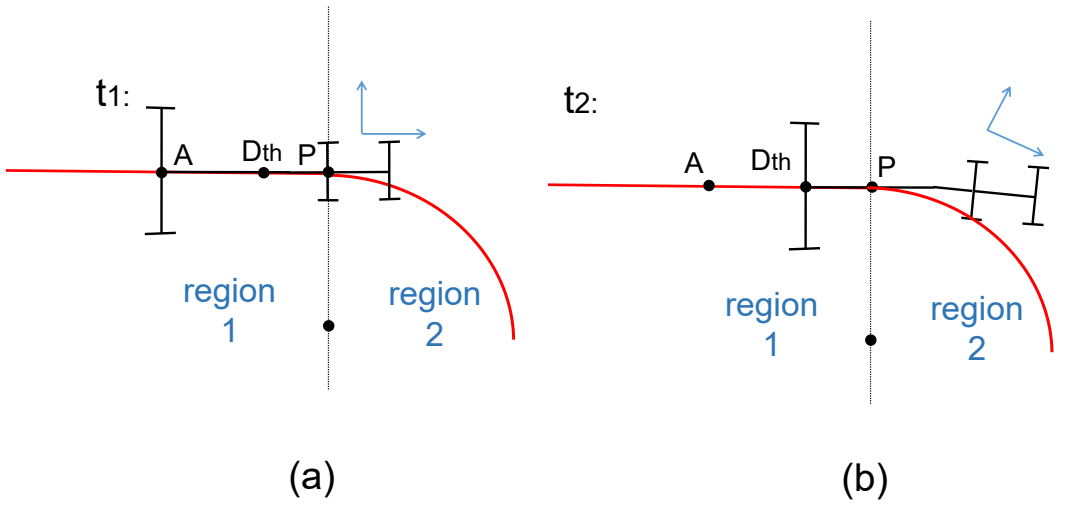

Figure 3.5: The new coordinate transformation strategy when reference path changes from line to curve

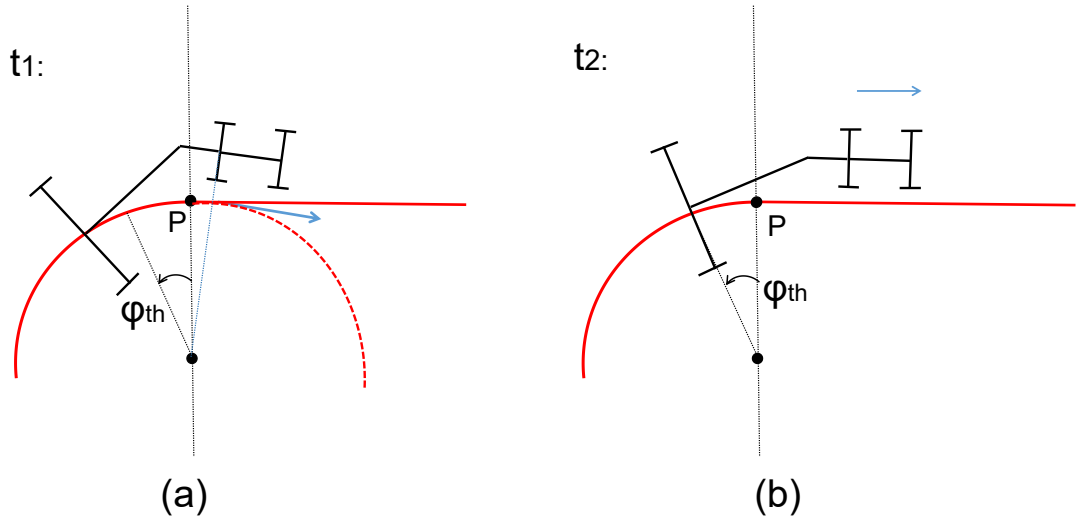

Figure 3.6: The new coordinate transformation strategy when reference changes from a curve

If the reference changes from a curved path, a threshold of angle φ_{th} rather than distance is defined. In Fig. 3.6, coordinate for the curved path is still used for the tractor from time t_1 to time t_2, until the trailer arrives at the setting angle φ_{th} (the moment shown in Fig. 3.6(b)).

The value of D_{th} or φ_{th} for each intersection can be determined by computer simulation with the assumption that there is no tracking error when the tractor arrives at the joint point. In other words, the location of each setting point is decided before the implementation without initial error and disturbances. The assumption of zero initial error is valid if the steady-state error for tracking straight and curved reference paths under a proper control law can be removed. The L_2 norm of trailer position error near the intersection, which is equal to $\sqrt{\sum error_i^2}$, is used to evaluate the system performance. Fig. 3.7 shows how this value changes with respect to the location of setting point for the case of reference from line to curve in Fig. 3.5. The vertical axis represents the L_2 norm of trailer lateral position error during the period before and after the intersection point P for three second respectively. Horizontal axis is the distance from the point A which is located at the reference path with a distance of $l_h + l_t$ from point P. It can be seen that the smallest L_2 norm of tracking error is 0.108, and this is obtained when the setting point is located at 3 meter from point A. As the comparison, if the tractor begins to apply new local coordinate when the trailer is at point A or point P, the L_2 norm of tracking error will be 1.627 and 1.592 respectively, which are much larger than the minimum.

The threshold of distance or angle mainly depends on the length of $l_h + l_t$ and how much the curvature changes. If the change of curvature between two reference path is larger, the setting point would be further to the joint point. Fig. 3.8 shows how the setting point changes with the curvature of region 2 in the case of Fig. 3.5. The setting point location for curvature change of $\frac{1}{7}$ is at 1.5 meter from the intersection point with error in L_2 norm of 0.072, while it's 1.75 meter for curvature change of $\frac{1}{4}$ with error in L_2 norm of 0.147.

In summary, the location of each setting point is pre-defined, and the calculation process can be easily computed in advance.

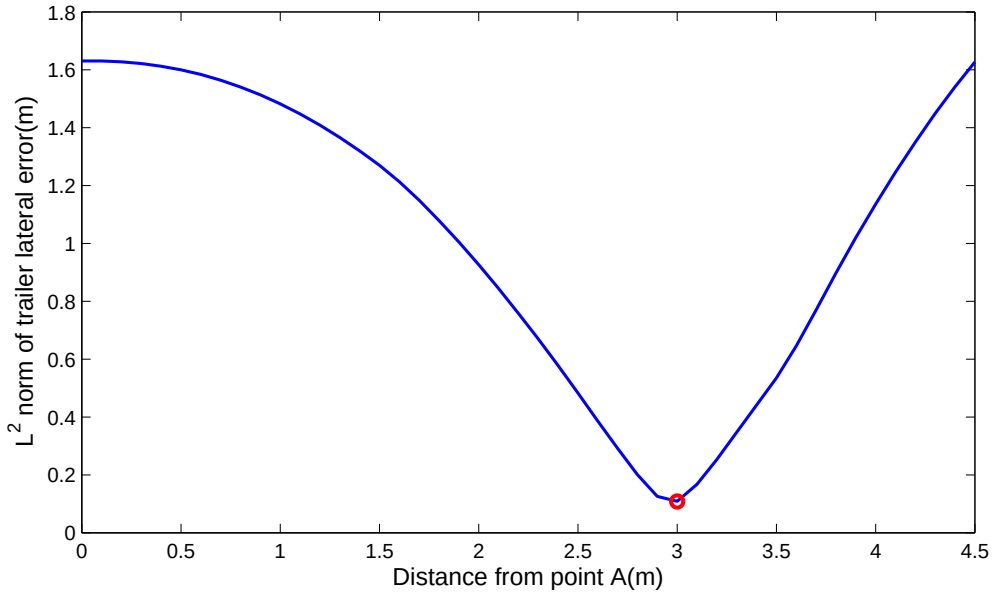

Figure 3.7: L_2 norm of tracking error with respect to different setting point location for Fig. 3.5

3.2.2 Model predictive control

In the last subsection, the method based on a new local coordinate transformation strategy is introduced to reduce the trailer tracking error near the intersections. Next, a straight-forward approach based on model predictive control (MPC) will be given.

The difficulty of obtaining a small tracking error near the intersection is that the system isn't under steady-state in this case. There is a transient process between two reference paths with different curvature. In other words, the curvature at the intersection is not continuous. Traditional methods just use the current state value and don't know how the reference path in the following steps will change. As a result, when the trailer just passes the intersection, the slow yaw rate can't match the desired one.

If the controller has the information of the following reference path, it is likely to output the proper control effort to track the path accurately. One can image the situation when a human driver makes a turn. The driver knows the paths in front of the car and turns the steering wheel to make the car move along the arc. Model predictive control can implement

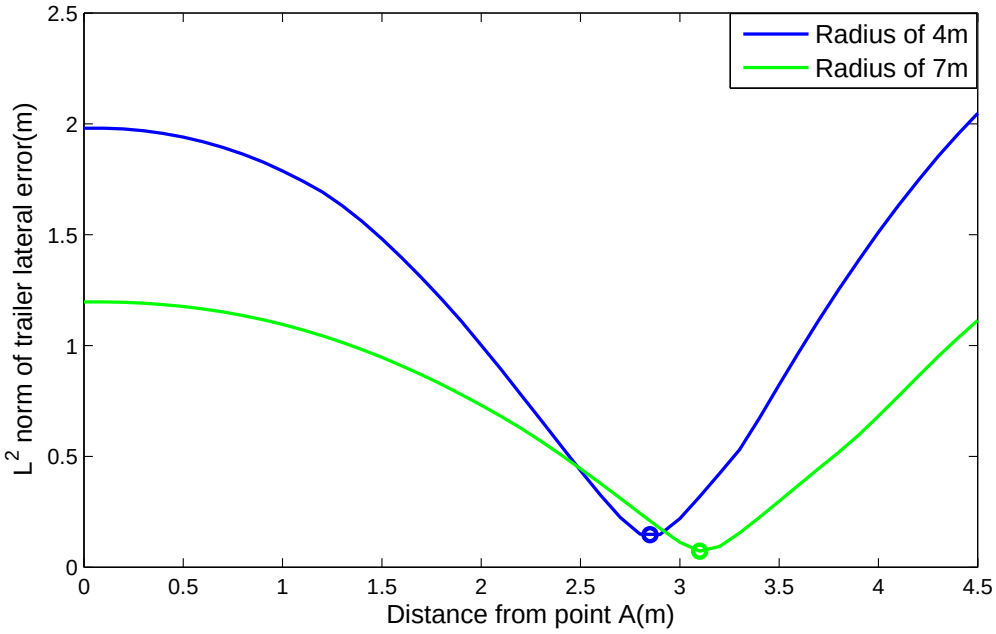

Figure 3.8: L_2 norm of tracking error with respect to different setting point location for different curvatures

this idea. With the development of computer technology, MPC becomes an alternative way to design a control law, especially for path tracking problem [21] [26]. MPC is an optimal controller minimizing a cost function, which considers the system error and control effort in a prediction horizon N_p.:

$$J = \sum_{k=1}^{N_p} [(y(k) - r(k))^T Q(y(k) - r(k)) + u(k)^T R u(k)] \tag{3.3}$$

where $y(k)$ is the system output, variable $r(k)$ is reference signal, variable $u(k)$ is control effort. Parameters Q and R are positive definite and weight the output error and control effort, respectively. The algorithm predicts the system output in the next N_p steps using a mathematical model, and then obtains the solution of u by minimizing J so that the tracking error can be optimized [27]:

$$u = [u(k), u(k+1), u(k+2) \cdots u(k+N_c)]^T \tag{3.4}$$

where N_c is control horizon, and $N_c \leq N_p$. The first element of u is applied only to the system. At the next time instant, the same procedure is done in a moving horizon manner.

It can be seen that MPC is very suitable for reducing the error where different reference paths join, which is a difficult problem for some other algorithms, such as linear quadratic regulator (LQR) or sliding mode control (SMC). Generally speaking, MPC can solve the following constrained optimal problem [28]:

$$\min_{u} J(x, u, r) \tag{3.5}$$

subject to

$$\begin{aligned} x_{k+n+1} &= f(x_{k+n}, u_{k+n}) \\ y_{k+n} &= h(x_{k+n}) \\ u_{min} &\leq u_{k+n} \leq u_{max} \\ y_{min} &\leq y_{k+n} \leq y_{max} \end{aligned} \tag{3.6}$$

where $n = 1, 2 \ldots N_p$. If the function f is nonlinear, it's a nonlinear model predictive controller (NMPC). The amount of computation of solving NMPC is very large because there is no closed-loop form solution and the control input must be calculated iteratively using numerical optimization. The computation burden is difficult to reduce. A spare control law may be still needed when NMPC fails to obtain the solution [29]. To avoid these drawbacks, a linear MPC approach is applied in this dissertation.

Using the approximation: $\sin(x) = x$ and the steering dynamic (3.1), the model (2.1)-(2.5) can be linearized as follows:

$$\begin{bmatrix} \dot{\varphi}_r \\ \dot{\varphi}_t \\ \dot{y}_t \\ \dot{\delta}_r \end{bmatrix} = \begin{bmatrix} 0 & 0 & 0 & \frac{v_r}{l_r} \\ \frac{v_r}{l_t} & -\frac{v_r}{l_t} & 0 & -\frac{l_h v_r}{l_r l_t}\cos\theta(t) \\ 0 & v_t(t) & 0 & 0 \\ 0 & 0 & 0 & -d^v \end{bmatrix} \begin{bmatrix} \varphi_r \\ \varphi_t \\ y_t \\ \delta_r \end{bmatrix} + \begin{bmatrix} 0 \\ 0 \\ 0 \\ K^v \end{bmatrix} u \tag{3.7}$$

Notice that there are two differences between (3.7) and (3.2). One is that the cosine term in the original nonlinear model is kept instead of being approximated by 1, because the approximation error of cosine term is much larger than the approximation of sine term. The other is that the trailer velocity is also kept instead of being approximated by the tractor velocity. In fact, the model (3.2) assumes that the hitch angle is always zero. But it's not true when the trailer tracks a curve.

The model (3.7) is time-varying and therefore it can't be used directly as the prediction model for MPC. In other words, the time-varying terms should be fixed during the prediction horizon. There are two ways to implement this. One is to use current value of time-varying terms so that the system matrix becomes linear time-invariant (LTI). In this case, the model can be expressed as:

$$x_{k+1} = A(k)x(k) + Bu(k) \tag{3.8}$$

Some research on MPC uses this approach and call it "Linear time varying MPC"(LTV-MPC) [30] [31]. Another method to make the system matrix linear-time-invariant is to use values under steady state of time-varying terms. Since the control objective is the trailer position, the steady state values with respect to the trailer reference path is used in the model. The model can be revised as:

$$x_{k+1} = A_{ss,k}x(k) + Bu(k) \tag{3.9}$$

where $A_{ss,k}$ contains the terms of $\cos\theta_{ss}$ and v_{tss}, which represent the steady-state value of hitch angle and trailer velocity respectively.

When the trailer reference path is a straight line ,then

$$\begin{aligned} \theta_{ss} &= 0 \\ \omega_{ss} &= 0 \\ v_{tss} &= v_r \end{aligned} \tag{3.10}$$

When the reference path is a curve,θ_{ss} is no longer zero, but the rate of θ_{ss} is zero [32] [13], which means the tractor and tailer have same yaw rate. Furthermore, the trailer velocity is proportional to the trailer yaw rate. Therefore, two equations can be obtained:

$$\begin{aligned} \dot{\theta}_{ss} &= 0 \\ v_{tss} &= \omega_r R \end{aligned} \tag{3.11}$$

where R is the reciprocal of reference curvature. Solving the equation set (3.10), and we have:

$$\begin{aligned} \omega_{ss} &= \sigma |v_r| \frac{\sqrt{l_t^2 + R^2 - l_h^2}}{l_t^2 + R^2 - l_h^2} \\ \theta_{ss} &= -2\sigma sign(v_r) \arctan(\frac{R - \sqrt{l_t^2 + R^2 - l_h^2}}{l_t - l_h}), \quad l_t \neq l_h \\ \theta_{ss} &= 2\sigma sign(v_r) \arctan \frac{l_t}{R}, \quad l_t = l_h \end{aligned} \tag{3.12}$$

Then, the trailer velocity with a curved reference path under steady state is :

$$v_{tss} = v_r \cos\theta_{ss} + l_h \omega_{ss} \sin\theta_{ss} \tag{3.13}$$

Using the result in (3.12) and (3.13), the system matrix can be linear time-invariant. It can be found that the former method, using current measurements in the model, requires more calculation because the system matrix at each sample may be different, and needs to be calculated each time, while the latter method can restore the values under steady state only. Later it will be shown that the two modeling approach are both valid for path following of a tractor-trailer.

To predict the system output in the next step, unified local coordinates should be used for both tractor and trailer. In other words, the error states of tractor and trailer need to be defined based on trailer only, and the cost function is calculated based on the trailer local coordinate. The definition of error state when the reference path changes from line

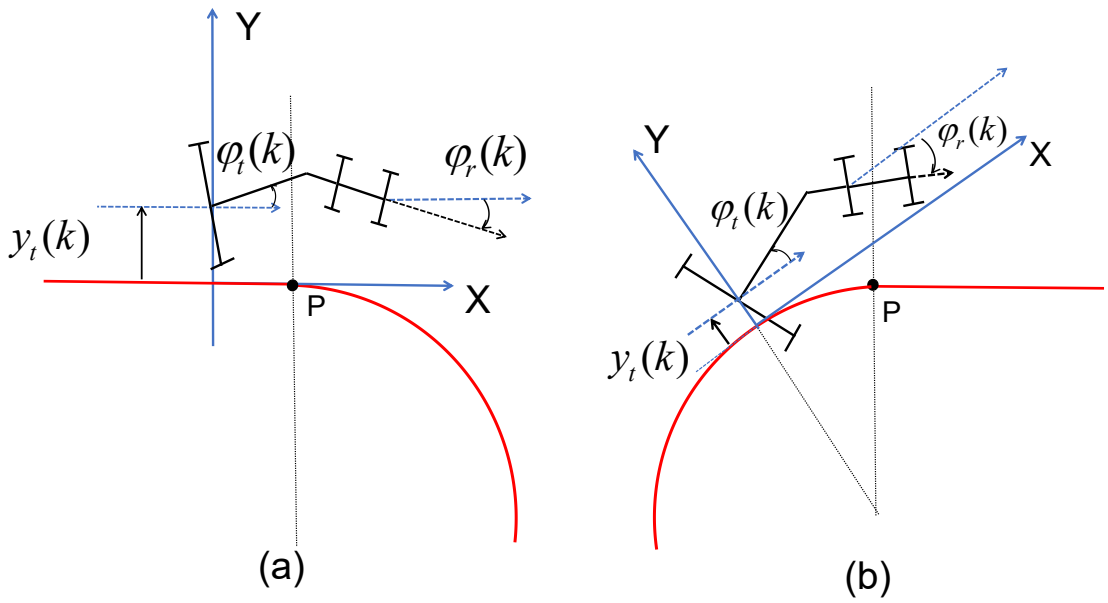

Figure 3.9: The local coordinate for MPC when reference path changes from line (a) and arc (b)

and arc are shown in Fig. 3.9 (blue line). Notice that this is different with traditional local coordinate in Fig. 3.1 and new coordinate transformation strategy in Fig. 3.5 and Fig. 3.6.

To minimize the cost function (3.3), the system output y should be selected. Obviously, the trailer lateral position should be taken as output. Additionally, the trailer heading is found to be important to the system performance, especially for the transient behavior. As a result, the output vector is:

$$y(k) = \begin{bmatrix} \varphi_t(k) \\ y_t(k) \end{bmatrix}$$

The reference signal $r(k+n)$ includes the trailer lateral position y_{td} and the trailer heading φ_{td}. The desired trailer heading is defined by the difference of the corresponding heading angle of reference position at time instant $k+n$ and the current trailer heading shown in Fig. 3.10 where the red curves represent the reference path and the blue lines with arrow represent the directions of local coordinate. When the desired position at time instant $k+1$

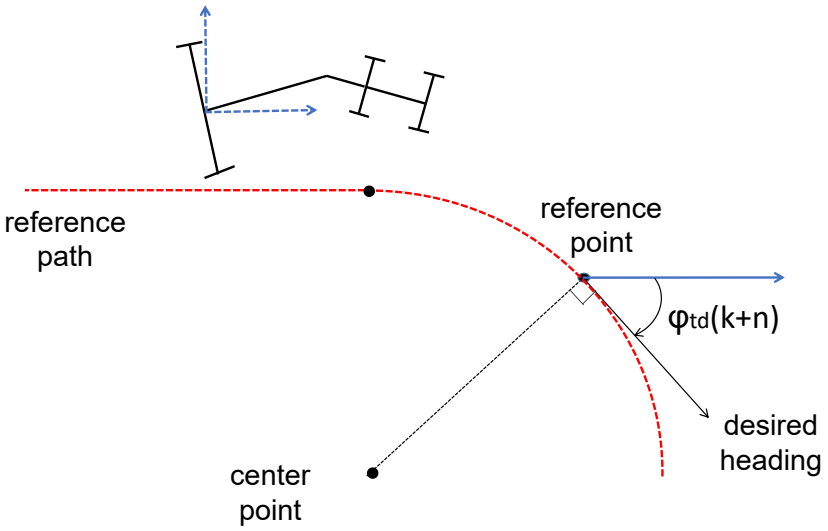

Figure 3.10: The definition of desired trailer heading

is located at a curve, the reference heading angle is:

$$\varphi_{td}(k+1) = \varphi_{td}(k) + \omega_d T \tag{3.14}$$

where T is the sampling time. Variable ω_d is the desired yaw rate and can be obtained by (3.9) and (3.11) for line and curved reference paths respectively.

In Fig. 3.10, the desired lateral position corresponding to the reference point is:

$$y_{td} = r - \cos\varphi_{td} R \tag{3.15}$$

Taking the derivative on both sides:

$$\dot{y}_{td} = \dot{\varphi}_{td} R \sin\varphi_{td} = v_{td} \sin\varphi_{td}$$

It's consistent with (2.4) that the derivative of lateral position is a function of $\sin\varphi_t$. However, the equation in the linearized model is:

$$\dot{y}_t = v_t\varphi_t$$

It can be seen that there is a linear relationship between $\dot{y}_t$ and φ_t. Since $|\sin\varphi_t| < |\varphi_t|$ for nonzero φ_t, the predicted lateral velocity in the model is always larger than the actual one if the desired trailer heading is nonzero. As a result, the tractor steering angle and tractor yaw rate would be smaller than the desired ones, and the trailer path would be outside the curved reference path.

Therefore, the reference signal of lateral position should be recalculated. As a solution, y_{td} is defined in such a way that it coincides with the linearized model. In other words, there should be a linear relationship between φ_{td} and $\dot{y}_{td}$. Therefore, the desired trailer lateral position at time instant k is:

$$y_{td,k} = y_{td,k-1} + \frac{1}{2}v_{td}(\varphi_{td,k} + \varphi_{td,k-1}) \tag{3.16}$$

Thus, at time instant k, the desired reference signal during the prediction horizon is:

$$r(k+n) = \begin{bmatrix} \varphi_{td,k+n} \\ y_{td,k+n} \end{bmatrix} \quad n = 1 \dots N_p \tag{3.17}$$

One advantage of MPC is that the system constraints can be integrated in the algorithm. The constraints at each sample are as follows:

$$\begin{aligned} u_{min} < u(k) < u_{max} \\ \theta_{min} < \theta(k) < \theta_{max} \end{aligned} \tag{3.18}$$

The first constraint is set on the control input, which is always restricted by energy or mechanics. The second constraint is set on the hitch angle. If the hitch angle is nearly 90 degree, the wheels of trailer would stop rolling and "jack-knife" phenomenon would occur, resulting in a strange path of trailer.

At each sample, the desired reference signal is calculated and the model is linearized to be linear time-invariant. The minimization of cost function can be done by quadratic programming [33]. A dual problem with Lagrange multipliers is solved instead to decrease the amount of computation and the constraints are treated as equality constraints in the computation [34].

3.2.3 Simulation results

Two proposed methods are studied to track an S-shape curve including three intersections: from line to curve, from curve to different curve and from curve to line. The S-shape path is a more complicated path than U-shape in [35] or eight-shape in [5] because it requires the trailer yaw rate to cross zero while the other two paths mentioned don't have such a demand. Each curved path is with a radius of 5 meter. The vehicle parameters are shown in Table 2.3 of the previous chapter. First, simulations are done without measurement noise. The sample time is 0.1 second. Fig. 3.11 shows the system performance using new coordinate transformation strategy (CTS) and previous method [22]. Under the previous control, the tracking error at each intersection point P_i are much larger than the error using the proposed approach, especially for the second intersection, where the desired yaw rate changes from negative (moving clockwise) to positive (moving counter-clockwise), and the trailer fails to track the second curved path. With the proposed method, the tractor starts to track new reference path at point S_i. The trailer path almost overlaps with the line and curved reference path. At the intersection of two consecutive curved path, the trailer can also track very well. Fig. 3.12 shows the comparison of lateral position error using these two methods. The alternating solid and dashed blue lines are used to distinguish different path

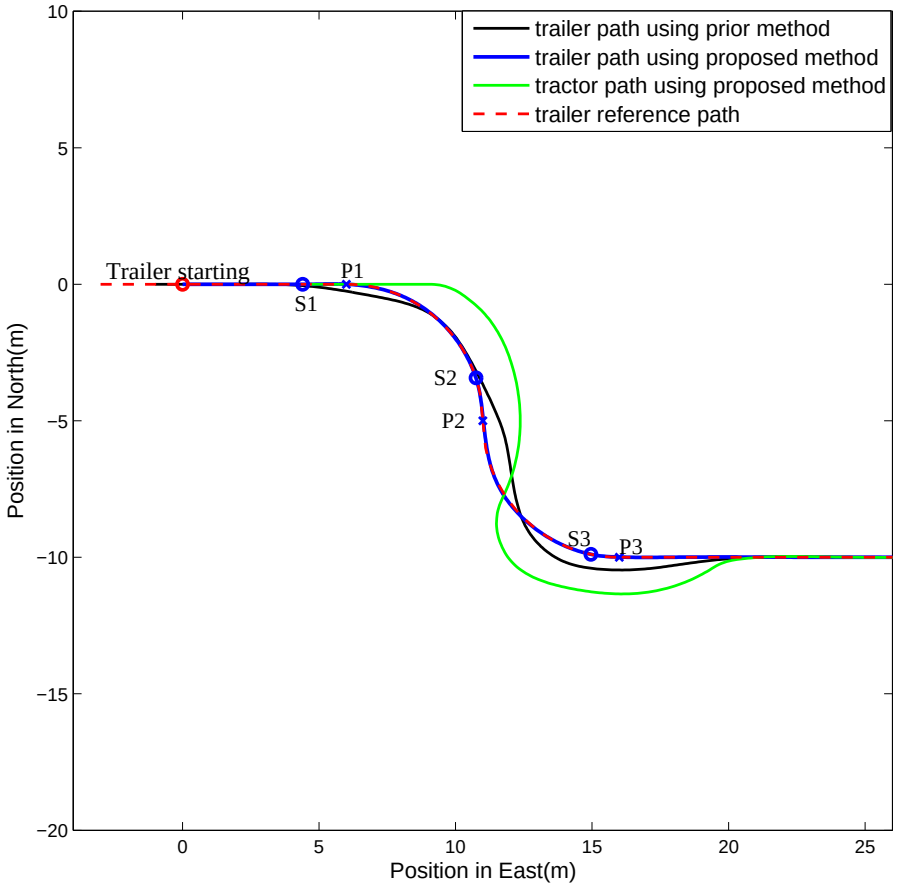

Figure 3.11: System performance using new coordinate strategy

sections. It can be seen clearly that the error near each intersection is significantly reduced. Using the proposed strategy, the root mean square error (RMSE) of trailer lateral position is 1.30 centimeter and the maximum absolute error is 5.27 centimeter.

Next, model predictive controllers based on two modeling methods, namely linear time-varying MPC (LTV-MPC) and using steady state values (SS-MPC) in the model, are tested. The prediction horizon N_p and the control horizon N_c are both 50, i.e. predicting the system behavior in the next 5 seconds. Notice that if current measurements are used in the model, the system response is faster than using steady state values, but are easier to be overshoot as well. Furthermore, the overshoot can be reduced by adjusting weighting matrix Q in

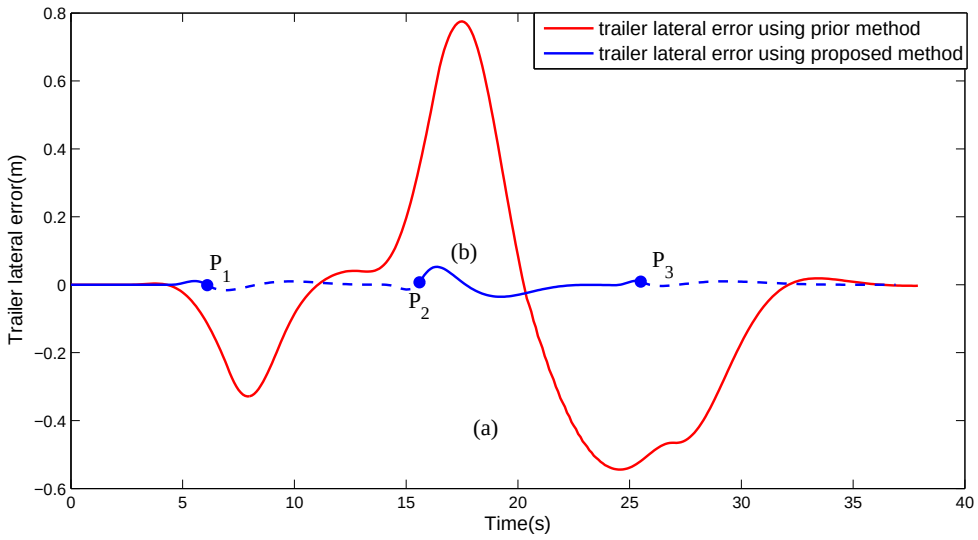

Figure 3.12: Comparison of lateral position error using new coordinate strategy (b) and previous approach (a)

Table 3.1: Error comparison for tracking S-curve using three methods without noise

	CTS	LTV-MPC	SS-MPC
Max. error	5.27 cm	4.57 cm	4.43 cm
RMSE	1.30 cm	1.41 cm	1.51 cm

(3.3). Fig. 3.14 shows how the parameter Q affects the system response. The system tracks a straight line and the initial error is 2 meter. The blue curve using SS-MPC and the green curve using LTV-MPC are generated by same control parameters Q and R. The tracking error in LTV-MPC reaches zero faster with a overshoot. The blue curve, however, are gentler when the trailer is close to reference. It is realized that the trailer heading error is larger using LTV-MPC when the trailer first arrives at the zero line. So the system response with more weighting on the trailer heading in Q is studied and drawn in magenta. Basically the response gets similar with the curve using SS-MPC, and has smaller overshoot than the previous case using LTV-MPC. In conclusion, the two modeling methods can have similar responses when the weighting on trailer heading for LTV-MPC is set to be a little larger than the value in SS-MPC.

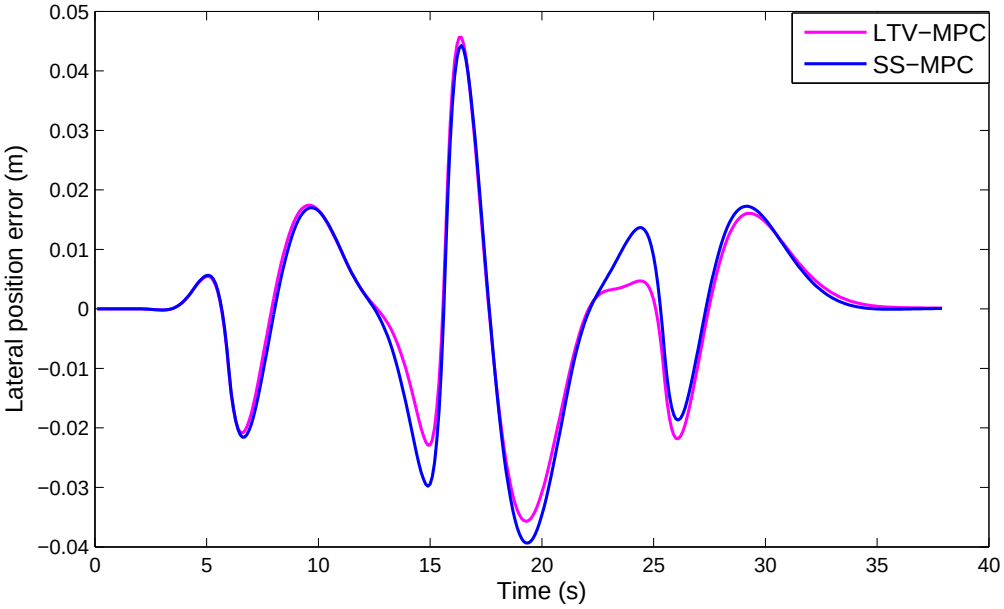

Figure 3.13: System response with different linearization methods

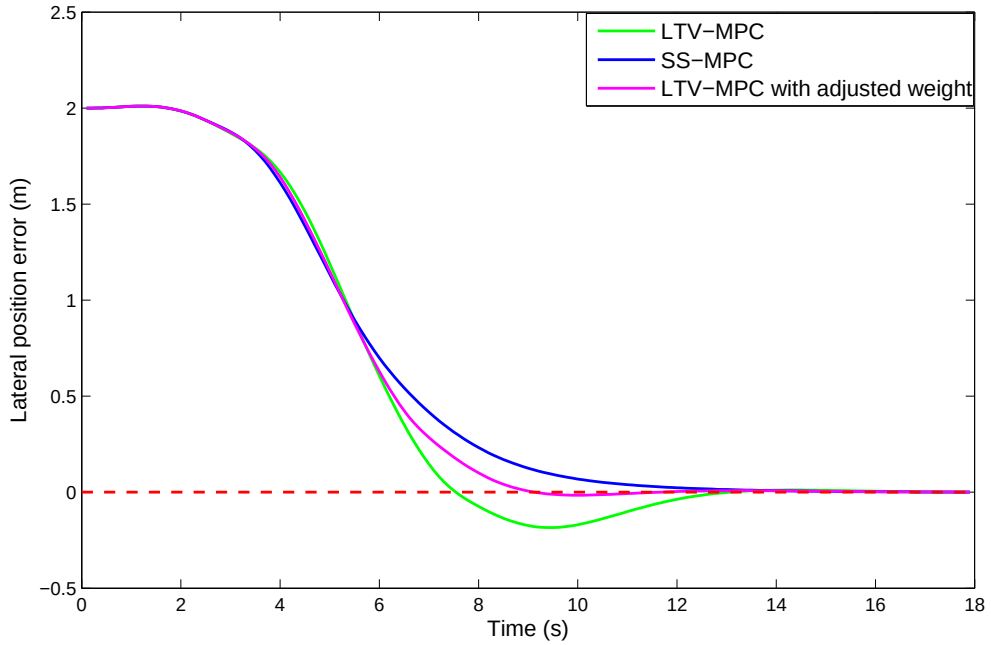

Figure 3.14: Lateral tracking error using different linearization methods

Then, the system tracks the same S-curve using the two modeling methods. Fig. 3.13 shows the lateral position error. The overall behaviors are quite similar. The tracking

error near the second intersection is larger than the errors near the other intersections, which is consistent with the situation using the proposed coordinate transformation strategy. Table 3.1 shows the maximum of absolute error (MAE) and RMSE using the three methods respectively. The controller using CTS has the largest MAE but smallest RMSE, because it works well near the intersection point P_1 and P_3, but works worse near P_2. MPC has smaller MAE , illustrating that MPC can do better when the curvature of reference path has a big change, such as crossing zero at P_2. Next, the simulation with initial error is done. Fig. 3.15 shows the trailer paths using coordinate transformation and LTV-MPC. The initial position error is 0.92 meter. Notice that the tracking error still exists at S_2. The trailer moves to the reference more quickly using LTV-MPC method. Both of the two controllers can track the second curved path very well. Fig. 3.16 shows the lateral position error with respect to time using the three methods. LTV-MPC and SS-MPC have faster response and less overshoot than CTS when the trailer near P_2. It's mainly because the setting point in CTS is calculated beforehand assuming no error at the setting point, and can't be adjusted adaptively according to the actual situation near the intersections, while the control effort in the two approaches based on MPC is calculated on-line. In conclusion, MPC can obtain better results when there is tracking error at the setting point.

3.2.4 System performance with the presence of noise

Noise usually exists in the measurement signals. It is assumed that all the states including heading angles and positions can be measured. Next, the system still tracks the S-curve with the same initial condition in Fig. 3.12, but Gaussian white noises are added with standard covariance of 0.02 radian for angle measurement and 0.02 meter for position measurement. The simulations are done for thirty times. Table 3.2 shows the MAE and RMSE using three methods. CTS has the largest RMSE while LTV-MPC and SS-MPC have the same RMSE. Recall from Table 3.1 that CTS has the smallest RMSE without the

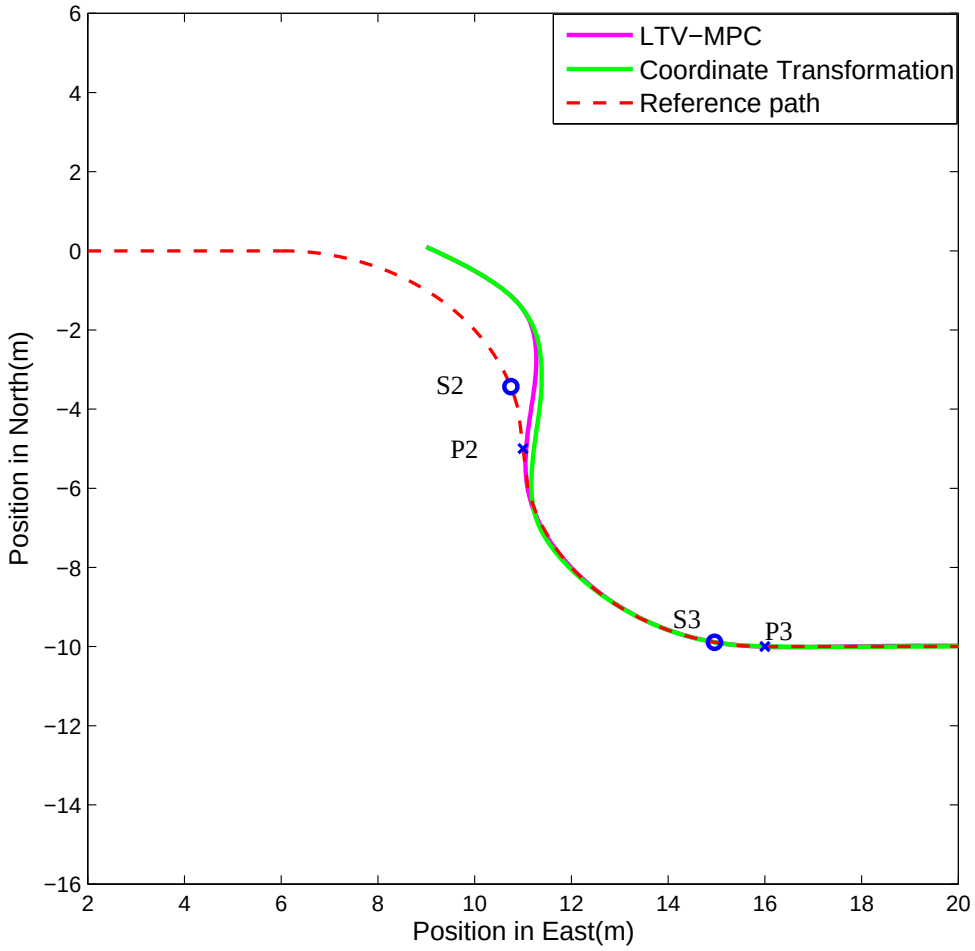

Figure 3.15: System paths with initial errors using two methods

Table 3.2: Error comparison for tracking S-curve using three methods with noise

	CTS	LTV-MPC	SS-MPC
Max. error	6.38 cm	5.58 cm	5.16 cm
RMSE	1.93 cm	1.78 cm	1.78 cm

presence of noise. This illustrate that MPC can have better results when measurements are noisy.

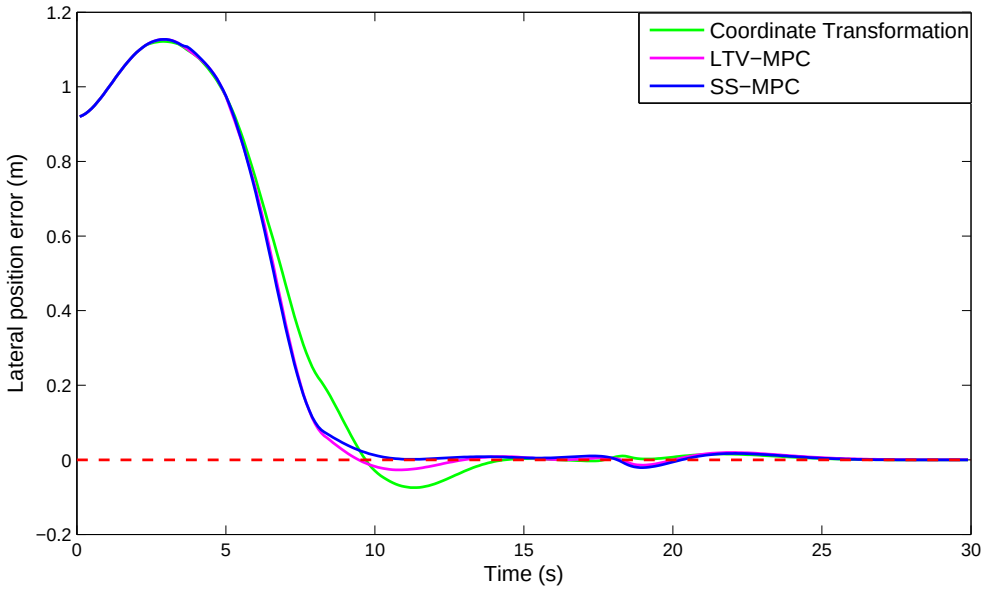

Figure 3.16: Lateral position error using three methods

3.2.5 Summary

In this section, two methods, based on coordinate transformation strategy (CTS) and MPC, are introduced to reduce the tracking error near the intersections of different reference paths. Two linearization approaches are given in MPC. All the proposed methods can provide much better results than traditional linear state feedback. CTS is simpler and easier to implement, requiring less computation, while MPC is less sensitive to measurement noise, and the tracking error can be smaller when non-zero steady-state error is considered.

Two methods of linearizing the nonlinear system is given. One is called LTV-MPC, using current values of time-varying terms in the system matrix. The other is called SS-MPC, using steady-state values instead. Two approaches can obtain similar responses when the trailer heading is weighted more in LTV-MPC. It's also found that the system tends to overshoot more when the prediction horizon becomes longer. Fig. 3.17 shows the tracking error versus time with different prediction horizon N_p. The control parameter Q and R are the same for the three situations. The initial position error is 2 meter. There is no overshoot when N_p equals 50. The overshoot exists when N_p becomes 65, and gets larger when the

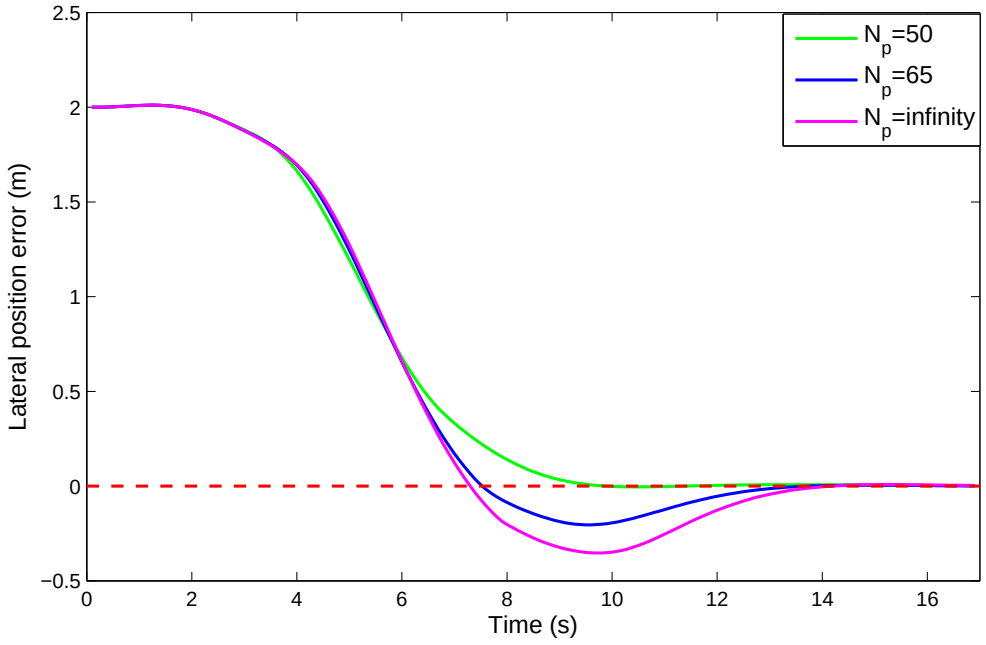

Figure 3.17: Lateral position error using LTV-MPC with different prediction horizon

prediction horizon is infinity, which is implemented by infinite-horizon LQR approach. In fact, in the most cases, the system would finally go to the steady state when time goes to the infinity. As a result, the larger the prediction horizon is, the more steady state values are included during the horizon. Therefore, LTV-MPC becomes less accurate when the prediction horizon gets larger. In a conclusion, LTV-MPC is not an appropriate approach for path following problem if the prediction is large, or even infinite.

3.3 Controller for the trailer far from the reference

In this section, an alternate controller for the trailer far from the reference is introduced.

3.3.1 Problem Statement

For the study of nonlinear systems, one common approach is to linearize the original nonlinear system at the operating point, and then analyze the linearized system instead using classical approaches. It's usually all right when the system works near the reference.

However, the global stability is not guaranteed. One of the differences between linear system and nonlinear system is that the system response of nonlinear system may depend on the initial condition, which doesn't have effect in linear systems. The tractor-trailer system suffers this problem as well. Fig. 3.18 shows a trailer path tracking a straight line (dashed red line), and the initial lateral position error is 12 meter and the heading errors of tractor and trailer are -60° and -75° respectively. State feedback is used as the controller:

$$u(k) = -kx(k) = -k_1\varphi_r(k) - k_2\omega_r(k) - k_3\varphi_t(k) - k_4 y_t(k) \tag{3.19}$$

The tractor and trailer just keep turning clockwise and fails to follow the reference path.

The reason of this phenomenon is that the trailer position error y_t is so large that it dominates the control law. Heading angles φ_r and φ_t are constrained in the range of $[-\pi, \pi]$. The tractor yaw angle is also limited. However, the lateral position error can be very large. Thus, the control effort u will totally depend on the sign of y_t. In the case of Fig. 3.18, position error y_t is positive, resulting in a negative control effort and a steering angle in clock-wise direction even if the other three variables contributes to a positive control effort. Therefore, no matter how the other variables change, the tractor keeps turning right as well as the trailer.

A nonlinear control algorithm considering control input constraints may solve the problem, obtaining global stability based on Lyapunov stability theory [7] [36], or state linearization [11]. In [36] and [11] different controllers for tracking lines and arcs are designed. In [7], the proposed control law is only valid for on-axle hitching system, and the transient behavior needs to be improved. In the next subsection, a method that can be applied for both on-axle hitching and off-axle hitching systems, and for both lines and arcs reference paths is given.

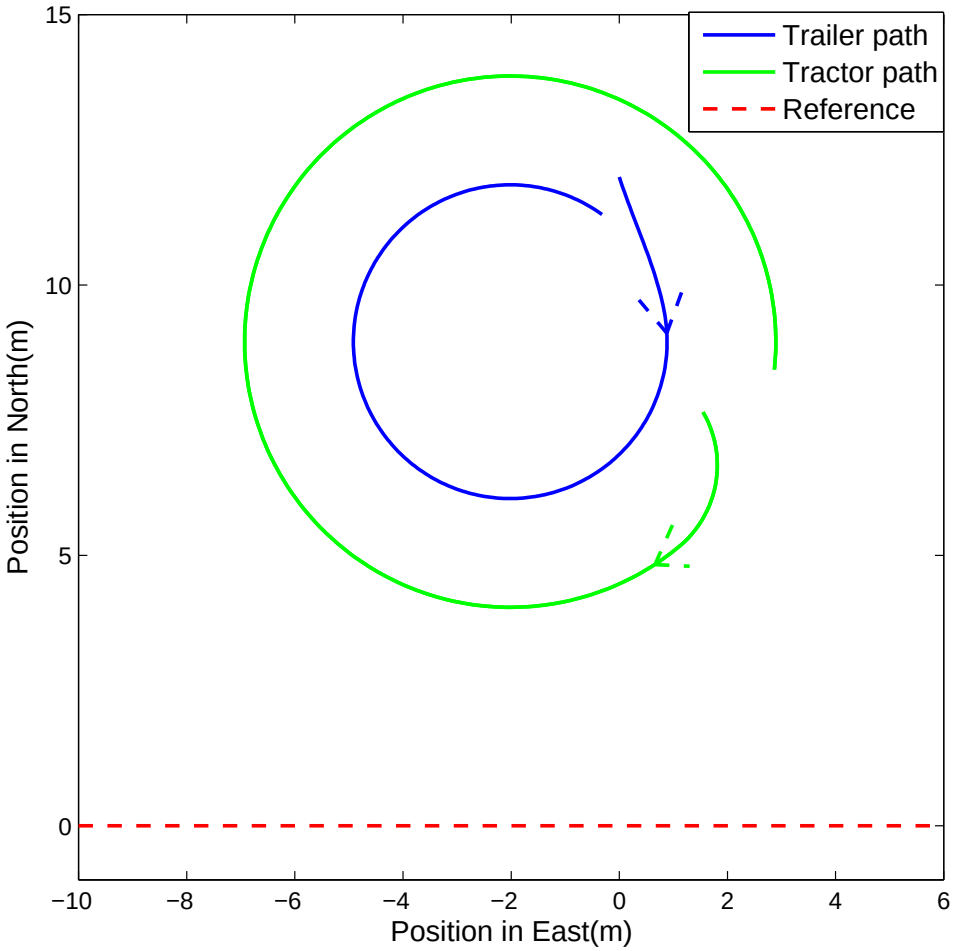

Figure 3.18: An example of system failing to follow the reference

3.3.2 Heading control

When the position error is very large and has opposite sign to the heading angle, the system may become unstable. It is realized that when the system is unstable, the heading angle errors are not properly controlled. In other words, the problem can be solved by adding weights to the heading angles. Fig. 3.19 illustrates this idea. For the two vehicles with different heading angles and large position errors, the desired control law should drive the vehicles to the reference path as soon as possible. One solution is shown in red arrows, which requires the heading angles to be $-90°$ for both vehicles. In other words, a control

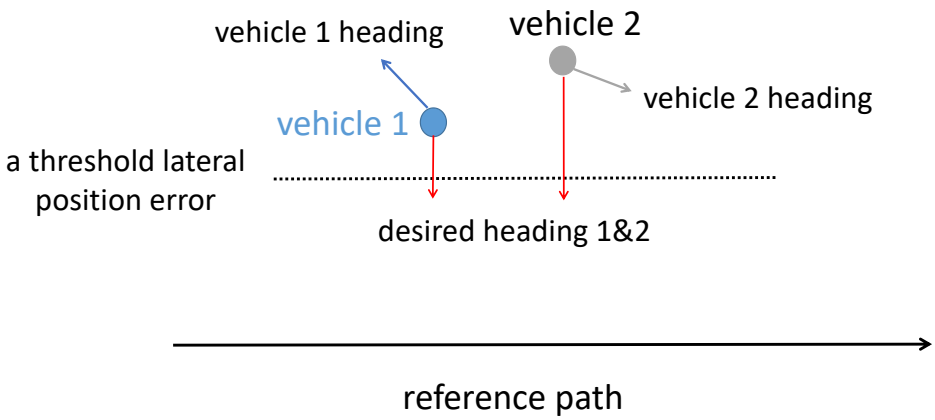

Figure 3.19: Illustrating the importance of correct heading when position error is large

law based on heading angles can be designed when y_t is large. A suitable control law is as follows:

$$u(k) = -k_1(\varphi_r + \frac{\pi}{2} sign(y_t)) - k_2\omega_r - k_3(\varphi_t + \frac{\pi}{2} sign(y_t)) \tag{3.20}$$

where $sign$ is the signum function, and the control gains k_1, k_2, and k_3 are the same as the gains in (3.19). There are some comments on the control law (3.20). First, the control effort is actually designed for the subsystem:

$$\begin{aligned} \dot{\varphi}_r &= \omega_r \\ \dot{\varphi}_t &= \frac{v_r \sin\theta - l_h\omega_r \cos\theta}{l_t} \\ \dot{\omega}_r &= -d^v\omega_r + K^v v_r \frac{\tan u}{l_r} \end{aligned} \tag{3.21}$$

where the state variable x_s is

$$x_s = \begin{bmatrix} \varphi_r \\ \omega_r \\ \varphi_t \end{bmatrix}$$

which contains variables of tractor heading, tractor yaw rate, and trailer heading. Equations (3.21) can be obtained by just removing the lateral position y_t in the original model. The desired value of x_s is:

$$x_{s,d} = \begin{bmatrix} -\frac{\pi}{2} sign(y_t) \\ 0 \\ -\frac{\pi}{2} sign(y_t) \end{bmatrix}$$

which makes the tractor and trailer move orthogonally toward to the reference path. The stability of the closed-loop subsystem is guaranteed if the original fourth-order system is stable because the eigenvalues of the subsystem is a part of original ones. Second, the control goal is actually changed by the new controller, to stabilizing the heading angles to 90° or -90° from stabilizing all the variables to zero. This change will avoid the unstable behavior in Fig. 3.18 because only the sign of position error is considered instead of the error value. The position error will not dominate the control law any more when it's very large. Last but not the least, this idea is also valid if the tractor moves backwards. In [14], an alternate controller based on tractor only is proposed. That approach is only valid when the vehicle moves forward. However, the controller (3.20) doesn't suffer that restriction because the trailer dynamic is also considered, and the model (3.21) of the subsystem is valid for both forward and backward motion.

3.3.3 The equivalent form of the alternate controller

Extending the control law (3.20), the following equations can be obtained:

$$\begin{aligned} u(k) &= -k_1\varphi_r - k_2\omega_r - k_3\varphi_t - \frac{\pi k_1}{2}sign(y_t) - \frac{\pi k_3}{2}sign(y_t) \\ &= -k_1\varphi_r - k_2\omega_r - k_3\varphi_t - k_4\frac{k_1+k_3}{k_4}\frac{\pi}{2}sign(y_t) \\ &= -k_1\varphi_r - k_2\omega_r - k_3\varphi_t - k_4 y_{t,sat} \end{aligned} \tag{3.22}$$

where k_4 is the same gain in (3.19). It can be found that the new control law can be still expressed as the form in (3.19) containing four variables, using $y_{t,sat}$ instead of y_t and

$$y_{t,sat} = \frac{\pi(k_1+k_3)}{2k_4}sign(y_t) \tag{3.23}$$

In other words, the controller (3.19) can be still applied with saturated trailer position error. In the case of Fig. 3.18, the value of y_t is used directly, resulting in undesired response. Therefore, variable y_t should be constrained and a maximum absolute value of y_t should be used instead when the position error is beyond the range. Fig. 3.20 shows the closed-loop system flow chart. The heading angle errors of tractor and trailer are saturated as well as the trailer position error before the signals enter the controller. Besides, the tractor yaw rate is also saturated by the constraint of control effort in the controller.

This equivalent form also provides the threshold of position error which indicates when the controller should switch to the other one. In the last subsection, the control law (3.19) is given, but it's not clear when to use such a control law. In other words, there is a question: How large should y_t be such that the alternate controller is used? The equivalent form (3.22) gives the answer. The threshold of trailer position error is $y_{t,sat}$. In fact, it can be realized that there is no switching operation because the two controllers can be regarded as one by (3.22). The control effort at $y_{t,sat}$ is continuous, so no additional smoothing function is needed.

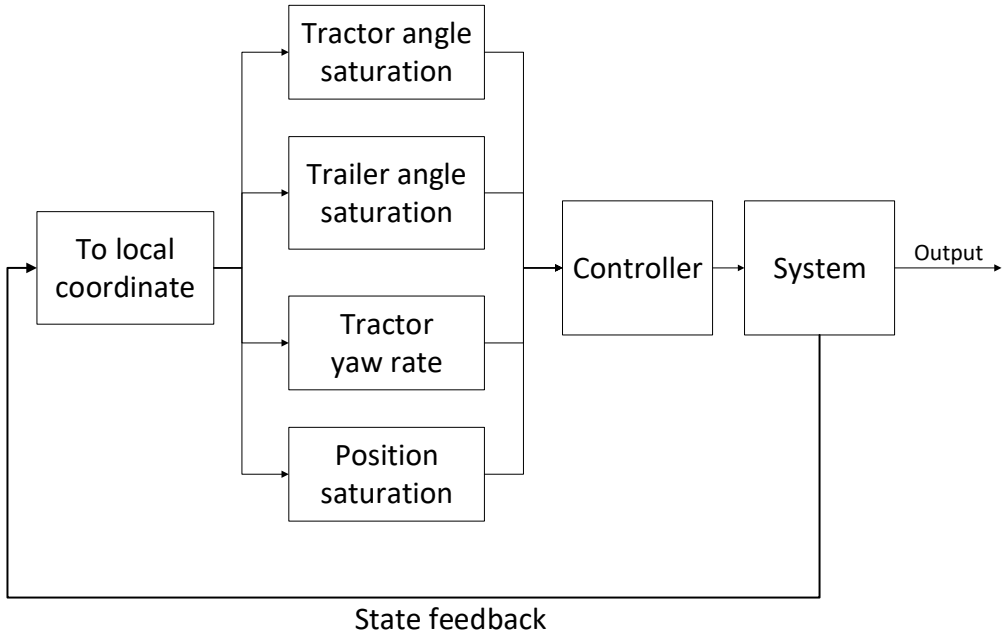

Figure 3.20: System flow chart with saturation

The idea of input saturation also exists in fuzzy systems. In a fuzzy system, an input is expressed by a combination of variables in a fuzzy set with a membership function via fuzzification [37]. Fig. 3.21 is an example of a typical membership function with a triangle shape [38]. Horizontal axis represents a regularized system input. One may notice that for the fuzzy variables NB (Negative big) and PB (Positive big), the membership function for absolute of inputs more than 1 is flat. It means that there is no difference for a regularized input with value of 2 and 3 because the system would transform the actual input to fuzzy variable PB with a membership of 1 for both cases. In other words, the system input is saturated by the fuzzifier.

Furthermore, the threshold of trailer position error $y_{t,sat}$ can be analyzed in another way. Fig. 3.22 shows the circular trailer path in clock-wise motion corresponding to the case of Fig. 3.18. Points L, M, and N correspond to the trailer heading of 90°, $-90°$ and 180° or (-180°). The reference path is from left to right. The circle path can be divided into three

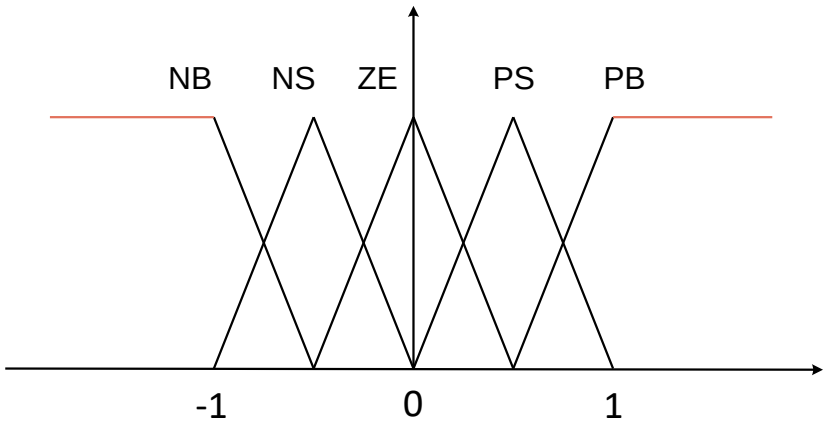

Figure 3.21: A typical triangle membership function in a fuzzy system

parts. The first part is from point N to L. The trailer heading changes from 180° to 90°. The path is reasonable because at point N the trailer moves in the opposite direction,and path NL makes the heading error smaller. The second part is from point L to M. Trailer heading changes from 90° to $-90°$. The path is also reasonable, because the trailer is on the right way to the reference. One can image that after point M, the vehicle can go down and finally follow the reference. The last part is form M to N. The heading changes from -90° to -180°. This path, however, is not reasonable, because the trailer should go towards the reference and reduce the heading error. In other words, the steering angle should be positive, i.e. the vehicle should turn left. But for the path MN, the vehicle turns right instead. Therefore, for the path from M to N:

$$u(k) = -k_1\varphi_r - k_2\omega_r - k_3\varphi_t - k_4 y_t > 0$$

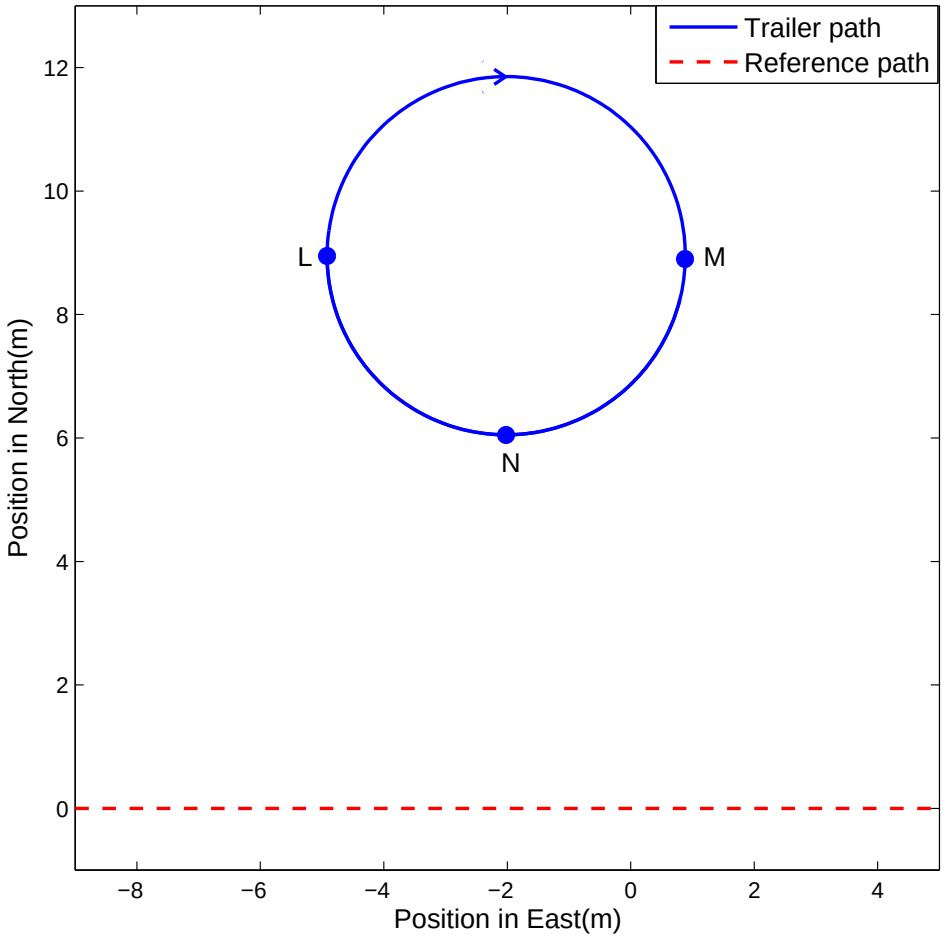

Figure 3.22: Trailer ends up with a clockwise motion, failing to follow the reference

Then,

$$y_t < \frac{-k_1\varphi_r - k_2\omega_r - k_3\varphi_t}{k_4}, k_4 > 0 \tag{3.24}$$

Thus, position error y_t should be smaller than the minimum of the right side of (3.24). For the path MN:

$$-180^\circ \leq \varphi_r, \varphi_t \leq -90^\circ \tag{3.25}$$

Besides, the desired tractor yaw rate is positive (turning left) for path MN, therefore

$$\omega_r \geq 0 \tag{3.26}$$

Combining (3.25) and (3.26), it can be derived that the minimum of the right side of (3.24), which is also the threshold of position error $y_{t,sat}$ is:

$$y_{t,sat} = \frac{\pi(k_1 + k_3)}{2k_4}, y_t > 0 \tag{3.27}$$

Similarly, for the negative position error:

$$y_{t,sat} = -\frac{\pi(k_1 + k_3)}{2k_4}, y_t < 0 \tag{3.28}$$

Combining (3.27) and (3.28), it can be easily realized that the result is as the same as (3.23).

3.3.4 Simulation results

Infinite-horizon discrete LQR technique is applied to determine the control gains. Furthermore, the constraints of steering angle and hitch angle are considered:

$$\begin{aligned} \delta_{min} \leq \delta \leq \delta_{max} \\ \theta_{min} \leq \theta \leq \theta_{max} \end{aligned} \tag{3.29}$$

There are some research on the LQR for constrained problems [39] [40]. Inspired by [33], the system response can be similar just applying the constraints on the next step compared to setting constraints during the whole horizon. One-step prediction is proposed and applied for the constraints. The control effort is first calculated without any constraints. Then, the control input and the hitch angle are predicted for the next step. If any constraint is violated, the control effort is recalculated to satisfy the active constraint, by regarding the active inequality constraint as an equality one. If there is a control delay in the system, two-steps prediction is needed.

Table 3.3: System parameters corresponding to Sec. 3.3.4

Variable	Value
a	0.75 m
b	1.21 m
c	0.53 m
d	3 m
e	1 m
v_r	1m/s
δ_{min}	-45°
δ_{max}	45°
θ_{min}	$-60°$
θ_{max}	60°

The system parameters used in the simulations are shown in Table 3.3. The weighting matrix on the state Q and weighting parameter on the system input R are:

$$Q = \begin{bmatrix} 0 & 0 & 0 & 0 \\ 0 & 0 & 0 & 0 \\ 0 & 0 & 4 & 0 \\ 0 & 0 & 0 & 2 \end{bmatrix}, \quad R = 0.6$$

The trailer heading is more weighted in matrix Q to get a smooth response with less overshoot. Gaussian white noises with a standard covariance of 0.02 are added on all states. The simulation is done first with a line reference path. Fig. 3.23 shows the paths of tractor and trailer with the same initial condition in Fig. 3.18. Instead of turning only clockwise and ending up with a circle path, the trailer moves vertically to the reference path, reducing the position error as soon as possible, then produces a smooth response when the trailer is near the reference.

Next, the reference path becomes a curve. In Fig. 3.24, the reference path is a circle with radius of 5 meter. Initially, the position error is 9.86 meter, and the trailer heading is almost opposite to the desired direction. The system first turns in clockwise and moves

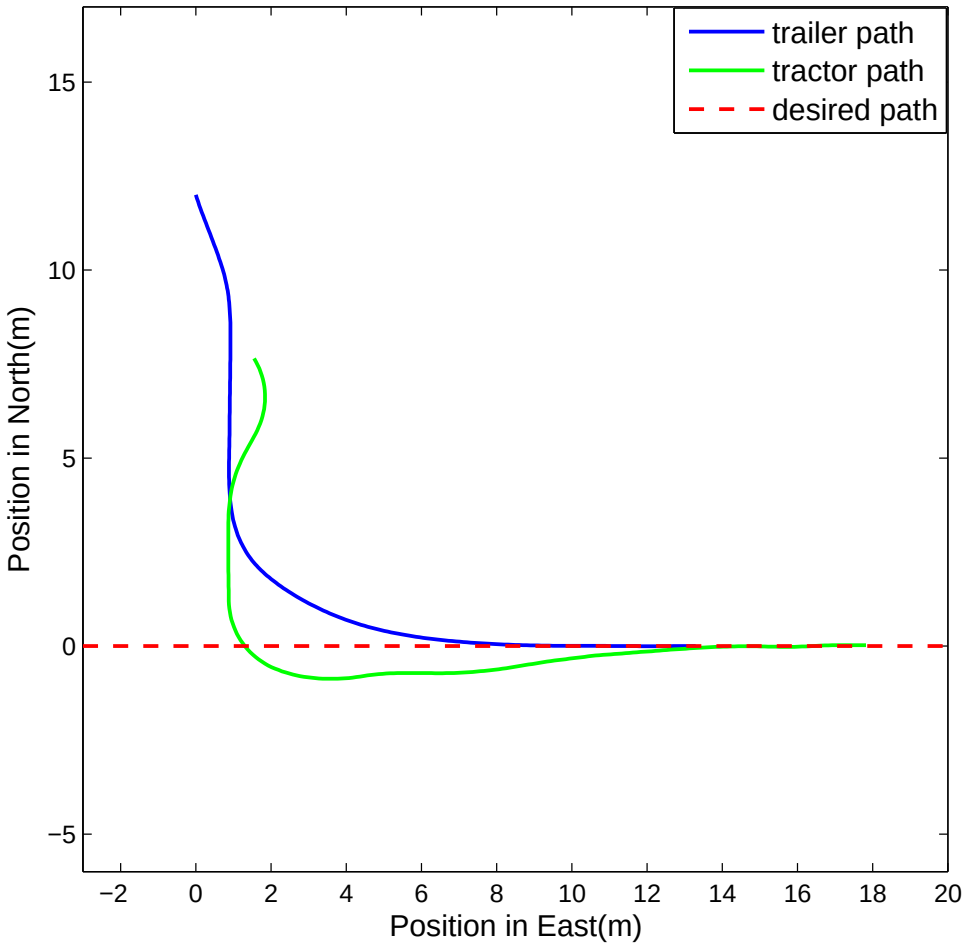

Figure 3.23: System response with large initial error: line reference path

towards the reference, then follows the curved line smoothly. The hitch angle with respect to time is shown in Fig. 3.25. The hitch angle keeps the lower bound of $-60°$ from 3 second to 16 second by setting the constraint on that angle, thus avoids the jack-knife phenomenon.

The controller is also able to reverse the system by setting the tractor velocity negative. Fig. 3.26 shows the paths in backward motion to track a straight line.The initial error is $180°$ for tractor and trailer headings and 10 meter for trailer position. The trailer adjusts the heading angle from $180°$ to $90°$ and then keeps that heading until the trailer reaches threshold position at 4.35 meter. After that both the heading angle error and the position

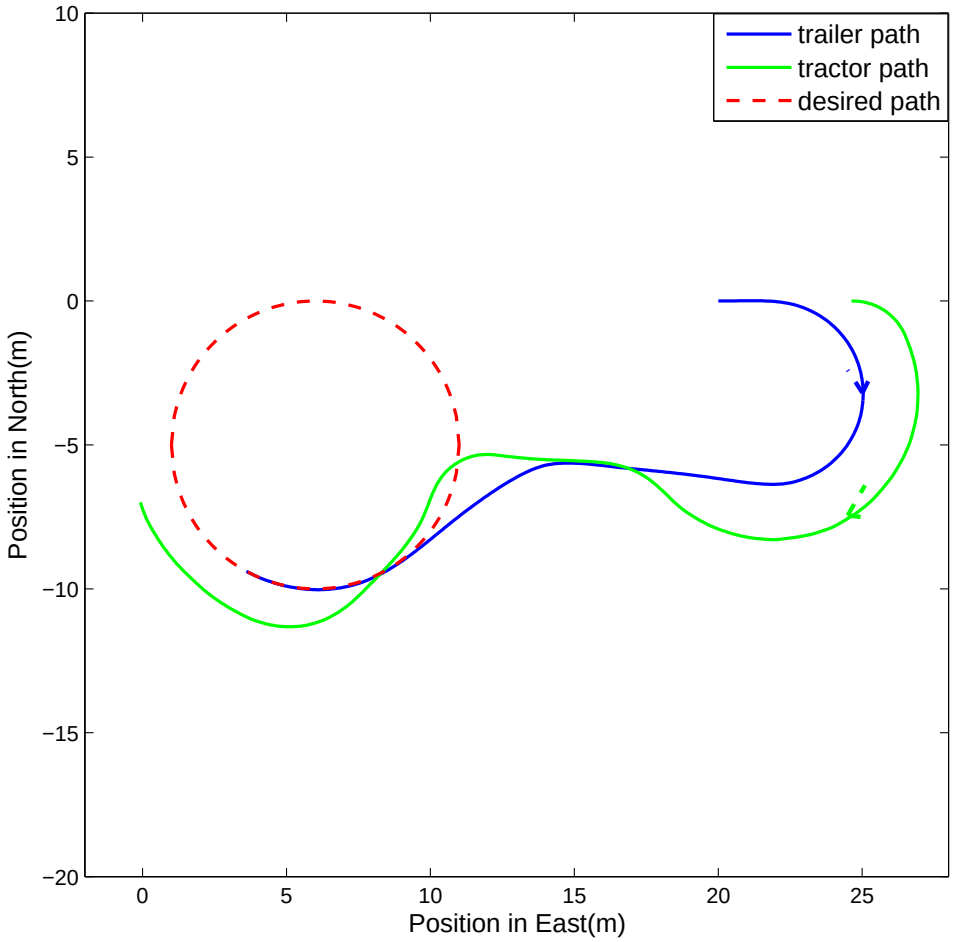

Figure 3.24: System response with large initial error: curved refrence path

error converge to zero. Notice that the constraint of hitch angle plays an important role in the path following in backward motion. The open-loop dynamic is unstable, and an improper large hitch angle may result in an undesired weird trailer path.

3.3.5 Summary

In this section, an alternate controller used when the system is far away from the reference path is proposed. The global space is segmented based on the trailer position error. When the position error is large, heading control has higher priority, and the controller drives

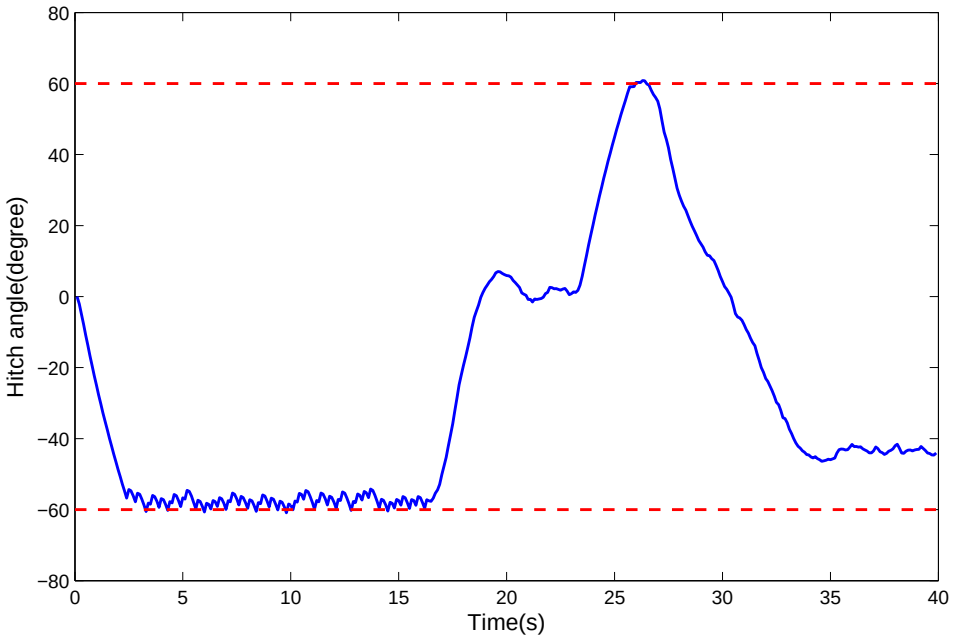

Figure 3.25: Hitch angle vs. time

the vehicle vertically, reducing the position error as fast as possible. Furthermore, the two controllers, used for trailer far or near the reference path, have the same structure. It is achieved by saturating the position error at an appropriate threshold. The proposed method is valid for both lines and arcs reference paths, and is able to drive the system in both forward and backward motion.

3.4 Chapter summary

Several control system contributions have been presented in this chapter. First, a local coordinate transformation strategy is proposed to reduce the tracking error near the joining point of two different reference path. Second, model predictive controller is designed to solve the same problem. Two linearizing approaches on the system matrix is analyzed. Last, an alternate controller focusing on heading control is designed so that the system is globally stable.

In the next chapter, control systems that eliminate steady-state error are presented.

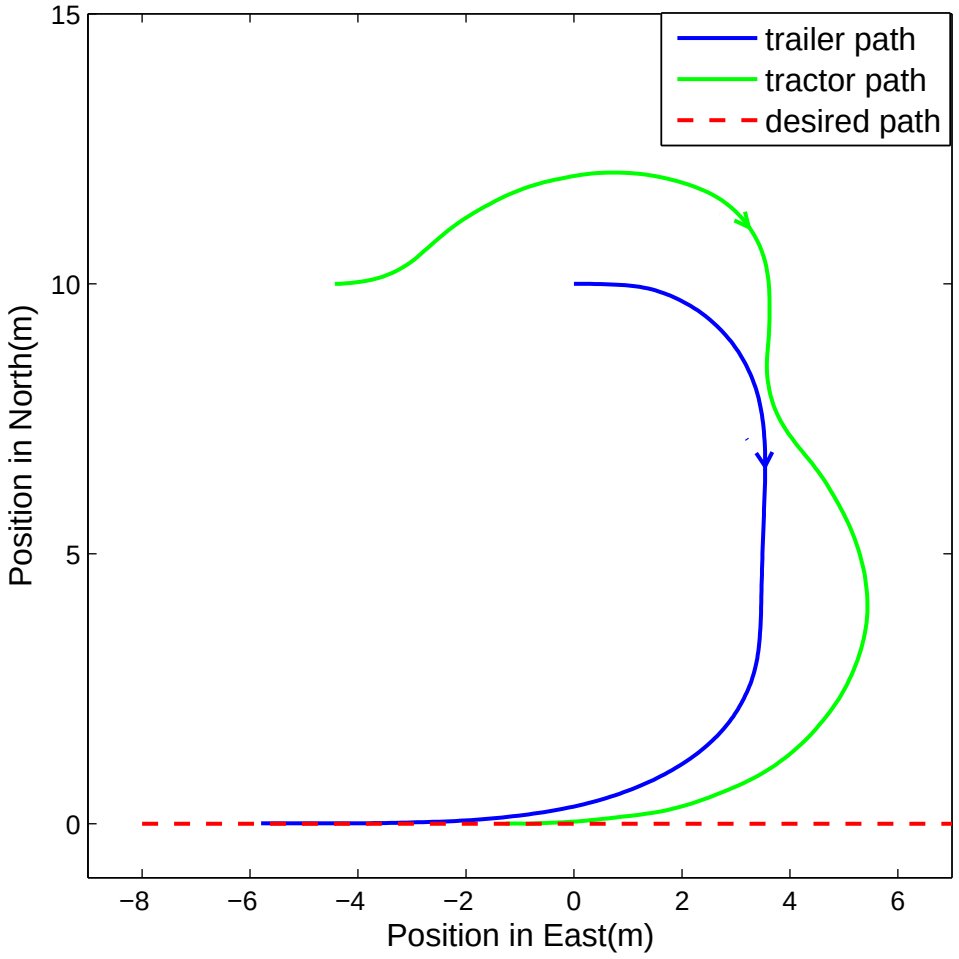

Figure 3.26: System response in backwards motion with a large initial error

Chapter 4

Controller to Remove the Steady-state Error for Tractor-trailer Systems

In the previous chapter, two problems are solved. One is reducing the tracking error near the intersections of different reference paths. The other is to stabilize the system when it's far form the reference. In this chapter, the problem of removing the steady-state error for line and arc segments is solved.

4.1 Problem Statement

One may notice that in Fig. 3.2, when the reference is a curve, the trailer path using state feedback does not exactly follow the reference path in red dash, because these two paths don't overlap. However, when the trailer tracks a straight line, the tracking error can be zero. In that figure, the measurement noise is not added. The error exists just due to the control algorithm. Therefore, there is a drawback of traditional state feedback: the steady-state error for curved reference path is nonzero.

The feedback approach has the robustness naturally. Furthermore, LQR approach is able to make the closed-loop system have at least 60° phase margin [1]. The stability of the overall system is still guaranteed with the presence of parameter uncertainty. Fig. 4.1 is such an example, showing the trailer and tractor path following a straight line, but with a velocity mismatch. The tractor velocity is 1 m/s in the model while the actual value is 0.9 m/s instead. Zero-mean Gaussian measurement noises are added. The system is still stable with a good response and the steady-state error is almost zero.

However, if the noise on the process or measurement is not zero-mean, a steady-state error often exists, and it can not be solved by state feedback. Fig. 4.2 shows the trailer position error at the same initial condition and using the same control gains, but adding

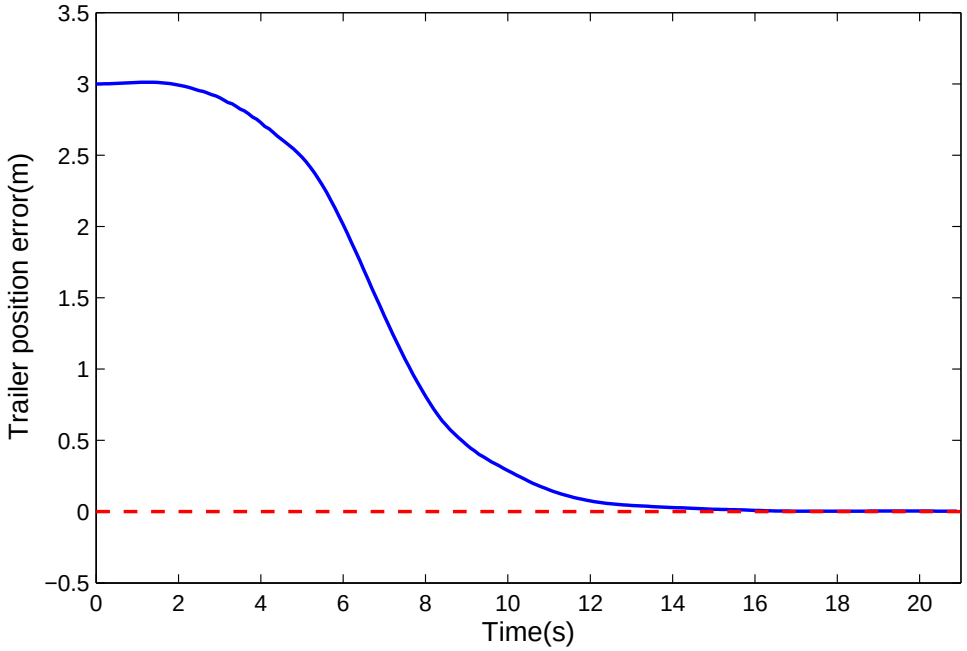

Figure 4.1: Lateral position error vs. time with the tractor velocity mismatch

measurement bias on the tractor heading and trailer heading of 0.57° and 1.14° respectively. It is found that the steady-state error occurs, with a value of about 5.5 centimeter.

In the following part, the steady-state error caused by the two reasons above will be removed respectively.

4.2 Controller to remove steady-state error when tracking a curve

A control law based on the traditional state feedback is the combination of state error. It implies that the control input, steering angle δ, is zero when the system tracks the reference path without errors. But such a strategy is not suitable on a curved reference path, because a non-zero steering angle is necessary to maintain zero tracking error on a curved path. Therefore, tracking error exists due to the non-zero control input. Next, two methods are proposed to solve this problem.

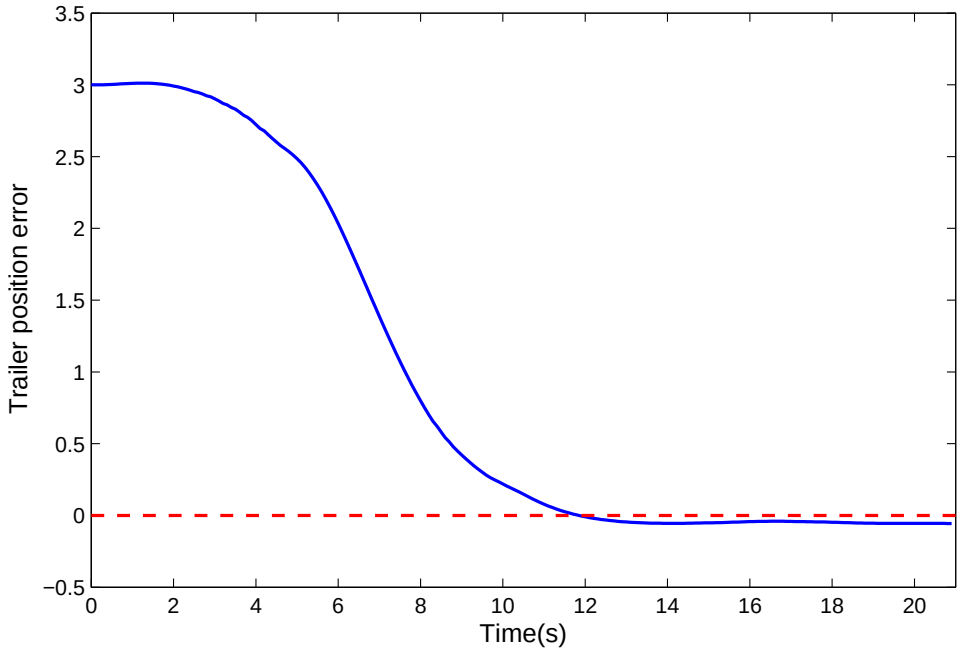

Figure 4.2: Lateral position error vs. time with the presence of measurement bias

4.2.1 Feed-forward control

Feed-forward control can be used to compensate for the nonzero steering angle. The whole control law consists of two parts: feed-forward part and feedback part:

$$u = u_{feedforward} + u_{feedback}$$

The feed-forward part takes charge of providing a proper steering angle when the system follows a curve assuming that there is no disturbance. The feedback control is used to eliminate the error in a closed loop with the presence of disturbances.

The feedforward part can be regarded as an offset. The idea of using an offset also exists in machine learning algorithm. Take neural network as an example. For a multiple layer perception (MLP) with one hidden layer [41], there is a neuron with a value of 1 at hidden layer and output layer respectively. This is the bias for the corresponding neurons and the

value of the bias equals the weights connected to the neurons [42]. The role of those neurons is quite similar with the role of feed-forward part in the controller.

The bias for each neuron in the hidden layer and output layer can be calculated based on a large of labeled data sets and supervised learning algorithms such as back propagation [43], while the feedforward control should be calculated based on the system dynamics and the desired curvature. Notice that the desired tractor yaw rate for a given desired curvature has been obtained by (3.12). If the tractor yaw rate and steering angle is modeled as a linear relationship, then the feedforward control, i.e. the desired steering angle for a reference curve with radius R is:

$$u_{feedforward} = \arctan(\sigma sign(v_r)\frac{l_r\sqrt{l_t^2 + R^2 - l_h^2}}{l_t^2 + R^2 - l_h^2}) \tag{4.1}$$

where σ distinguishes the clockwise motion (σ=-1) and counter-clockwise motion (σ=1). The feedback controller can be designed using linear or nonlinear approaches, as long as the closed-loop system is stabilized.

This method to remove the steady-state error tracking a curved path is actually applied in the subsection 3.2.3 and subsection 3.3.4. For the simulations in 3.2.3, when the trailer is not near the intersection points, the controller above, consisting of feedforward control and feedback control, is used. For section 3.2.4, the proposed scheme is applied in the simulations shown in Fig. 3.24. It can be found that the trailer exactly follows the desired curved path in red dash without steady-state error.

4.2.2 Controller using steering rate as input

The steady-state error when the system tracks a curved path can be removed by the feed-forward control. However, there is a drawback of this approach. A linear relationship between the steering rate and tractor yaw rate is assumed. It may be not accurate with the change of the weight of the trailer. The dc gain from steering angle to tractor yaw rate transfer function, which can be found by the dynamic model, changes with the corner stiffness at the hitch, regarding the implement as additional tire at the hitch [44]. It means

that the feedforward control effort may be inaccurate since the dc gain from δ to ω_r varies with the weight of the trailer. Furthermore, the feed-forward control forms a open-loop without feedback. It's more sensitive to the parameter uncertainty than feedback control. As a result, a steady-state error may also exist, but the error is smaller than the one under the traditional state feedback approach.

Therefore, a method which avoids using the feed-forward control can solve this problem better. It's realized that the zero value doesn't hold for the steering angle under the steady-state for a curved reference path, but the rate of steering angle does. No matter the reference is a straight line or an arc, the rate of steering angle $\dot{\delta}$ should not change. When tracking and heading errors are zero, then the steering rate is zero, which more closely coincides with the human driving experience.

Thus, the steering rate is taken as the new system input, and an additional state variable is added in the system matrix correspondingly. Concretely, the system model becomes [15]:

$$\begin{aligned} \dot{\varphi}_r &= \omega_r \\ \dot{\omega}_r &= \frac{v_r}{l_r \cos^2 \delta} u \\ \dot{\varphi}_t &= \frac{v_r \sin\theta - l_h \omega_r \cos\theta}{l_t} \\ \dot{y}_t &= v_t \sin\varphi_t \end{aligned} \tag{4.2}$$

With small angle assumption, the model (4.2) can be linearized as:

$$\begin{bmatrix} \dot{\varphi}_r \\ \dot{\omega}_r \\ \dot{\varphi}_t \\ \dot{y}_t \end{bmatrix} = \begin{bmatrix} 0 & 1 & 0 & 0 \\ 0 & 0 & 0 & 0 \\ \frac{v_r}{l_t} & -\frac{l_h}{l_t} & -\frac{v_r}{l_t} & 0 \\ 0 & 0 & v_r & 0 \end{bmatrix} \begin{bmatrix} \varphi_r \\ \omega_r \\ \varphi_t \\ y_t \end{bmatrix} + \begin{bmatrix} 0 \\ \frac{v_r}{l_r} \\ 0 \\ 0 \end{bmatrix} u \tag{4.3}$$

The additional state variable is the tractor yaw rate. Note that there are two extra benefits from the new steering rate input. First, for the steering angle control, the feedback

sensor should be carefully aligned to the system, so that zero angle is correctly measured. However, the speed sensor for steering rate control is easier to install, and requires less alignment work. Second, the new augmented model naturally adds an integrator at the input channel, thus the noise from the input is filtered since the integrator can be regarded as a low pass filter.

Furthermore, even if the steering angle is the system input in the actual vehicle, the proposed new model can be still applied to remove the steady-state error. When the vehicle tracks a curve path, the steering angle would take a proper position according to the controller output, and finally find the correct steering angle to track the desired curvature naturally, even if a bias on the steering angle exists. When the sample period T is small, the steering angle can be calculated by numerical integration:

$$\delta(k) = \delta(k-1) + Tu \tag{4.4}$$

4.2.3 Simulation

The proposed method using steering rate as new input is next verified by simulations. LQR technique is used to determine the control gains. The constraints on the system input, steering angle and hitch angle are considered:

$$\begin{aligned} -u_{max} \leq u \leq u_{max} \\ -\delta_{max} \leq \delta \leq \delta_{max} \\ -\theta_{max} \leq \theta \leq \theta_{max} \end{aligned} \tag{4.5}$$

Table 4.1: Simulation Parameter for Sec. 4.2.3

Variable	Value
a	0.75 m
b	1.21 m
c	0.53 m
d	3 m
e	1 m
v_r	$\pm$1m/s
u_{max}	$90°/s$
δ_{max}	45°
θ_{max}	60°

The weighting matrix on the state is:

$$Q = \begin{bmatrix} 0 & 0 & 0 & 0 \\ 0 & 0 & 0 & 0 \\ 0 & 0 & 4 & 0 \\ 0 & 0 & 0 & 4 \end{bmatrix}$$

where the trailer heading error and the trailer position error are weighted only. The weighting parameter on the system input is $R = 1$. The other parameters are shown in Table 4.1. Gaussian zero-mean noises are added with a standard covariance of 0.02 for all states. The situation of moving forward is first simulated. The reference path is a circle with a radius of 6 meter. Fig. 4.3 shows the paths of tractor and trailer with trailer initial position at (3,1)m and heading angles of 22° and 30° for tractor and trailer respectively. Fig. 4.4 shows the trailer lateral position error with respect to time. Under the steady state, the tracking error is not exactly zero due to the measurement noise, but the mean value of the error under the steady state is nearly zero (about 10^{-3}).

Next, the case of moving backwards is tested by setting the tractor velocity to be negative. Fig. 4.5 is the system response tracking the same reference path above, but with backward motion. The initial position of the trailer is located at (3.1)m, and the initial

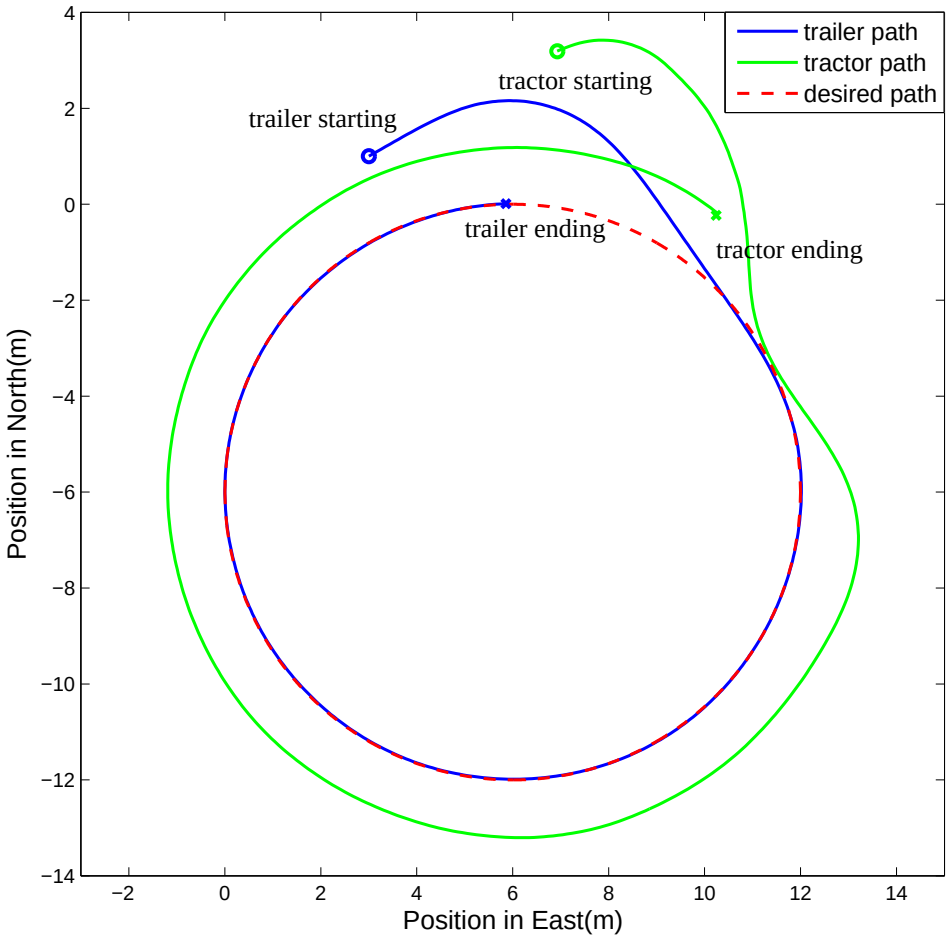

Figure 4.3: System response using steering rate input: forward motion

heading angles of tractor and trailer are zeros. The proposed controller stabilizes the system, and the tracking error converges to zero after a few seconds.

4.2.4 Summary A

In this section, two methods to remove the tracking error for a curved reference path is proposed. One is to use a feed-forward control. A suitable steering angle should be calculated and added in the control law. The other is to use steering rate as system input instead of steering angle. For the new control input, the model is augmented by an additional state

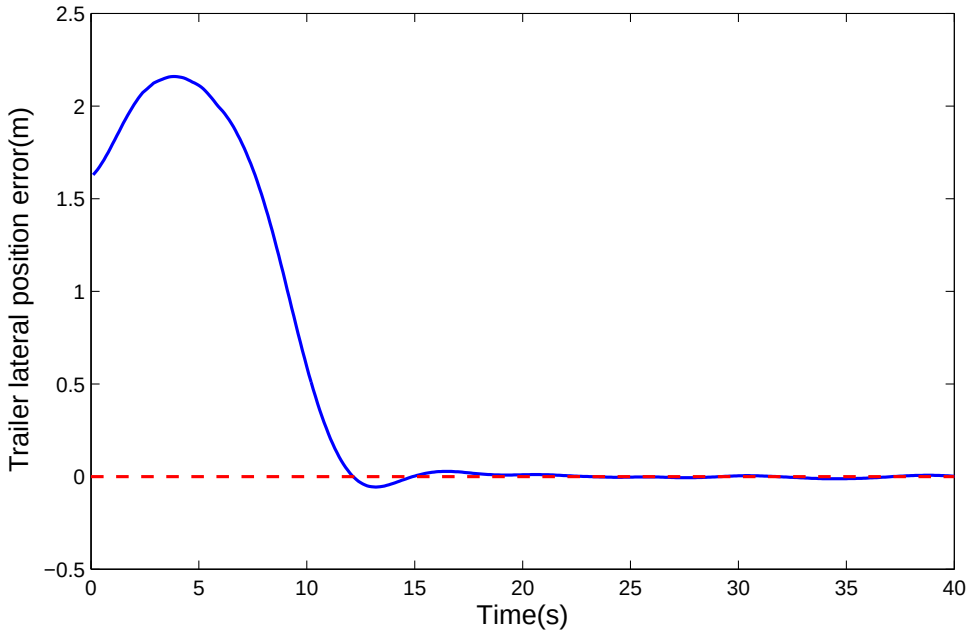

Figure 4.4: Lateral position error vs. time using steering rate input: forward motion

ω_r. The latter method have some advantages over the former one, such as more robust to model uncertainty, filtering the noise from the input, and easier to implement for the velocity control (steering rate) than the position control for the steering angle. The simulation results verify the method with both forward and backward motion.

4.3 Controller to remove the steady-state error with the presence of bias

Up to the last section, the steady-state error is removed for both curved and straight reference paths. Using the steering rate as control input in the model, the error can be still eliminated with the presence of steering angle bias. It's assumed that the measurement noise is zero-mean. However, a bias in the measurement can result in a steady-state error. Furthermore, the road or driving surface condition may produce a bias in the process noise. In this case, the closed-loop system may be still stable, but the bias in the model can generate a steady-state error. The idea of extended state observer (ESO) [45] [46], which estimates the disturbances in the system, can't solve this problem because the measurement

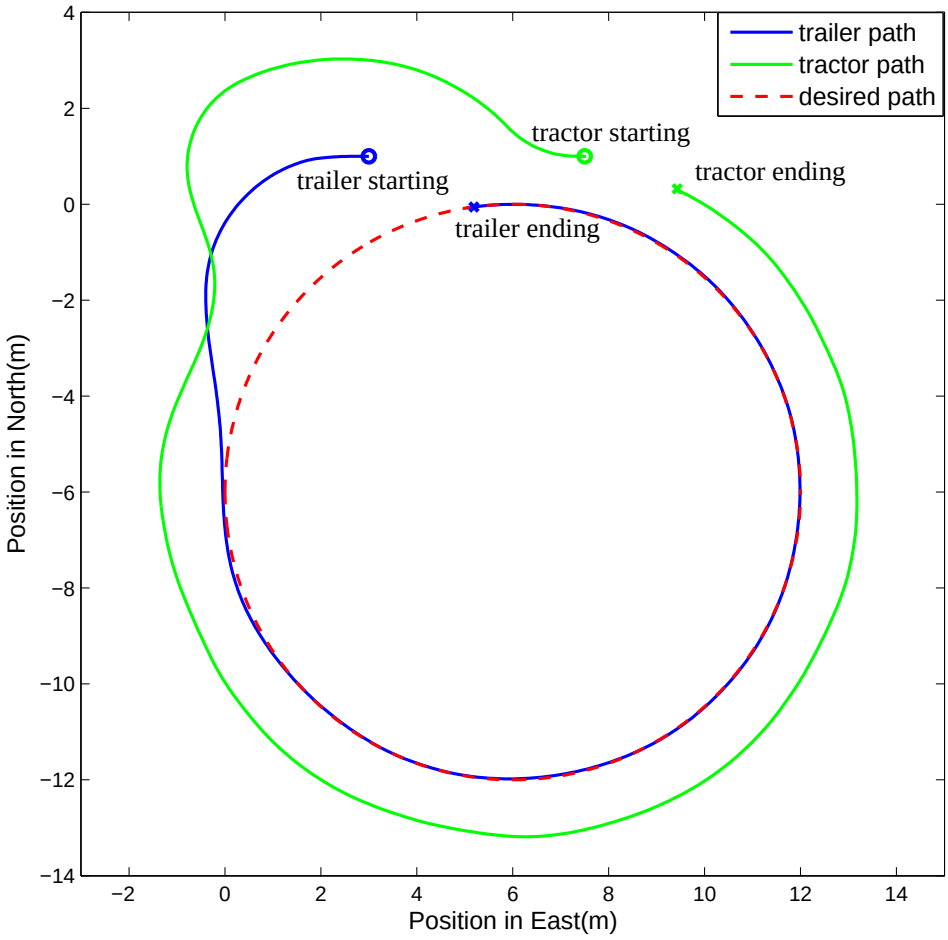

Figure 4.5: Paths of the tractor and the trailer using steering rate input: backward motion

bias is unobservable. Han proposed a scheme to remove the error for the system with the disturbances using active disturbances rejection control (ADRC) [47][48]. However, there are too many control parameters that are difficult to tune.

PID control is usually used in a wide rage of applications. The integral part can reject system disturbances and eliminate the output error. It's an attractive method because it's model-independent and it's effective for many situations. On the other hand, there are some drawbacks of integral control. First, the system is easier to oscillate and it may cause an excessive response, making the system output beyond the acceptable range. The setting time

may become longer than expected [1]. Second, since the control action has an effective range limit, the actuator may saturate since the integral control keeps accumulating the output error. Thus, the future control effort would be ignored until the saturation is offset [49].

4.3.1 State-space model with an integrator

As mentioned above, the tractor-trailer system may still have a steady-state error if there are disturbances and measurement bias. The proposed approach based on state feedback in the previous chapter can't eliminate this tracking error. The state variable used in the control law is:

$$x(k) = \begin{bmatrix} \varphi_r(k) \\ \omega_r(k) \\ \varphi_t(k) \\ y_t(k) \end{bmatrix}$$

The last variable in the state vector, $y_t(k)$ is the position error at time instant k. It's also the tracking error that should be totally eliminated. The time derivative of y_t is a function of the third variable $\varphi_t(k)$. The time derivative of φ_t is a function of the first variable $\varphi_r(k)$. And the second variable ω_r is the time derivative of $\varphi_r(k)$. In other words, the control effort related to $y_t(k)$ plays a similar role with the proportional control in PID, and the control efforts related to the other three variables have similar contribution to the system compared with the derivative control in PID. Therefore, there is no control effort corresponding to integral control to reject the bias.

To remove the steady-state error with the presence of disturbances and bias, an integrator is needed to be added in the model. Thus, the original model is augmented by an additional state y_I with the following dynamic:

$$\dot{y}_I = k_a y_t \tag{4.6}$$

where y_I is accumulated position error, and variable k_a is a positive gain to determine how fast the position error is accumulated. The larger k_a is, the faster the error is accumulated. Note that there is a difference from the integrator control in many research where the gain k_a equals one [50] [51].

4.3.2 Integral separation control

Some approaches have been proposed to overcome the "wind-up" phenomenon of integral control. An observer-based approach can be used to compensate for the input saturation [52] [53]. A conditioning technique is used to weaken the integral term in order to mitigate the windup of integration when the actuator saturation occurs [54].

The algorithms mentioned above mainly focus on the problem of actuator saturation. For the tractor-trailer systems, it's realized that it's unnecessary to introduce integral when the tracking error is large because the traditional controller without integration is able to reduce the error. The key attraction of integral control is to remove the steady-state error effectively. In other words, the author believes that the integral control should be used when the system gets close to the steady-state rather than the transient process. Furthermore, the bad response of system caused by integral control is basically from the excessive accumulation of output error. Note that the error would accumulate very fast when the trailer is not near the reference. Fig. 4.6 shows the step response of a typical second order system with a PI controller. Basically, the integral control is not needed until the output reaches point A. Generally speaking, if the initial error is large, the system response with integral control is usually unsatisfactory such as large overshoot and long settle time, due to the integration from the staring point. Therefore, integral separation is used for the tractor-trailer system. Concretely, when the absolute of position error is larger than a threshold ϵ_y, normal controller can be used to make the error converge, When the absolute of position error is smaller than the threshold, the integral control is added to remove the steady-state error. As a result, the error is integrated only when it's small. Thus, the possibility of actuator saturation

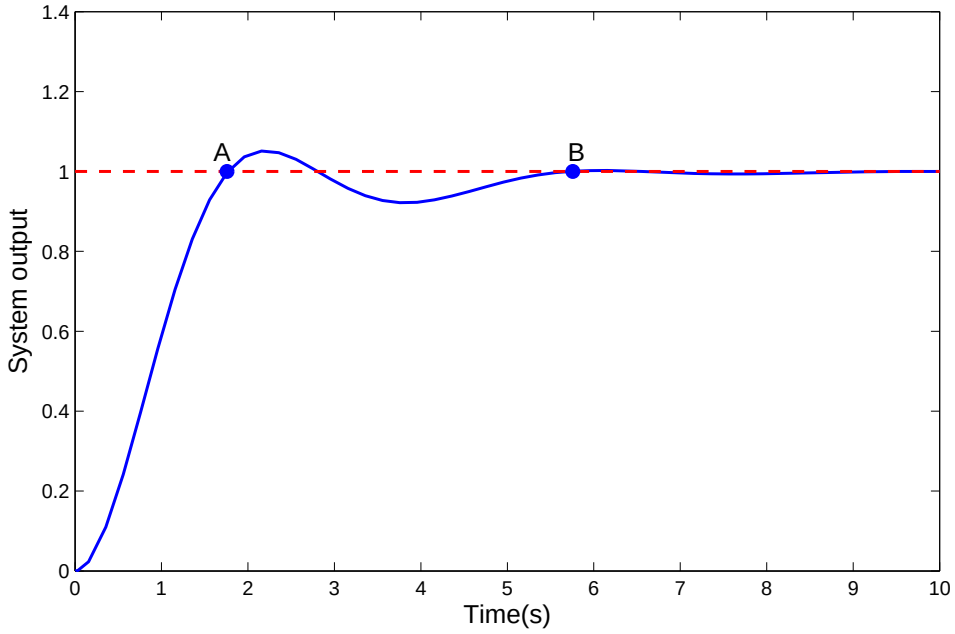

Figure 4.6: Step response of a typical second order system with PI controller

is greatly reduced. Moreover, when the trailer moves towards the reference path from a far initial point, the integral doesn't make an action until the system is near the reference. The excessive error accumulation is avoided. Therefore, the transient response would be acceptable with small overshoot, less osculation, and short settle time. In summary, with the integral separation, the disadvantage of integral control is avoided and the benefit is kept.

In PID controller, the integral separation has the following control law [51]:

$$u(k) = k_p[e(k) + \gamma k_i T \sum_{0}^{k} e(k) + \frac{k_d}{T}(e(k) - e(k-1)] \tag{4.7}$$

where T is the sample time, variable $e(k)$ is the output error:

$$e(k) = y(k) - r(k)$$

The variables k_p, k_i and k_d are the control gains for the proportional part, integral part and derivative part. Variable γ is an coefficient of integral control where

$$\gamma = \begin{cases} 0 & |e(k)| > \epsilon_y \\ 1 & |e(k)| \leq \epsilon_y \end{cases}$$

The algorithm of integral separation for a tractor-trailer system in state feedback approach is implemented as follows. Suppose state vector x is the variable in the normal controller without integral. The augmented state vector x_a which includes the integration of trailer position error is:

$$x_a(k) = \begin{bmatrix} x(k) \\ y_I(k) \end{bmatrix}$$

Then the controller is designed as:

$$u(k) = \begin{cases} k_n x(k) & |y_t| > \epsilon_y \\ k_n' x(k) + k_I y_I & |y_t| \leq \epsilon_y \end{cases} \tag{4.8}$$

and y_I is calculated by integration separation:

$$\dot{y}_I = \begin{cases} 0 & |y_t| > \epsilon_y \\ k_a y_t & |y_t| \leq \epsilon_y \end{cases} \tag{4.9}$$

where the gain k_a is from (4.6).

There is one problem remaining: how to decide the threshold position error ϵ_y. If the threshold is too large, the separation will have less effect on the system response and the drawback of integral control may still exist. If the threshold is too small, the integrator works only in a small range. the "wind-up" phenomenon may be avoided. However, the steady-state error maybe exist because y_I doesn't change if the absolute error is large than

ϵ_y. As a result, the steady-state error larger than ϵ_y will not be eliminated by the integral control.

From the analysis above, it can be expected that the transient behavior will be acceptable if ϵ_y is small, but a small threshold probably fails to totally remove the steady-state error. An adaptive approach is proposed here to adjust the threshold position as needed. A very important task is to identify the steady state and then check the output error. In the example of Fig. 4.6, the system can be regarded to be under the steady state after the point B because the system oscillate slightly. Therefore, if the output doesn't change heavily, the system is considered to be under the steady state. From the initial condition to point A, the system isn't under the steady state because the output increases rapidly. The response between A and B is not the steady state because the output oscillates. Therefore, the variance, or the standard variance of the output signal can be calculated to examine whether the system is under the steady state. if the variance is large, it illustrates that the system is going through the transient behavior.

Furthermore, the mean value of the output during the last several seconds, y_{ave} is used to compare with the threshold ϵ_y. If the mean value is larger than ϵ_y, it implies that the threshold is not big enough to remove the error, and ϵ_y should be a little larger. Thus, initial value of ϵ_y at the starting point can be set to be relatively small. The initial ϵ_y is also considered to be the normal value of the threshold position to get a satisfactory transient behavior, avoiding accumulating the error too much. Next, the mean value and the variance of the position error are examined every a few sample period. A receding horizon is used to obtain the statistical features of the error above. If the following conditions are satisfied simultaneously:

$$|y_{ave}| > \epsilon_y(k) \tag{4.10}$$

$$var(y_t) < \sigma_{th}^2 \tag{4.11}$$

where σ_{th} is a parameter to indicate how much the variance of position error is considered to be acceptable under the steady state. Then, ϵ_y should increase a bit. The algorithm runs every a few samples period rather than at each sample instant because the new position threshold may make the integrator start working and the system needs some time to respond the change of new y_I.

In summary, the adaptive ϵ_y is adjusted as the following pseudo code. where M is an

Algorithm 1 Adaptive ϵ_y algorithm

```
function "SETTING THRESHOLD POSITION ERROR"
    if mod(k, M) == 0 then
        ε_y = ε_base
        y_ave = mean(Σ_{i=k−N+1}^{k} e(i))
        y_std = std(e(i)),   i = k − N − 1 ... k
        if |y_ave| > ε_y  &&  y_std^2 < σ_th^2 then
            if |y_ave| − ε_y > ε_d then
                ε_y = ε_y + 2ε
            else
                ε_y = ε_y + ε
            end if
        else if y_ave < ε_base  &&  y_std^2 < σ_th^2 then
            ε_y = max(ε_y − ε, ε_base)
        end if
    end if
end function
```

integer to indicate the frequency of the algorithm execution, and the algorithm is executed every MT seconds where T is the sample period. Variable N is the time window for calculating the mean and variance of the error, and σ_{th} is the accepted total standard variance under the steady state, and can be calculated by:

$$\sigma_{th}^2 = \sigma_y^2 + \sigma_{noise}^2 \tag{4.12}$$

which means that σ_{th} can be determined by the sum of accepted output variance and the variance of measurement noise.

Furthermore, if y_{ave} during the past NT seconds is much larger than the threshold ϵ_y, ϵ_y would increase faster (added by 2ϵ). On the contrast, ϵ_y would increase relatively slower (added by ϵ) if the difference between the mean value and the threshold position is not big. Besides, when the tracking error goes back into a small range (in the range of $[-\epsilon_{base}, \epsilon_{base}]$), the threshold position ϵ_y will decrease until it's equal to the minimum, i.e. the initial value ϵ_{base}.

4.3.3 Simulation results

The controller with integral separation is verified by simulations. Differently from the simulations above, the system with two trailers are used instead of one trailer. The control goal is to make the center of the second trailer axle track a given path.

As mentioned earlier, the kinematic model of the tractor-trailer system can be extended to multiple trailers. For the system with two trailers, the nonlinear dynamic model is as follows:

$$\dot{\varphi}_r = \omega_r \tag{4.13}$$

$$\dot{\varphi}_{tf} = \frac{v_r \sin\theta_f - l_{hf}\omega_r \cos\theta_f}{l_{tf}} \tag{4.14}$$

$$\dot{\varphi}_{ts} = \frac{v_{tf} \sin\theta_s - l_{hs}\omega_{tf} \cos\theta_s}{l_{ts}} \tag{4.15}$$

$$\dot{x}_{ts} = v_{ts} \cos\varphi_{ts} \tag{4.16}$$

$$\dot{y}_{ts} = v_{ts} \sin\varphi_{ts} \tag{4.17}$$

where φ_{tf} and φ_{ts} are the heading angle of the first trailer and the second trailer.Variables l_{hf} and l_{hf} are the hitch lengths of the first trailer and the second trailer. Variables l_{tf} and l_{ts} are the lengths of the first trailer and the second trailer. Variables θ_f and θ_s are two hitch

angles:

$$\theta_f = \varphi_r - \varphi_{tf} \tag{4.18}$$

$$\theta_s = \varphi_{tf} - \varphi_{ts} \tag{4.19}$$

Besides, the velocities of the first trailer v_{tf} and the second trailer v_{ts} are:

$$v_{tf} = v_r \cos\theta_f + l_{hf}\omega_r \sin\theta_f$$

$$v_{ts} = v_{tf} \cos\theta_s + l_{hs}\omega_{tf} \sin\theta_s$$

With the small angle assumption, the linearized state-space model with steering rate as input, a fifth-order model can be derived:

$$\begin{bmatrix} \dot{\varphi}_r \\ \dot{\omega}_r \\ \dot{\varphi}_{ts} \\ \dot{\varphi}_{tf} \\ \dot{y}_{ts} \end{bmatrix} = \begin{bmatrix} 0 & 1 & 0 & 0 & 0 \\ 0 & 0 & 0 & 0 & 0 \\ a_{31} & a_{32} & a_{33} & 0 & 0 \\ a_{41} & a_{42} & a_{43} & a_{44} & 0 \\ 0 & 0 & 0 & v_r & 0 \end{bmatrix} \begin{bmatrix} \varphi_r \\ \omega_r \\ \varphi_{tf} \\ \varphi_{ts} \\ y_{ts} \end{bmatrix} + \begin{bmatrix} 0 \\ \frac{v_r}{l_r} \\ 0 \\ 0 \\ 0 \end{bmatrix} u \tag{4.20}$$

where a_{ij} is expanded in the Appendix. The model (4.20) is used when

$$|y_t(k)| > \epsilon_y(k) \tag{4.21}$$

Table 4.2: Parameter values for a tractor-two trailers system

Variable	Value
l_r	1.2 m
l_{hf}, l_{hs}	0.3 m
l_{tf}, l_{ts}	3.0 m
v_r	1m/s
u_{max}	$90°/s$
δ_{max}	$45°$
$\theta_{f,max}$	$60°$
ϵ_{base}	0.1m
ϵ	0.02m
σ_y	0.03
σ_{noise}	0.02

An augmented sixth-order model with the integral of error as an additional state can be obtained:

$$\begin{bmatrix} \dot{\varphi}_r \\ \dot{\omega}_r \\ \dot{\varphi}_{ts} \\ \dot{\varphi}_{tf} \\ \dot{y}_{ts} \\ \dot{y}_I \end{bmatrix} = \begin{bmatrix} 0 & 1 & 0 & 0 & 0 & 0 \\ 0 & 0 & 0 & 0 & 0 & 0 \\ a_{31} & a_{32} & a_{33} & 0 & 0 & 0 \\ a_{41} & a_{42} & a_{43} & a_{44} & 0 & 0 \\ 0 & 0 & 0 & v_r & 0 & 0 \\ 0 & 0 & 0 & 0 & k_a & 0 \end{bmatrix} \begin{bmatrix} \varphi_r \\ \omega_r \\ \varphi_{tf} \\ \varphi_{ts} \\ y_{ts} \\ y_I \end{bmatrix} + \begin{bmatrix} 0 \\ \frac{v_r}{l_r} \\ 0 \\ 0 \\ 0 \\ 0 \end{bmatrix} u \tag{4.22}$$

The model (4.22) is used when:

$$|y_t(k)| \leq \epsilon_y(k) \tag{4.23}$$

The system parameter is listed in Table 4.2. The sample time is 0.1 second. According to the rule (4.12), variable σ_{th}^2 in (4.11) is selected to be 0.036^2. Variable M in the algorithm is 4, i.e. the adaptive ϵ_y is revised every 0.4 second, and the receding window N for calculating the mean and variance is 12. Gaussian noises with the standard variance of 0.02 are added for all the state measurements.

LQR technique is used to determine the control gains in (4.8), balancing the system error and control effort, as well as obtaining large phase margin and magnitude margin.

Notice that the gains k'_n and k_I in (4.8) for the controller with integral are calculated as a whole. In other words, the gains above are obtained together based on the model (4.22). The weighting matrix on the states in the model (4.20) is

$$Q_1 = \begin{bmatrix} 0 & 0 & 0 & 0 & 0 \\ 0 & 0 & 0 & 0 & 0 \\ 0 & 0 & 1 & 0 & 0 \\ 0 & 0 & 0 & 5 & 0 \\ 0 & 0 & 0 & 0 & 3 \end{bmatrix}$$

The weight on the trailer heading error is a little bigger than the weight on the position since a smooth transient response is expected. The weighting matrix on the states for the model (4.22) is

$$Q_2 = \begin{bmatrix} 0 & 0 & 0 & 0 & 0 & 0 \\ 0 & 0 & 0 & 0 & 0 & 0 \\ 0 & 0 & 1 & 0 & 0 & 0 \\ 0 & 0 & 0 & 5 & 0 & 0 \\ 0 & 0 & 0 & 0 & 3 & 0 \\ 0 & 0 & 0 & 0 & 0 & 0.2 \end{bmatrix}$$

The last element of matrix Q_2 is on the weight on the error integral y_I. This parameter determines how much the variable of error integral affects the control input. The hitch angle between the tractor and the first trailer is also constrained by one-step prediction approach [15].

First, the reference path is a circle with a radius of 5 meter, and the center point is located at (5,-5)m. The measurement bias is added on the variables of tractor heading, tractor yaw rate, the first trailer heading, and the second trailer heading with a magnitude of 0.02 rad, 0.02 rad/s, 0.02 rad, and 0.01 rad respectively. The initial position of the second trailer is (0.5,0)m and the initial position error is 2.43 meter. Fig. 4.7 shows the paths of

three vehicles using the proposed control algorithm with integral separation. The second trailer gets close to the reference quickly and follows the given path with a small overshoot. Fig. 4.8 shows the comparison of position error with respect to time using the proposed algorithm, the control based on the model (4.20) without integral, and the control with integral term but no integral separation. The controller without the integral has a steady state error for about 8.5 centimeter. For the controller with integral control but without integral separation, the overshoot becomes very big. The maximum overshoot is about -1.95 meter. That's because the integral always works no matter how much the error is, resulting in a unnecessarily big y_I when the second trailer approaches the reference at the first time. Compared to the other two controller, the proposed methods has much smaller overshoot (the maximum overshoot is only -0.12 meter). Furthermore, the steady-state error is almost removed. The blue curve in Fig. 4.8 is very close to zero after 25 second.

Next, the reference paths becomes a straight line. The measurement bias is added on the variables of tractor heading, tractor yaw rate, the first trailer heading, and the second trailer heading with a magnitude of 0.01 rad, -0.02 rad/s, -0.02 rad, and -0.02 rad respectively. Besides, biased process disturbances are also added on the dynamic of the second trailer positions:

$$\dot{x}_{ts} = v_{ts} \cos \varphi_{ts} + 0.01$$

$$\dot{y}_{ts} = v_{ts} \sin \varphi_{ts} + 0.01$$

The initial position error is 2.5 meter. Fig. 4.9 shows the vehicles paths in global coordinate. The vehicles first moves towards the reference, reducing the tracking error quickly, then make the second trailer approach the reference smoothly, and finally the second trailer tracks the given path very accurately. Notice that due to the biased process disturbances, the tractor and the first trailer don't follow the reference path of the second trailer (drawn in red dash). Fig. 4.10 shows the comparison of the position error y_{ts} versus time using three

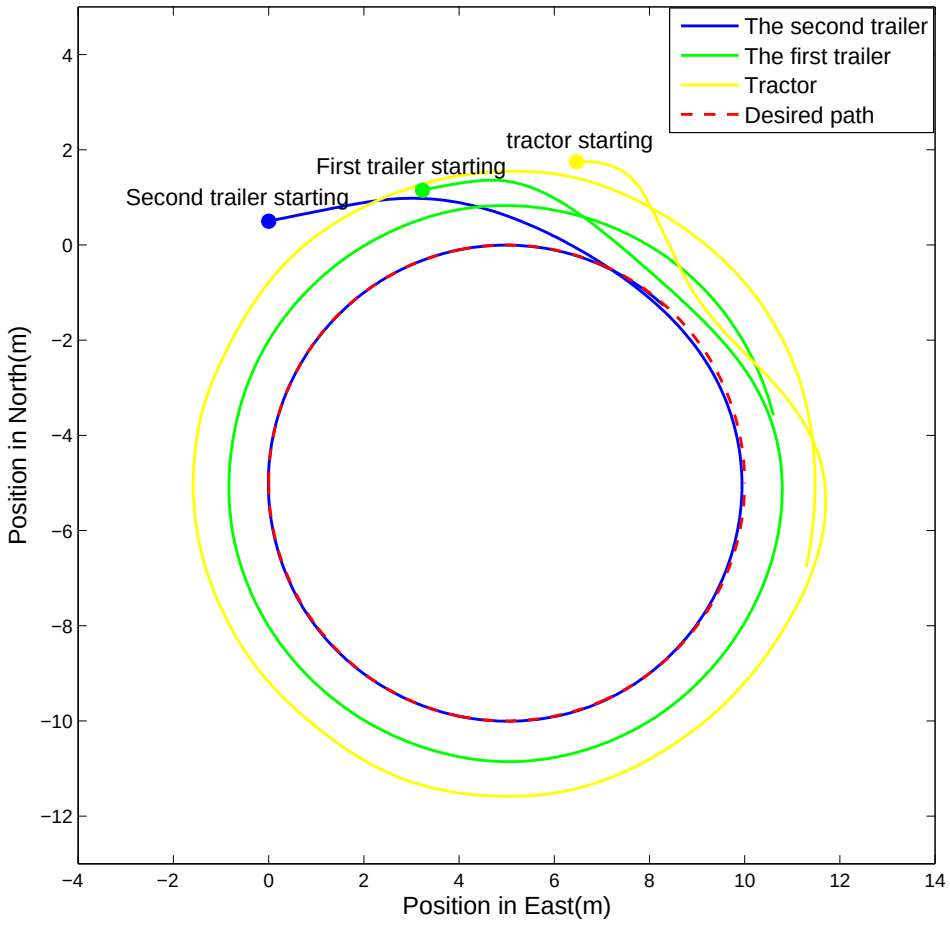

Figure 4.7: System response using integral separation to track a curved reference path

methods. Similar phenomenon with Fig. 4.8 can be observed that the controller without integral term has a steady-state error for about 16 cm. The blue curve generated by the proposed algorithm has the same shape with the curve generated by the former controller at the beginning. From the seventeenth second, however, the error begins to converge to zero, rather than keeping nearly constant. The approach with integral control, but without using the integral separation has very large overshoot and longer settle time, which are possibly unacceptable.

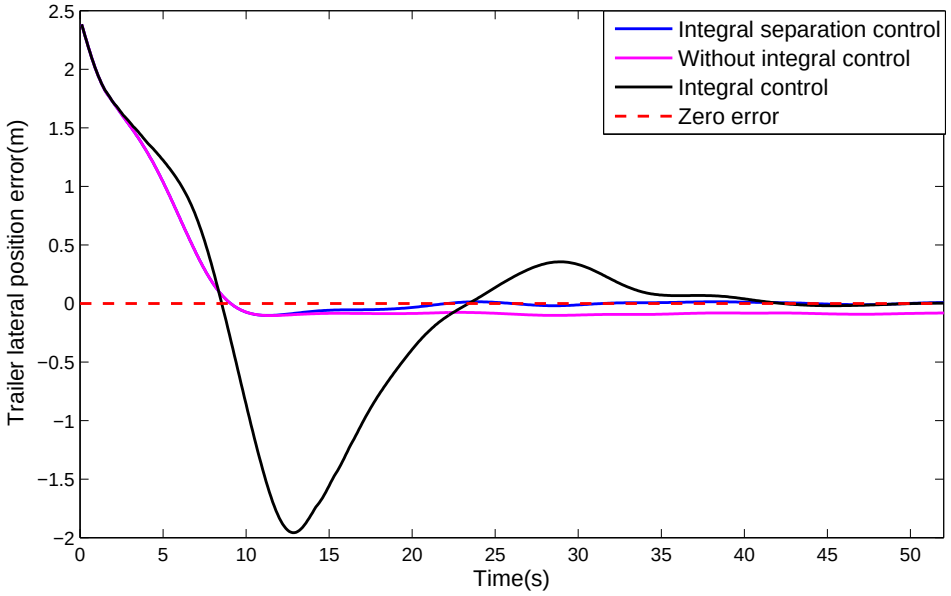

Figure 4.8: Lateral position errors tracking a curved reference path using three methods

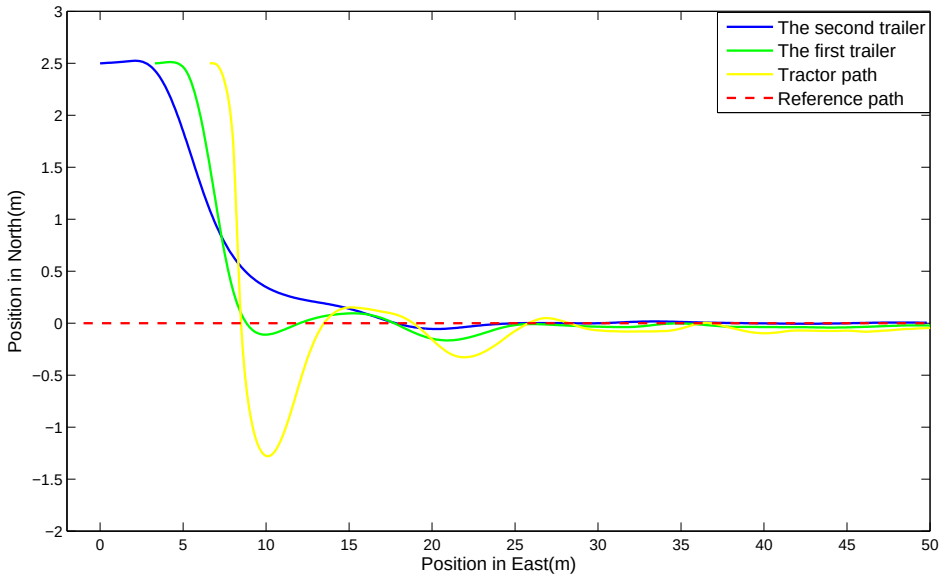

Figure 4.9: System response using integral separation to track a straight line

4.3.4 Summary B

In this section, a controller based on integral separation algorithm is proposed for tractor-trailer system to remove the steady-state error with the presence of bias. An extra state variable is introduced to calculated the integral term of output error. Integral

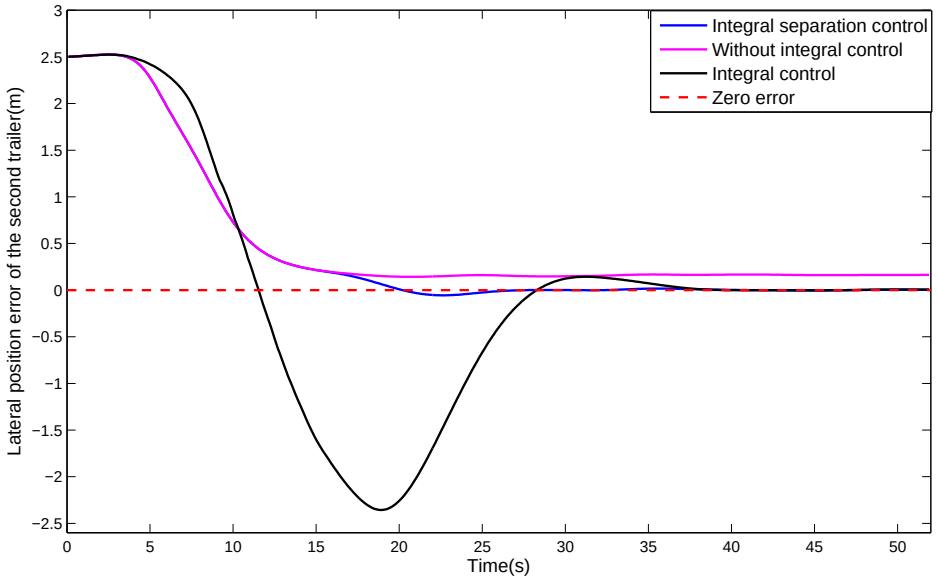

Figure 4.10: Lateral position errors tracking a straight line using three methods

separation is applied in a such way that the error is accumulated only when the tracking error is relatively small to avoid the integral of error becoming unnecessarily large. A system with two trailers is used to verify the proposed method. Results show that the algorithm is able to remove the measurement bias on heading angles and yaw rate as well as constant process disturbance. Moreover, the system response is satisfactory with a good transient behavior when compared to the method without the integral separation algorithm.

It's also found that the proposed approach can't remove the bias from the position measurement of the controlled trailer. Concretely, for the case of a tractor with two trailers system, the position bias can be removed if it's from the measurements of the tractor or the first trailer. If the position measurement of the second trailer has bias, it can't be removed because the system can't realize that bias from other variables. This problem can be solved if other sensor, such as computer vision, is introduced to the system.

4.4 Chapter summary

The problems of steady-state error on both straight and curved path have been completely solved by the methods presented here. In the next chapter, the problem of reducing the feedback instrumentation requirement is addressed by state estimation theory.

Chapter 5

State Estimation of a Tractor-trailer System Based on Unscented Kalman Filter

State estimation is usually used when some variables are not measurable in the system. In this chapter, an state observer based on unscented Kalman filter is proposed to estimate the states of a tractor-trailer system.

5.1 Introduction

5.1.1 Problem Statement

In the previous chapters, the tracking error when the system is near the intersections of different reference paths, or far form the reference path is reduced successfully. The position error may be also reduced even a measurement bias exists. For the controllers above, it's assumed that all the states in the system, including positions, heading angles and yaw rate, are available. It's feasible if two sets of global positioning system (GPS)/inertial navigation system (INS) are equipped on both the tractor and the trailer. However, the implement cost becomes very high. To decrease the cost, an optical encoder can be installed to measure the hitch angle so that the tractor heading can be calculated rather than measured, and only one GPS/INS system is used for the measurement of trailer position and the trailer heading. The positions of the tractor can be obtained by the trailer positions and the heading angles of the tractor and trailer:

$$\begin{aligned} x_r &= x_t + l_t \cos\varphi_t + l_h \cos\varphi_r \\ y_r &= y_t + l_t \sin\varphi_t + l_h \sin\varphi_r \end{aligned} \tag{5.1}$$

where x_r and y_r are the tractor positions in global coordinate. However, in the past experience (Hodo, Payne and Singh), the encoder is very difficult to mount securely and robustly.

It's also easily damaged. In this dissertation, the author tries to reduce the hardware cost further. Differential GPS (DGPS) sensors with real-time kinematic correction (RTK) are used only to measure the positions of the trailer, which has the accuracy of about 2 centimeter [3][12]. Thus, the heading angles of the tractor and trailer are estimated from the position measurements. Furthermore, the tractor yaw rate can be obtained by the tractor heading if needed.

5.1.2 Linear full-order observer

A full-order observer can be designed for linear systems so that the estimation error converges to zero. The system equations are:

$$\begin{aligned} \dot{x} &= Ax + Bu \\ y &= Cx \end{aligned} \tag{5.2}$$

To design a state observer, the output error, which is the difference between the system output and the model output, is used as the feedback variable to correct the model estimation continuously [1]. This structure is shown in Fig. 5.1. The closed-loop dynamic for the state estimator is:

$$\begin{aligned} \dot{\hat{x}} &= A\hat{x} + Bu + L(y - C\hat{x}) \\ \hat{y} &= C\hat{x} \end{aligned} \tag{5.3}$$

where L is the estimator gain and y is the system output. Define the error state:

$$\tilde{x} = x - \hat{x}$$

Subtract (5.2) by (5.3), the error dynamic can be obtained:

$$\dot{\tilde{x}} = (A - LC)\tilde{x} \tag{5.4}$$

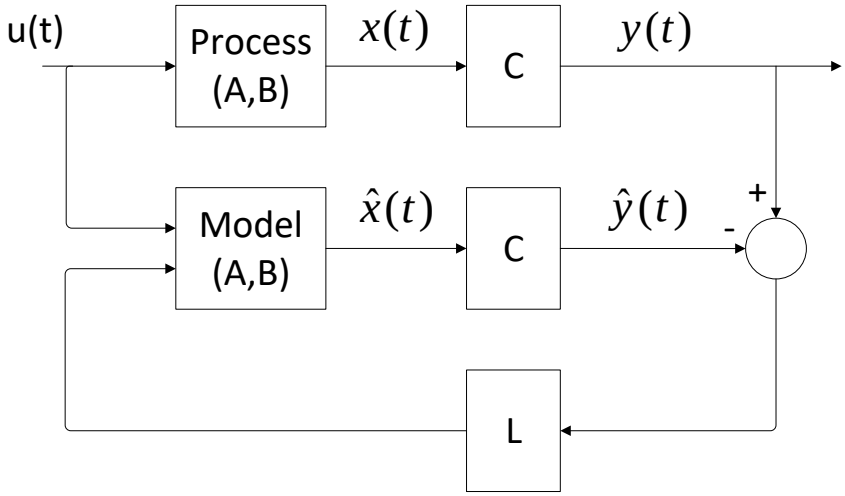

Figure 5.1: System structure of a full-order state observer

Therefore, the estimated state will converge to the real value as long as all the eigenvalues of $(A - LC)$ have negative real component, i.e. the closed system (5.4) is stable.

5.2 Kalman filter

In the last section, a state observer can be designed when an appropriate observer gain L can be determined. Kalman proposed an optimal way to calculate the estimator gain considering the model dynamic and the characteristics of process and measurement noise [55]. This method is called Kalman filter. It is able to provide an unbiased estimation for a linear system in a statistical sense, and the estimator gain, i.e. Kalman gain is obtained in such a way that the trace of process covariance matrix is minimized. The discrete Kalman filter has been successfully used in a large amount of applications [56].

5.2.1 Kalman filter

The process to be estimated can be modeled as:

$$\begin{aligned} x_{k+1} &= Fx_k + Gu_k + w_k \\ y_k &= Hx_k + v_k \end{aligned} \tag{5.5}$$

where w_k and v_k represent the process noise and measurement noise respectively, and the noises are assumed to be independent, white and Gaussian:

$$w_k \sim N(0, Q_k), \quad v_k \sim N(0, R_k) \tag{5.6}$$

where Q_k and R_k are covariance of the noises respectively.

The process of computing estimated state at each sample can be divided into two steps. The first step is time update. In the time update, a priori state estimation is predicted by the system model based on a posteriori estimation at the last time instant. The following equations are calculated:

$$\hat{x}_{k+1}^- = F\hat{x}_k + Gu_k \tag{5.7}$$

$$P_{k+1}^- = FP_k^+F + Q_k \tag{5.8}$$

where P_k^+ is a posterior process uncertainty calculated at the last sample. In the measurement update, a new output measurement is introduced to improve the a priori estimation. Then a posteriori estimations of state and process uncertainty are calculated:

$$K_k = P_k^- H^T (HP_k^- H^T + R_k)^{-1} \tag{5.9}$$

$$\hat{x}_{k+1}^+ = \hat{x}_{k+1}^- + K_k(y_{k+1} - H\hat{x}_{k+1}^-) \tag{5.10}$$

$$P_{k+1}^+ = (I - K_k H)P_{k+1}^- \tag{5.11}$$

After the pair of time update and measurement update, the process is repeated in such a recursive way that the a posteriori estimation at current sample is used to compute the a priori estimation for next sample.

5.2.2 Extended Kalman filter

Kalman filter can be used as a powerful approach to estimate state for linear systems. For nonlinear systems, extended Kalman filter (EKF) can be used instead. EKF has been applied in many fields such as navigation and electronics [57][58].

In general, the system dynamic in continuous-time domain can be expressed by the following differential equation:

$$\dot{x} = f_c(x, u) + B_w w \tag{5.12}$$

A discrete form of (5.12) with the system output can be expressed as follows:

$$\begin{aligned} x_k &= f(x_{k-1}, u_{k-1}) + w_{k-1} \\ y_{k-1} &= h(x_{k-1}) + v_{k-1} \end{aligned} \tag{5.13}$$

where f and h are nonlinear generally. In time update, a priori estimation is obtained by:

$$\hat{x}_k^- = f(\hat{x}_{k-1}^+, u_{k-1}) \tag{5.14}$$

$$\hat{y}_k^- = h(\hat{x}_{k-1}^+) \tag{5.15}$$

Instead of using the system matrix F in the linear case, Jacobian matrix with respect to the state is used to calculated a priori process uncertainty:

$$P_k^- = A_{k-1} P_{k-1}^+ A_{k-1} + Q_k \tag{5.16}$$

where

$$A_{k-1} = \left.\frac{\partial f}{\partial x}\right|_{x=\hat{x}_{k-1}^+} \tag{5.17}$$

In the measurement update, the Kalman gain and the a posteriori estimations of state and process uncertainty matrix are:

$$K_k = P_k^- H_k^T (H_k P_k^- H_k^T + R_k)^{-1} \tag{5.18}$$

$$\hat{x}_k^+ = \hat{x}_k^- + K_k(y_k - H\hat{x}_k^-) \tag{5.19}$$

$$P_k^+ = (I - K_k H_k) P_k^- \tag{5.20}$$

where

$$H_k = \left.\frac{\partial h}{\partial x}\right|_{x=\hat{x}_k^-}$$

5.3 Adaptive unscented Kalman filter

In EKF, Jacobian matrix is calculated at each sample. In fact, the state distribution is propagated through the first order approximation of the original nonlinear system using Taylor series expansion. The linearization is not accurate enough, resulting in an appreciable estimation error on the state as well as the process uncertainty [59].

Instead of using Jacobian matrix, unscented Kalman filter (UKF), however, uses some discrete carefully chosen points, called sigma points to capture the mean and the distribution of the state [59]. The estimation using UKF has been proved to be more accurate than EKF, and the number of computations in UKF scales with the dimensions at the same rate as the lineaization method in EKF [60]. The classical UKF algorithm is introduced first, then an adaptive UKF approach is proposed.

5.3.1 Unscented Kalman filter

The unscented Kalman filter uses unscented transformation to obtain sigma points which capture the state distribution. Those points then propagate through the state equation, and are used to calculate a priori estimated state, process uncertainty and system outputs in

the time update step. In the measurement update step, a posteriori estimation of state and process uncertainty are calculated. The algorithm of a standard UKF is first reviewed.

The filter works in discrete domain, The nonlinear process in continuous-time domain and discrete-time domain are expressed by (5.12) and (5.13) respectively. There are $(2n+1)$ sigma points selected where n is the dimension of the system.

$$\begin{aligned}
&\chi_{0,k-1} = \hat{x}_{k-1} \\
&\chi_{i,k-1} = \hat{x}_{k-1} + (\gamma\sqrt{P_{x,k-1}})_i, i = 1, ..., n \\
&\chi_{i,k-1} = \hat{x}_{k-1} - (\gamma\sqrt{P_{x,k-1}})_i, i = n+1, ..., 2n
\end{aligned} \tag{5.21}$$

where $\gamma = \alpha\sqrt{n+\kappa}$. κ is a scaling parameter, and α is used to determine the spread of sigma points [61]. Variable $\hat{x}_{k-1}$ is the estimated state at sample $k-1$, Parameter γ is a scaling vector and $P_{x,k-1}$ is state error covariance matrix at last sample. Here the square root of $P_{x,k-1}$ matrix is needed. There are some algorithms to deal with it such as Cholesky, diagonalization, and Schur methods [62].

The UKF still has two steps at each sample. In the time update, a priori estimations of state, output and state error covariance are calculated:

$$\chi^i_{k|k-1} = f(\chi_{k-1}, u_{k-1}) \tag{5.22}$$

$$\hat{y}_k = \sum_{i=0}^{2n} W_i^m h(\chi_{k|k-1}) \tag{5.23}$$

$$\hat{x}_k^- = \sum_{i=0}^{2n} W_i^m \chi^i_{k|k-1} \tag{5.24}$$

$$P^-_{x,k} = \sum_{i=0}^{2n} W_i^c (\chi^i_{k|k-1} - \hat{x}_k^-)(\chi^i_{k|k-1} - \hat{x}_k^-)^T + Q_k \tag{5.25}$$

$$W_0^m = \frac{\alpha^2(n+\kappa) - n}{\alpha^2(n+\kappa)} \tag{5.26}$$

$$W_0^c = W_0^m + (1 - \alpha^2 + \beta) \tag{5.27}$$

where $\hat{y}_k$ is the estimated system output, $\hat{x}_k^-$ is a priori state estimate and $P_{x,k}^-$ is a priori state error covariance matrix. Parameter β is used to tune the filter. In the measurement update following equations are calculated:

$$P_{y,k} = \sum_{i=0}^{2n} W_i^c (h(\chi_{k|k-1}) - \hat{y}_k)(h(\chi_{k|k-1}) - \hat{y}_k)^T + R_k \tag{5.28}$$

$$P_{xy,k} = \sum_{i=0}^{2n} W_i^c (\chi_{k|k-1}^i - \hat{x}^-)(h(\chi_{k|k-1}) - \hat{y}_k) \tag{5.29}$$

$$K_k = P_{xy,k} P_{y,k}^{-1} \tag{5.30}$$

$$\hat{x}_k = \hat{x}_k^- + K_k(y_k - \hat{y}_k) \tag{5.31}$$

$$P_{x,k} = P_{x,k}^- - K_k P_{y,k} K_k^T \tag{5.32}$$

where K_k is the Kalman gain, y_k is actual measurement at sample k, and $P_{x,k}$ is a posteriori state error covariance.

The UKF is able to estimate the a priori state error covariance P_k^- more accurately by using unscented transformation than Jacobian matrix in (5.16). However, the UKF still suffers some drawbacks from traditional Kalman filter due to the fixed process noise covariance Q_k in (5.16). For the state estimation of a mobile robot, the vehicle may work in various road conditions. So the characteristic of process noise is difficult to determine before the implementation. Thus, a mismatch between real process noise characteristic and the one in the filter usually occurs and the performance of the filter degrades. Besides, fixed Q_k matrix may lead to a slow respond if the disturbance occurs and measurements have a sudden change.

5.3.2 Adaptive unscented Kalman filter

As mentioned before, an adaptive process noise covariance is helpful to provide a better observer performance. Xia, Rao *et al.* developed an adaptive fading Kalman filter (AFKF) for linear systems, which ensured the Kalman gain was optimal by making the

auto-covariance of residual equal zero [63]. Cao and Tian designed an AUKF algorithm to correct the process uncertainties by an adaptive gain acting on the a priori process uncertainty matrix [64]:

$$P_{k,a}^{-} = \eta P_k^{-} \tag{5.33}$$

Song and Han revised the UKF by using MIT rule to adjust the process uncertainties adaptively [65], but the computation burden became much heavier due to many time-derivative functions.

In this dissertation, an AUKF is designed by adjusting the process noise covariance matrix Q_k at each sample with an adaptive gain. The gain is calculated based on the optimal feature in [63]. Furthermore, a real-time estimated $\hat{Q}_k$ is calculated based on the approach in [66], and the elements of the estimated noise covariance matrix are properly constrained rather than being used directly to guarantee the positive definite of the matrix.

Instead of (5.27), the estimated a priori state error covariance matrix is modified by

$$P_{x,k}^{-} = \sum_{i=0}^{2n} W_i^c (\chi_{k|k-1}^i - \hat{x}_k^-)(\chi_{k|k-1}^i - \hat{x}_k^-)^T + \eta(k) Q_{a,k-1} \tag{5.34}$$

where $\eta(k)$ is a positive gain, and $Q_{a,k-1}$ is the adjusted process noise covariance at the last time instant in discrete-time domain. The advantage of using $\eta(k)Q_{a,k-1}$ instead of original fixed noise covariance matrix Q_k is that the process uncertainty as well as the characteristic of each noise can be estimated adaptively.

An estimation algorithm for process noise covariance matrix is designed [16]. In [66], process noise covariance matrix is estimated on-line by:

$$\hat{Q}_k = \frac{1}{N} \sum_{j=k-N+1}^{k} (\Delta x_j \Delta x_j^T) + P_{x,k} - A_k P_{x,k-1} A_k^T \tag{5.35}$$

where A_K is Jacobian matrix in (5.17) and Δx_j is the difference between a posterior and a priori estimated state:

$$\Delta x_j = \hat{x}_j - \hat{x}_j^- = K_k(y_j - \hat{y}_j)$$

Use (5.35) in UKF scheme and use fading factor ρ_1 instead of the average operation to overweight the recent values, the real-time $\hat{Q}_k$ is:

$$\hat{Q}_k = C_{x,k} + Q_{k-1} - K_k P_{y,k} K_k^T \tag{5.36}$$

where

$$C_{0,k} = \frac{\rho_1 C_{x,k-1} + \Delta x_j \Delta x_j^T}{\rho_1 + 1} \tag{5.37}$$

where $0 < \rho_1 \leq 1$. However, as mentioned earlier, (5.36) may yield a $\hat{Q}_k$ which is not positive-definite. To deal with this problem, some constraints have to be made. If the noises are uncorrelated, $\hat{Q}_k$ should be diagonal. Thus, the constraints can be made so that each element on the diagonal becomes positive. If the process noises are correlated, the assumption of diagonal Q_k is not valid. However, the noise covariance in continuous-time domain $\hat{Q}_c$ is usually diagonal. Without generality, when the sample time is small, the estimated $\hat{Q}_c$ can be obtained if $B_w' B_w$ is non-singular:

$$\hat{Q}_c = \frac{1}{T}(B_w' B_w)^{-1} B_w' \hat{Q}_k B_w (B_w' B_w)^{-1} \tag{5.38}$$

To guarantee the positive definiteness, the constraints for the diagonal terms in $\hat{Q}_c$ are as follows:

$$\hat{Q}_c(i,i) \geq Q_c(i,i), \quad i = 1 \ldots d \tag{5.39}$$

where d is the number of disturbances in (5.12), $\hat{Q}_c(i,i)$ is the ith diagonal element of $\hat{Q}_c$, and Q_c is a pre-defined process noise covariance in continuous time domain. Normalize the

constrained $\hat{Q}_c$ so that:

$$min(\frac{\hat{Q}_c(i,i)}{Q_c(i,i)}) = 1, \quad i = 1 \dots d$$

Notate this adjusted matrix as $\hat{Q'}_c$, then the process noise covariance matrix $Q_{a,k}$ in (22) can be derived:

$$Q_{a,k} = B_w \hat{Q'}_c B'_w T \tag{5.40}$$

Since a posteriori state estimation is needed in the calculation of $Q_{a,k}$, $Q_{a,k-1}$ obtained at the last time instant is used in (5.34).

In [63], Xia *et al.* proposed an adaptive fading linear Kalman filter which ensured that the sequence of residuals was uncorrelated by the following equation:

$$H_k P^-_{x,k} H^T_k = C_{0,k} - R_k \tag{5.41}$$

where H_k is output matrix, and $C_{0,k}$ is the covariance of the residual. This idea is extended in UKF scheme in this dissertation. Define the residual:

$$z_k = y_k - h(\hat{x}_k)$$

Then $C_{0,k}$ is expressed as:

$$C_{0,k} = E[z_k z^T_k].$$

A fading factor ρ_2 is applied on the estimation of $C_{0,k}$:

$$C_{0,k} = \frac{\rho_2 C_{0,k-1} + z_k z^T_k}{\rho_2 + 1} \tag{5.42}$$

To utilize this result in UKF, substitute (5.34) into (5.41):

$$\sum_{i=0}^{2n} W^c_i (h(\chi_{k|k-1}) - \hat{y}_k)(h(\chi_{k|k-1}) - \hat{y}_k)^T + \eta(k) Q_{a,k} = C_{0,k} - R_k \tag{5.43}$$

Taking trace in both sides of (5.43):

$$\eta(k) = \frac{trace(C_{0,k} - R_k) - trace(\sum_{i=0}^{2n} W_i^c (h(\chi_{k|k-1}) - \hat{y}_k)(h(\chi_{k|k-1}) - \hat{y}_k)^T)}{trace(HQ_{a,k}H^T)} \tag{5.44}$$

Since relatively large process noise covariance can contribute to a quick response after a disturbance acts on the system, $\eta(k)$ is set to be larger than 1:

$$\eta(k) = max(1, \eta(k)) \tag{5.45}$$

Up to (5.45), the gain $\eta(k)$ and the process noise covariance $Q_{a,k-1}$ in (5.34) are obtained. Thus, compared to EKF, the estimation of process uncertainty is improved in two aspects. One is to apply UKF instead of EKF, using sigma points rather than first-order linearization to propagate the state. The other is to estimate the covariance of process noise at each sample.

5.3.3 Initial value of estimated state

Suppose that the observer starts working at time t_k. The measurement of position estimation at t_k can be selected to be the initial position estimation. Furthermore, the trailer heading can be roughly calculated from the position measurement difference between t_k and t_{k-1}:

$$\varphi_{es} = \arctan \frac{Y_k - Y_{k-1}}{X_k - X_{k-1}} \pm m\pi$$

where Y and X are the position measurements in global coordinate. Parameter m is used to extend the domain of φ_{es} from $(-\pi/2, \pi/2)$ to $(-\pi, \pi)$, and its value can be 0 or 1. This estimation is not accurate especially when the path of the trailer is a curve. But it's still reasonable to be used as an initial value of heading angle estimation. Therefore, the initial

Table 5.1: Parameters for tractor-trailer system

Variable	Description	Value
l_r	Length from front tire of tractor to rear tire of tractor	0.96 m
l_h	Length from back tire of the tractor to hitch	0 m
l_t	length from hitch to the rear tire of trailer	2.5 m
v_r	Longitudinal velocity of tractor	1m/s

estimation x_0 can be:

$$x_0 = \begin{bmatrix} \varphi_{r,0} \\ \varphi_{t,0} \\ e_{t,0} \\ n_{t,0} \end{bmatrix} = \begin{bmatrix} \varphi_{es} \\ \varphi_{es} \\ X_k \\ Y_k \end{bmatrix} \tag{5.46}$$

5.4 Simulation results

System parameters used in the simulation are shown in Table 5.1. It's an on-axle hitching system, and the system input is the tractor yaw rate. The sample rate is 10 Hz, and B_w is an identity matrix. Tuning parameter κ in (5.26) α and β in (5.27) are 0, 0.01 and 2 respectively. Fading factor ρ_1 in (5.37) and ρ_2 in (5.42) are 0.4. The parameter in the filter is:

$$Q_k = \begin{bmatrix} 10^{-6} & 0 & 0 \\ 0 & 10^{-6} & 0 \\ 0 & 0 & 10^{-6} \end{bmatrix}$$

The measurement noise covariance matrix is:

$$R_k = \begin{bmatrix} 0.0004 & 0 \\ 0 & 0.0004 \end{bmatrix}$$

Notice that the initial value of estimated state is not obtained from (5.46). Instead, estimated state at the beginning is chosen so that the initial estimation error is relatively large in order to observe the error convergence.

Table 5.2: Estimation RMSE using three methods when process noise mismatches

	EKF	SUKF	The proposed method
Tractor heading	3.07°	2.60°	2.07°
Trailer heading	1.76°	1.32°	1.11°
Trailer position in North	2.25 cm	1.46 cm	1.10 cm
Trailer position in East	2.44 cm	1.21 cm	1.01 cm

Two different scenarios are tested. In the first case, the process noise covariance in the filter mismatches the real one. It is implemented by multiplying actual noise covariance with a constant number of 20. EKF, Standard UKF (SUKF), and the proposed AUKF are used to estimate the states of tractor heading φ_r, trailer heading φ_t, trailer positions n_t and e_t. Initial estimation error is 0.8 rad, 1 rad, -1 m and 1 m respectively. Fig. 5.2 shows the estimation errors of tractor heading and trailer heading using EKF and the proposed method. The estimation errors by EKF converges slowly,and it's also larger than using the proposed AUKF approach at the most of samples after six second. Table 5.2 shows the root-mean-square errors of the estimated four states using three approaches during the period from 4 second for thirty times simulations. Standard UKF and the proposed AUKF have better result than EKF, which coincides with the theoretical analysis. Moreover, the estimation errors by the propsed AUKF are the smallest for all the states, reducing 20.38%, 15.91%, 24.66% and 16.53% respectively compared with SUKF. Next, the process noise covariance matches the real value, but a disturbance is added on the tractor at time $T = 4.5s$. It is implemented by adding 18° to the tractor heading φ_r. Fig. 5.3 shows the estimation errors of tractor heading and trailer heading using standard UKF and the proposed AUKF algorithm. AUKF algorithms respond faster than SUKF when a sudden change occurs for the two heading angles. Fig. 5.4 shows the estimation errors of positions in two directions. After the disturbance occurs, the estimated states using the proposed method are very close to the real values, while the estimation errors using SUKF first increase to about 7.8 cm, then converge slowly for both state variables. Table 5.3 presents the root-mean-square estimation

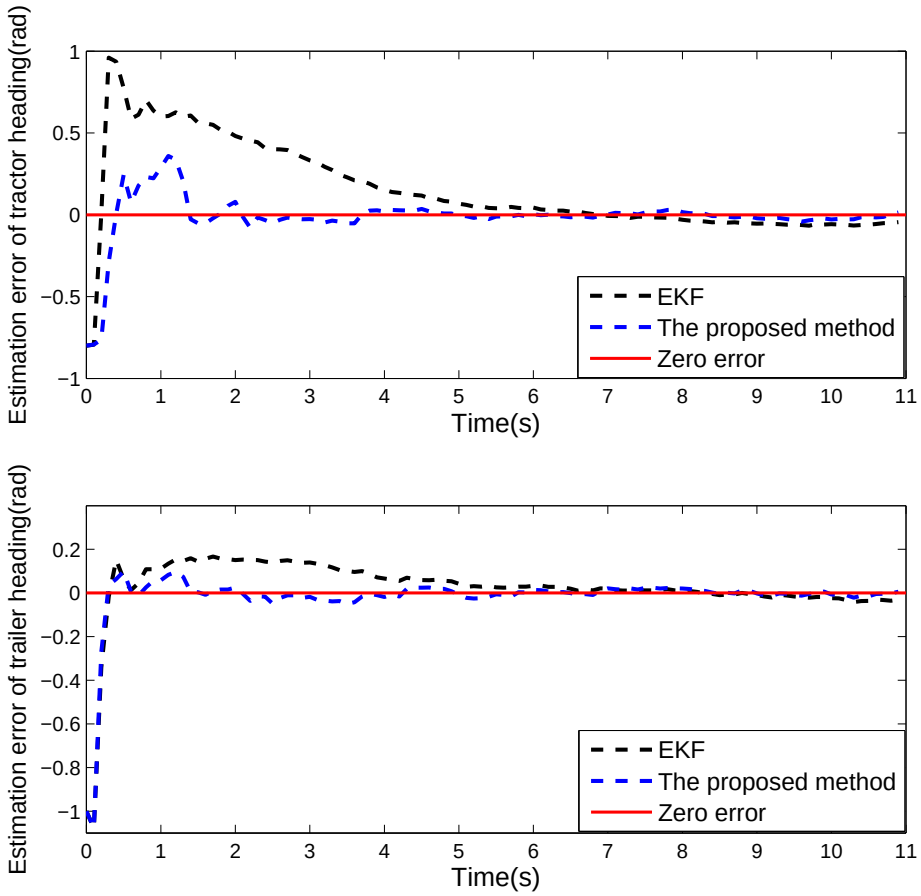

Figure 5.2: Estimations of heading angles when process noise covariance mismatches

errors using three methods from 4.5 second for thirty times simulations. The simpler AUKF algorithm still applies adaptive UKF with the gain $\eta(k)$ in (5.34), but uses original Q_k to calculate the a priori process uncertainty rather than $Q_{a,k-1}$ .The proposed algorithm stands out which has the smallest estimation error. Compared with the simpler AUKF algorithm, the RMSE values for tractor heading angle, trailer heading angle and trailer positions in two directions reduce 1.90°, 1.34°, 2.16 cm and 1.82 cm respectively.

5.5 Summary

In this chapter, a state observer is designed using an adaptive unscented Kalman filter with the measurements of trailer positions. The proposed observer works without the

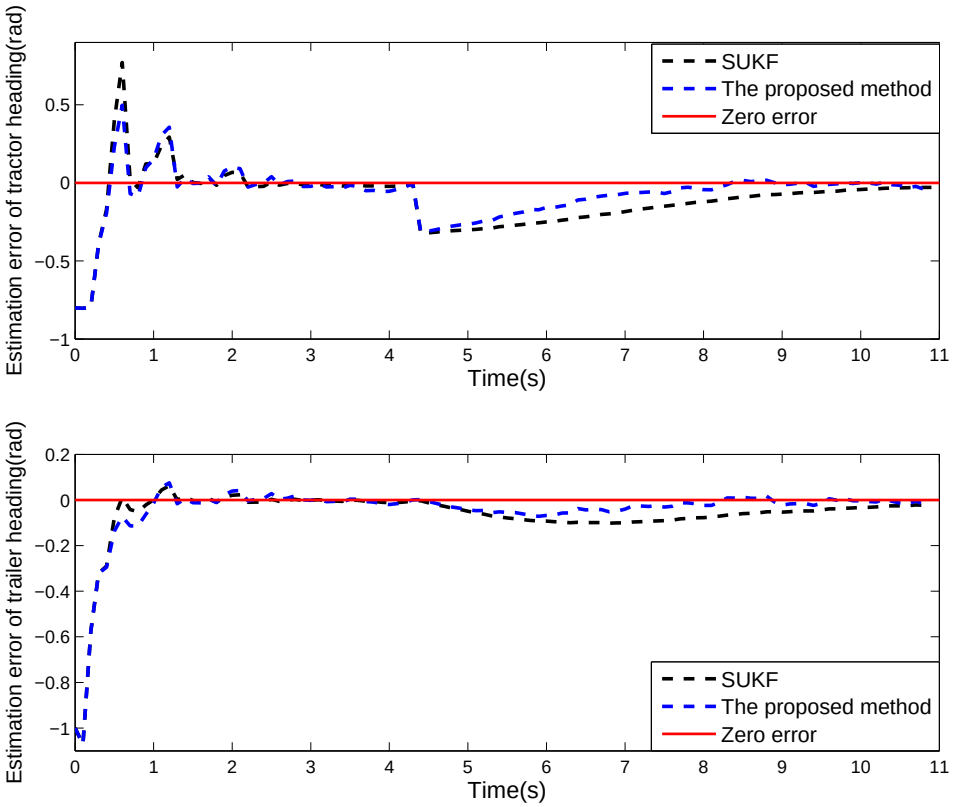

Figure 5.3: Heading angle estimations when a sudden disturbance is added

Table 5.3: Estimation RMSE using three methods when a disturbance acts on the tractor

	SUKF	A simpler AUKF	The proposed method
Tractor heading	10.43°	9.69°	7.79°
Trailer heading	3.95°	3.43°	2.09°
Trailer position in North	6.03 cm	3.41 cm	1.25 cm
Trailer position in East	4.87 cm	3 cm	1.18 cm

coordinate transformation, which is needed in a linear observer [67]. It adjusts the process uncertainty adaptively by estimating process noise covariance at each sample, which is applied to calculate the a priori process uncertainty at the next sample. Compared to EKF and standard UKF, the proposed filter is able to provide more accurate estimation with the presence of different operation conditions and disturbances. Notice that the proposed

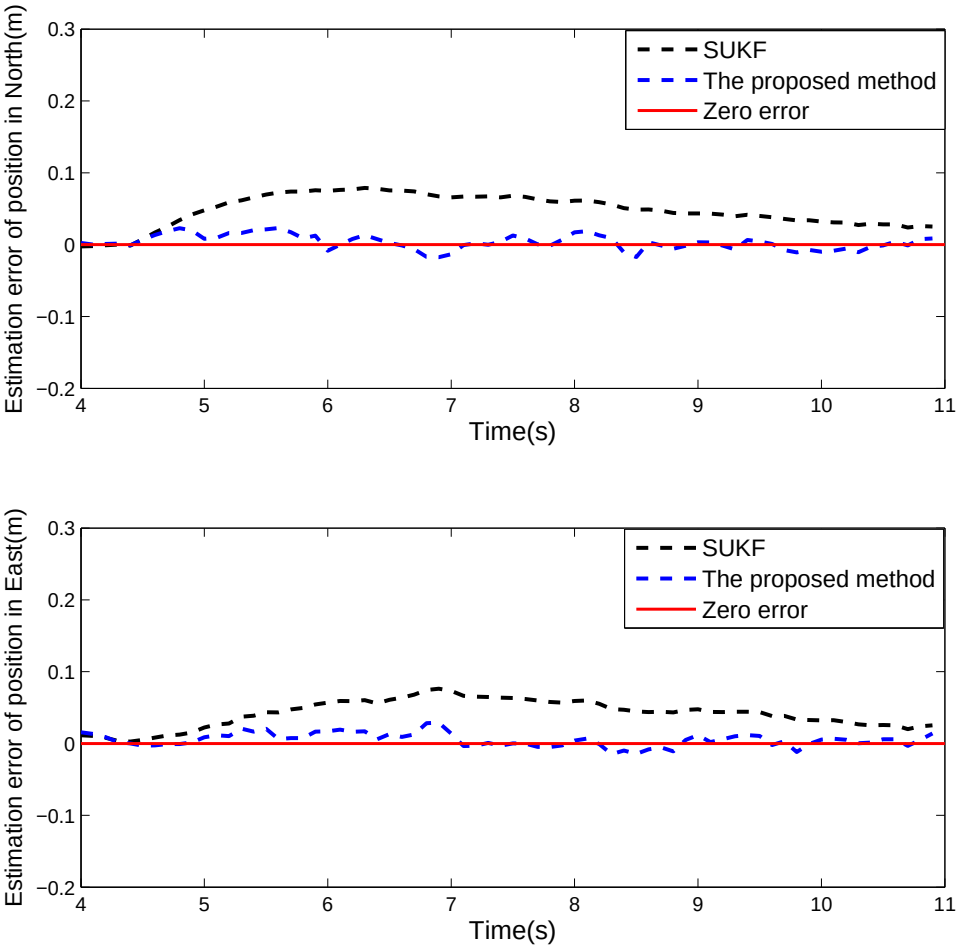

Figure 5.4: Position estimations when a sudden disturbance is added

algorithm requires that the output has a linear relationship with the state, i.e. the function $h(x_k)$ in (5.13) is linear.

Chapter 6

Contributions and Future Work

6.1 Main contributions

In this dissertation, path following problem of a tractor-trailer system is studied. For the space-based reference path, the existing approaches can make the trailer track a straight line with very small error. This work mainly solves the following four problems.

First, the tracking error near the intersections between two different reference paths are reduced. Two methods are proposed. One is to select a proper coordinate transformation for the tractor. A distance or an angle is chosen and compared for each intersection beforehand to indicate when the tractor begins to track new reference path. The other method is model predictive control (MPC). The model can be linearized based on current measurement (LTV-MPC) or the steady-state values of the time-varying terms (SS-MPC). The error under MPC can be smaller than using the former approach considering measurement noise, but the computation burden becomes heavier.

An alternate controller which focuses on the heading errors is proposed to be applied when the system is far away from the reference path. It can be implemented by saturating the position error before the controller receives the signal.

To remove the steady-state error when the trailer tracks a curved path, two methods are given. One is feedforward control, which can be regarded as an offset of the desired curvature. The other is to use steering rate as control input. The latter method is considered as a better solution mainly because it's more robust to modeling error. Integral control is introduced to reduce the tracking error if measurement bias exists. Integral separation is applied to get a good transient response. In addition, the threshold in integral separation can be adjusted adaptively.

Finally, the state estimation of a tractor-tailer system is investigated. A state observer based on an unscented Kalman filter is proposed. The trailer positions are used as measurements. The process uncertainty can be adaptively adjusted to give a better estimation when the process noise characters are unknown.

6.2 Future work

In this work, the obstacles are not considered. It would be worthwhile to further study the obstacle avoidance algorithm for a tractor-trailer system.

Another interesting area is nonlinear control. Considering both the system transient response and the global stability is very challenging. Recently artificial intelligence becomes very popular. It's interesting to introduce machine learning technique in the controller design. For example, the nonlinear model predictive control is very time-consuming during the optimization process. Machine leaning technique, such as neural network may be able to map the nonlinear relationship between the system state, the desired path in the future and the suitable control effort.

Bibliography

[1] Gene F Franklin, J David Powell, and Abbas Emami-Naeini. *Feedback control of dynamic systems*, volume 3.

[2] David W Hodo, John Y Hung, David M Bevly, and D Scott Millhouse. Analysis of trailer position error in an autonomous robot-trailer system with sensor noise. In *Industrial Electronics, 2007. ISIE 2007. IEEE International Symposium on*, pages 2107–2112. IEEE, 2007.

[3] Michael L Payne, John Y Hung, David M Bevly, and Bob J Selfridge. Control of a robot-trailer system using a single non-collocated sensor. In *IECON 2012-38th Annual Conference on IEEE Industrial Electronics Society*, pages 2674–2679. IEEE, 2012.

[4] Paolo Falcone, Francesco Borrelli, Jahan Asgari, H Eric Tseng, and Davor Hrovat. A real-time model predictive control approach for autonomous active steering. *Nonlinear Model Predictive Control for Fast Systems, Grenoble, France*, 2006.

[5] Erkan Kayacan, Erdal Kayacan, Herman Ramon, and Wouter Saeys. Learning in centralized nonlinear model predictive control: application to an autonomous tractor-trailer system. *IEEE Transactions on Control Systems Technology*, 23(1):197–205, 2015.

[6] Pushkar Hingwe, Jeng-Yu Wang, Meihua Tai, and Masayoshi Tomizuka. Lateral control of heavy duty vehicles for automated highway system: Experimental study on a tractor semi-trailer. *California Partners for Advanced Transit and Highways (PATH)*, 2000.

[7] Aditya Singh, John Y Hung, and Bob J Selfridge. A hybrid backstepping-like nonlinear control of a robot-trailer system. In *IECON 2012-38th Annual Conference on IEEE Industrial Electronics Society*, pages 2109–2114. IEEE, 2012.

[8] Kazuo Tanaka and Hua O Wang. *Fuzzy control systems design and analysis: a linear matrix inequality approach*. John Wiley & Sons, 2004.

[9] Jing Yuan and Yalou Huang. Path following control for tractor-trailer mobile robots with two kinds of connection structures. In *Intelligent Robots and Systems, 2006 IEEE/RSJ International Conference on*, pages 2533–2538. IEEE, 2006.

[10] Jin Cheng, Yong Zhang, and Zhonghua Wang. Curve path tracking control for tractor-trailer mobile robot. In *Fuzzy Systems and Knowledge Discovery (FSKD), 2011 Eighth International Conference on*, volume 1, pages 502–506. IEEE, 2011.

[11] Mitsuji Sampei, Takeshi Tamura, Tadaharu Kobayashi, and Nobuhiro Shibui. Arbitrary path tracking control of articulated vehicles using nonlinear control theory. *IEEE Transactions on Control Systems Technology*, 3(1):125–131, 1995.

[12] Samuel Gan-Mor, Rex L Clark, and Bruce L Upchurch. Implement lateral position accuracy under rtk-gps tractor guidance. *Computers and Electronics in Agriculture*, 59(1):31–38, 2007.

[13] Tong Wu and John Y Hung. Path following for a tractor-trailer system using model predictive control. In *Proceedings of IEEE SoutheastCon*, pages 1–5. IEEE, 2017.

[14] Tong Wu and John Y Hung. Lateral position control for a tractor-trailer system using coordinate transformation and hybrid controllers. In *Proceedings of IEEE SoutheastCon*, pages 1–6. IEEE, 2017.

[15] Tong Wu and John Y Hung. Lateral position control for a tractor-trailer system using steering rate input. In *Industrial Electronics (ISIE), 2017 IEEE 26th International Symposium on*, pages 1–5. IEEE, 2017.

[16] Tong Wu and John Y Hung. State estimation for a tractor-trailer system using adaptive unscented kalman filter. In *Proceedings of IEEE SoutheastCon*, pages 1–5. IEEE, 2017.

[17] Florent Lamiraux, Sepanta Sekhavat, and J-P Laumond. Motion planning and control for hilare pulling a trailer. *IEEE Transactions on Robotics and Automation*, 15(4):640–652, 1999.

[18] Thomas Bell. Automatic tractor guidance using carrier-phase differential gps. *Computers and electronics in agriculture*, 25(1):53–66, 2000.

[19] J Benton Derrick and David M Bevly. Adaptive control of a farm tractor with varying yaw dynamics accounting for actuator dynamics and saturations. In *2008 IEEE International Conference on Control Applications*, pages 547–552. IEEE, 2008.

[20] Manoj Karkee. *Modeling, identification and analysis of tractor and single axle towed implement system*. PhD thesis, Iowa State University, 2009.

[21] James T Salmon. Guidance of an off-road tractor-trailer system using model predictive control. Master's thesis, Auburn University, 2013.

[22] David Hodo. Development of an autonomous mobile robot-trailer system for UXO detection. Master's thesis, Auburn University, 2007.

[23] Zhong-Ping Jiang, Erjen Lefeber, and Henk Nijmeijer. Saturated stabilization and tracking of a nonholonomic mobile robot. *Systems & Control Letters*, 42(5):327–332, 2001.

[24] Khac Duc Do. Bounded controllers for global path tracking control of unicycle-type mobile robots. *Robotics and Autonomous Systems*, 61(8):775–784, 2013.

[25] Thomas Bell. *Precision robotic control of agricultural vehicles on realistic farm trajectories*. PhD thesis, Stanford University, 1999.

[26] Xiaolong Cao. Design and experimental validation of longitudinal controller of connected vehicles using model predictive control. Master's thesis, Auburn University, 2015.

[27] Lars Grüne and Jürgen Pannek. Nonlinear model predictive control. In *Nonlinear Model Predictive Control*, pages 43–66. Springer, 2011.

[28] Timm Faulwasser, Benjamin Kern, and Rolf Findeisen. Model predictive path-following for constrained nonlinear systems. In *Decision and Control, 2009 held jointly with the 2009 28th Chinese Control Conference. CDC/CCC 2009. Proceedings of the 48th IEEE Conference on*, pages 8642–8647. IEEE, 2009.

[29] J Backman, T Oksanen, and A Visala. Navigation system for agricultural machines: nonlinear model predictive path tracking. *Computers and Electronics in Agriculture*, 82:32–43, 2012.

[30] Paolo Falcone, Francesco Borrelli, H Eric Tseng, Jahan Asgari, and Davor Hrovat. A hierarchical model predictive control framework for autonomous ground vehicles. In *American Control Conference, 2008*, pages 3719–3724. IEEE, 2008.

[31] Tamás Keviczky and Gary J Balas. Flight test of a receding horizon controller for autonomous uav guidance. In *American Control Conference, 2005. Proceedings of the 2005*, pages 3518–3523. IEEE, 2005.

[32] Jae-Hyoung Lee, Woojin Chung, Munsang Kim, and Jae-Bok Song. A passive multiple trailer system with off-axle hitching. *International Journal of Control Automation and Systems*, 2:289–297, 2004.

[33] Liuping Wang. *Model predictive control system design and implementation using MATLAB®*. Springer Science & Business Media, 2009.

[34] David G Luenberger. *Optimization by vector space methods*. John Wiley & Sons, 1969.

[35] Erkan Kayacan, Erdal Kayacan, and Herman Ramon. Distributed nonlinear model predictive control of an autonomous tractor-trailer system. *Mechatronics*, 24(8):926–933, 2014.

[36] Alessandro Astolfi, Paolo Bolzern, and A Locatelli. Path-tracking of a tractor-trailer vehicle along rectilinear and circular paths: a lyapunov-based approach. *IEEE transactions on robotics and automation*, 20(1):154–160, 2004.

[37] William WL Cheung, Tony J Pitcher, and Daniel Pauly. A fuzzy logic expert system to estimate intrinsic extinction vulnerabilities of marine fishes to fishing. *Biological conservation*, 124(1):97–111, 2005.

[38] Chih-Lyang Hwang, Chang-Chia Yang, and John Y Hung. Path tracking of an automatic ground vehicle with different payloads by hierarchical improved fuzzy dynamic sliding-mode control. *IEEE Transactions on Fuzzy Systems*, 2017.

[39] Alberto Bemporad, Manfred Morari, Vivek Dua, and Efstratios N Pistikopoulos. The explicit linear quadratic regulator for constrained systems. *Automatica*, 38(1):3–20, 2002.

[40] Donald Chmielewski and V Manousiouthakis. On constrained infinite-time linear quadratic optimal control. *Systems & Control Letters*, 29(3):121–129, 1996.

[41] Simon Haykin. A comprehensive foundation. *Neural Networks*, 2(2004):41, 2004.

[42] Bogdan M Wilamowski. Neural network architectures and learning algorithms. *IEEE Industrial Electronics Magazine*, 3(4), 2009.

[43] Jing Li, Ji-hang Cheng, Jing-yuan Shi, and Fei Huang. Brief introduction of back propagation (bp) neural network algorithm and its improvement. *Advances in Computer Science and Information Engineering*, pages 553–558, 2012.

[44] J Benton Derrick and David M Bevly. Adaptive steering control of a farm tractor with varying yaw rate properties. *Journal of Field Robotics*, 26(6-7):519–536, 2009.

[45] Xiaoxia Yang and Yi Huang. Capabilities of extended state observer for estimating uncertainties. In *American Control Conference, 2009. ACC'09.*, pages 3700–3705. IEEE, 2009.

[46] Robert Miklosovic, Aaron Radke, and Zhiqiang Gao. Discrete implementation and generalization of the extended state observer. In *American Control Conference, 2006*, pages 6–11. IEEE, 2006.

[47] Jingqing Han. From PID to active disturbance rejection control. *IEEE transactions on Industrial Electronics*, 56(3):900–906, 2009.

[48] Zhiqiang Gao. Active disturbance rejection control: a paradigm shift in feedback control system design. In *American Control Conference, 2006*, pages 7–13. IEEE, 2006.

[49] Kiam Heong Ang, Gregory Chong, and Yun Li. Pid control system analysis, design, and technology. *IEEE transactions on control systems technology*, 13(4):559–576, 2005.

[50] Zhang Yachen and Hu Yueming. On PID controllers based on simulated annealing algorithm. In *Control Conference, 2008. CCC 2008. 27th Chinese*, pages 225–228. IEEE, 2008.

[51] Shuwang Du, Zhilin Feng, and Zhiming Fang. Design of improved PID algorithm for position control of servo unit. In *Computer and Communication Technologies in Agriculture Engineering (CCTAE), 2010 International Conference On*, volume 3, pages 333–335. IEEE, 2010.

[52] Karl Johan Astrom and Lars Rundqwist. Integrator windup and how to avoid it. In *American Control Conference, 1989*, pages 1693–1698. IEEE, 1989.

[53] Navneet Kapoor, Andrew R Teel, and Prodromos Daoutidis. An anti-windup design for linear systems with input saturation. *Automatica*, 34(5):559–574, 1998.

[54] Raymond Hanus, Michel Kinnaert, and J-L Henrotte. Conditioning technique, a general anti-windup and bumpless transfer method. *Automatica*, 23(6):729–739, 1987.

[55] Rudolph Emil Kalman et al. A new approach to linear filtering and prediction problems. *Journal of basic Engineering*, 82(1):35–45, 1960.

[56] Greg Welch and Gary Bishop. An introduction to the kalman filter. 1995.

[57] Matthew Lashley, David M Bevly, and John Y Hung. Performance analysis of vector tracking algorithms for weak gps signals in high dynamics. *IEEE Journal of selected topics in signal processing*, 3(4):661–673, 2009.

[58] Rached Dhaouadi, Ned Mohan, and Lars Norum. Design and implementation of an extended kalman filter for the state estimation of a permanent magnet synchronous motor. *IEEE Transactions on Power Electronics*, 6(3):491–497, 1991.

[59] Simon J Julier and Jeffrey K Uhlmann. A general method for approximating nonlinear transformations of probability distributions. Technical report, Technical report, Robotics Research Group, Department of Engineering Science, University of Oxford, 1996.

[60] Simon J Julier. The scaled unscented transformation. In *Proceedings of the 2002 American Control Conference (IEEE Cat. No. CH37301)*, volume 6, pages 4555–4559. IEEE, 2002.

[61] Eric A Wan and Ronell Van Der Merwe. The unscented kalman filter for nonlinear estimation. In *Adaptive Systems for Signal Processing, Communications, and Control Symposium 2000. AS-SPCC. The IEEE 2000*, pages 153–158. IEEE, 2000.

[62] Matthew Rhudy, Yu Gu, Jason Gross, and Marcello R Napolitano. Evaluation of matrix square root operations for UKF within a UAV GPS/INS sensor fusion application. *International Journal of Navigation and Observation*, 2011, 2012.

[63] Qijun Xia, Ming Rao, Yiqun Ying, and Xuemin Shen. Adaptive fading kalman filter with an application. *Automatica*, 30(8):1333–1338, 1994.

[64] Yuping Cao and Xuemin Tian. An adaptive UKF algorithm for process fault prognostics. In *Intelligent Computation Technology and Automation, 2009. ICICTA'09. Second International Conference on*, volume 2, pages 487–490. IEEE, 2009.

[65] Zhe Jiang, Qi Song, Yuqing He, and Jianda Han. A novel adaptive unscented kalman filter for nonlinear estimation. In *Decision and Control, 2007 46th IEEE Conference on*, pages 4293–4298. IEEE, 2007.

[66] AH Mohamed and KP Schwarz. Adaptive Kalman filtering for INS/GPS. *Journal of geodesy*, 73(4):193–203, 1999.

[67] Michael L Payne. Non-collocated control of an autonomous vehicle-trailer system using state estimation. Master's thesis, Auburn University, 2012.

Appendices

Appendix A

Matrix N in the dynamic model of a tractor-trailer system

$$n_{11} = -\frac{C_f^r + C_r^r + C_r^t}{v_x^r}$$

$$n_{12} = -\frac{(a+b+c)C_f^r + cC_r^r}{v_x^r}$$

$$n_{13} = -\frac{d(C_f^r + C_r^r) - eC_r^t}{v_x^r} - (m_r + m_t)v_x^r$$

$$n_{15} = C_f^r + C_r^r$$

$$n_{16} = -C_f^r - C_r^r$$

$$n_{21} = -\frac{aC_f^r - bC_r^r - (b+c)C_r^t}{v_x^r}$$

$$n_{22} = \frac{a(a+b+c)C_f^r - bcC_r^r}{v_x^r}$$

$$n_{23} = -\frac{adC_f^r - bdC_r^r + (b+c)eC_r^t - (b+c)m_t(v_x^r)^2}{v_x^r}$$

$$n_{25} = aC_f^r - bC_r^r$$

$$n_{26} = -aC_f^r + bC_r^r$$

$$n_{31} = \frac{(d+e)C_r^t}{v_x^r}$$

$$n_{33} = -\frac{(d+e)eC_r^t}{v_x^r} + dm_t v_x^r$$

Appendix B

Matrix parameters in the model (4.20) and (4.22)

$$a_{31} = \frac{v_r}{l_{tf}}$$

$$a_{32} = -\frac{l_h}{l_{tf}}$$

$$a_{33} - \frac{v_r}{l_{tf}}$$

$$a_{41} = -\frac{v_r l_{hs}}{l_{ts} l_{tf}}$$

$$a_{42} = \frac{l_{hf} l_{hs}}{l_{tf} l_{ts}}$$

$$a_{43} = \frac{v_r}{l_{ts}} + \frac{v_r l_{hs}}{l_{ts} l_{tf}}$$

$$a_{44} = -\frac{v_r}{l_{ts}}$$